VOLATILIZATION OF ARSENIC AND ANTIMONY IN THE FIRE REFINING OF LEAD

By

Richard Joseph McClincy

T 1171

A thesis submitted to the Faculty and the Board of Trustees of the Colorado School of Mines in partial fulfillment of the requirements for the degree of Doctor of Science in Metallurgical Engineering.

Signed: R. J. McClincy
R. J. McClincy

Golden, Colorado

Date: May 22, 1968

Approved: A. H. Larson
A. H. Larson
Thesis Advisor

A. W. Schlechten
A. W. Schlechten
Head, Department of
Metallurgical Engineering

Golden, Colorado

Date: MAY 22, 1968

ABSTRACT

The activity of Sb_2O_3 in PbO-Sb_2O_3 slags containing less than 50 mole % Sb_2O_3 was determined by the inert-gas saturation method at 700°C. In this composition range, the activity of Sb_2O_3 shows a strong negative deviation from ideality. The activity of PbO in PbO-Sb_2O_3 slags containing less than 50 mole % Sb_2O_3 was calculated by application of the Gibbs-Duhem integration to the Sb_2O_3 activity data. The activity of PbO in slags containing more than 63 mole % PbO is found to deviate in the positive direction from ideality while for slags containing less than 63 mole % PbO, the activity of PbO deviates in the negative direction from ideality.

The activity of Sb_2O_3 in PbO-SiO_2-Sb_2O_3 ($\frac{PbO}{SiO_2} = 2$) slags containing less than 25 mole % Sb_2O_3 was also determined by the inert-gas saturation method at 700°C. In this composition range, the activity of Sb_2O_3 shows a negative deviation from ideality.

The vacuum removal of As and Sn as oxides from artificial lead-softening slags was shown not to be technically feasible at the concentrations and temperatures normally

encountered in the conventional fire refining of lead. The vacuum removal of Sb as Sb_2O_3 from artificial lead-softening slags was found to be a relatively fast, efficient method for the recovery of as much as 80% of the Sb_2O_3 contained in a 30 wt % Sb_2O_3-SiO_2-PbO slag at 750°C. This removal was accomplished in 8 hr at 200μ Hg pressure by adding 8-10 wt % SiO_2 to the slag. The condensate produced in this process contained 99 wt % Sb_2O_3.

The activity of As in Pb-As alloys containing less than 10 mole % As was determined by the inert-gas saturation method at 703°C. In this composition range, the activity of As exhibits near-ideal-solution behavior.

TABLE OF CONTENTS

LIST OF FIGURES

Number Page

Number Page

LIST OF TABLES

LIST OF APPENDICES

ACKNOWLEDGMENTS

The author wishes to express his appreciation to Dr. A. H. Larson, Professor, Department of Metallurgical Engineering, Colorado School of Mines, for his guidance throughout the course of this investigation.

The author's gratitude is also expressed to Dr. J. P. Hager, Assistant Professor; Mr. B. Harris, Visiting Professor, on leave from the University of New South Wales; Mr. J. D. Miller, Graduate Student; and Mr. D. A. Rice, Graduate Student, Department of Metallurgical Engineering, Colorado School of Mines, for their assistance and counsel in the experimental work connected with this investigation.

The author wishes to thank the Department of Health, Education, and Welfare, United States Government, for providing the financial assistance necessary to complete this investigation. The author also wishes to express his appreciation to the National Science Foundation, United States Government, for providing the financial assistance required for the investigation of the Pb-As system under NSF Grant GK-196.

INTRODUCTION

The introduction to this investigation is presented in three parts: 1) the statement of the problem, outlining the subject of the investigation, 2) the organization of the problem, outlining the methods by which the problem was studied, and 3) the importance of the study, outlining the reasons for which the problem was studied.

Statement of the Problem

This investigation makes a survey of the feasibility of removing impurity oxides, Sb_2O_3 in particular, from artificial lead-softening slags under reduced pressure at elevated temperature. The impurity oxides are recovered as a pure, solid condensate. In order to describe more fully the results obtained, a thermodynamic activity study was carried out on Sb_2O_3 dissolved in a slag of optimum composition. Before any thermodynamic measurements could be made, however, it was necessary to design and construct a laboratory apparatus capable of determining vapor pressures in the range of interest. The necessary equipment was constructed and used to verify the available data in the

literature for the vapor pressure of pure Sb_2O_3.

Since arsenic is a common impurity in lead blast-furnace bullion and has an exceptionally high vapor pressure, a brief thermodynamic study was made on the Pb-As system at 700°C.

Organization of the Problem

The problem was attacked experimentally by first making a survey of the relative rates of removal under reduced pressure of As_2O_3, Sb_2O_3, and SnO_2 from PbO-based slags. Artificial lead-softening slags containing the various impurity oxides singly or in combination were prepared and subjected to reduced pressure at various elevated temperatures. When it became apparent that only Sb_2O_3 showed an appreciable rate of removal, fluxing agents, temperature, and pressure were varied in an effort to define a set of optimum operating conditions for the removal of Sb_2O_3.

The second portion of the investigation dealt with the measurement of certain thermodynamic properties of the slag systems. An apparatus was constructed to measure the vapor pressure of a volatile material over the range from 10^{-6} to 10^{-3} atm. Vapor-pressure data for pure cadmium were obtained and compared with available data in the literature to establish the reliability of the apparatus. A vapor-pressure study on pure Sb_2O_3 was then made to evaluate the

accuracy of the very limited data available in the literature for this compound. After the vapor pressure of pure Sb_2O_3 was established, an activity study was conducted on Sb_2O_3 dissolved in an artificial lead-softening slag of the optimum composition as defined by the vacuum-removal experiments.

The thermodynamic activity study on the Pb-As system was confined to dilute alloys of As dissolved in Pb for two reasons: 1) the vapor pressure of As_4 above Pb-As alloys containing more than 3.5 wt % As exceeds the operating range of the experimental apparatus, and 2) the concentration of arsenic in normal lead blast-furnace bullion rarely exceeds 1 wt %.

Importance of the Study

The commercial softening of lead blast-furnace bullion is accomplished either by selective oxidation of the impurities by using air and/or PbO as the oxidizing agent or by chemical means which produce a sodium antimonate. In the former case, a high-antimony slag is produced which must be retreated in a reverberatory fuming operation or resmelted with carbon to produce an antimonial-lead product. The sodium antimonate produced in the latter case can be reduced to metal or converted into some other antimony compound, usually Sb_2O_3.

No work has yet been done to examine the feasibility of recovering antimony from lead-softening slags by the application of vacuum techniques. The experimental work involved in this study provides a basis for the development of such a process. The vacuum removal of antimony from lead-softening slags could be desirable because both the time and temperature of slag treatment would be reduced, and the antimony would be recovered as a pure oxide without the necessity of extensive dust- and fume-recovery equipment.

SURVEY OF THE LITERATURE

No studies are reported in the literature on the application of vacuum techniques to the treatment of lead-softening slags. Other lead metallurgy processes involving the use of vacuum techniques such as the vacuum dezincing of lead bullion and Parkes' crusts are well documented in the literature but do not bear directly on this study. Conventional lead softening and by-product recovery are represented in the published literature by a great many articles which are too numerous to mention individually.

A number of studies have been reported in the literature that were concerned with the PbO-Sb_2O_3 phase diagram. Maier and Hincke (1932, p. 3-12) determined the melting-point diagram for the PbO-Sb_2O_3 system and identified the compound $PbO \cdot Sb_2O_3$. They found the phase diagram for this system to be two simple eutectics located on either side of the single compound. They also determined a very limited amount of vapor-pressure data for Sb_2O_3 above PbO-Sb_2O_3 melts at 697°C. A second phase-diagram investigation was done by Henning and Kohlmeyer (1957, p. 8-15), who confirmed the existence of the compound $PbO \cdot Sb_2O_3$ as well as the form

of the diagram. A disagreement was noticed, however, in that their liquidus temperatures over nearly the entire diagram were higher than those reported by Maier and Hincke. Barthel (1957, p. 630) and Pelzel (1959, p. 558-561) redetermined the liquidus curve at the PbO-rich end of the $PbO-Sb_2O_3$ system and agree very closely with the results of Maier and Hincke. None of the investigators mentioned above reported any mutual solid solubility in the $PbO-Sb_2O_3$ system. Zunkel and Larson (1967, p. 473-477) have determined the phase diagram for the PbO-rich end of the $PbO-Sb_2O_3$ system by slag-metal equilibria in the $Pb-(PbO+Sb_2O_3)$ system and thermal analysis in the $PbO-Sb_2O_3$ system. Their results agree favorably with those of Maier and Hincke.

The vapor pressure of antimony trioxide in the temperature range from 470° to 800°C has been determined by Hincke (1930, p. 3869-3877). His results below the melting point are the only data reported in the published literature. Myzenkov and Klushin (1965, p. 1709-1718), using the boiling-point method, have determined the pressure of Sb_4O_6 above liquid Sb_2O_3 in the temperature range from 715° to 1025°C. The agreement between these two studies is not very close. A portion of the discrepancy lies in the fact that Hincke used silica crucibles which were attacked by the liquid Sb_2O_3 at high temperatures. This fact does not account, however, for the large difference at the melting point.

Maier (1934, p. 23) gives a brief summary of vapor-pressure data for Sb_4O_6 above pure liquid Sb_2O_3, which agree quite well with the data of Myzenkov and Klushin at temperatures near the melting point.

Although arsenic has a very high vapor pressure and vacuum distillation appears to be a likely method for its removal from lead, the literature offers virtually no information concerning the vacuum removal of arsenic from lead. Caldwell, Spendlove, and St. Clair (1960, p. 1-12) mention arsenic in their investigation on the removal of volatile metals from lead by vacuum distillation. They do not, however, give any data for arsenic removal or refer to any actual experimental work involving arsenic dissolved in lead.

EXPERIMENTAL APPARATUS AND PROCEDURE

The experimental techniques used in this study required apparatus and procedures

1) to determine the loss in weight of a sample in contact with a dynamic gas phase saturated with the vapor of the sample under conditions of constant but different inert-gas flow rates at a controlled, elevated temperature,
2) to run distillation experiments on binary and ternary oxide systems in an inert atmosphere and at reduced pressure at a controlled, elevated temperature,
3) to equilibrate slag-metal systems in an inert atmosphere at atmospheric pressure at a controlled elevated temperature,
4) to analyze chemically the various phases produced in each experiment, and
5) to analyze by X-ray diffraction techniques the slag and condensate phases produced in each experiment.

Apparatus

The apparatus used in this study consisted of the transportation system for the inert-gas saturation experiments,

the vacuum distillation system, which was used at atmospheric pressure for the slag-metal equilibration experiments, and the X-ray diffraction system.

The Transportation System. The transportation system, shown schematically in Fig. 1 and pictorially in Fig. 2, allowed for the equilibration of a 1- to 5-gm sample of a metal or oxide phase with an inert carrier gas stream moving at a known, constant flowrate. Experiments were carried out at atmospheric pressure at a controlled, elevated temperature.

The apparatus consisted of two separate gas-purification trains and a reaction system. In order to avoid any possible segregation of the carrier gas and the sample vapor due to large differences in molecular weight, argon was selected for the carrier gas. One gas-purification train admitted the argon carrier gas to the reaction system containing the sample to be studied. A second gas train admitted argon at a high flow rate to flush the volatile species away from the reaction zone. Both gas trains were constructed entirely of Pyrex brand glass tubing.

The gas purification train used for the inert carrier gas contained a flow meter for the measurement of the gas flow rate. After passage through the flow meter, the gas was led first through silica gel and then through anhydrous magnesium perchlorate drying chambers to remove most of the

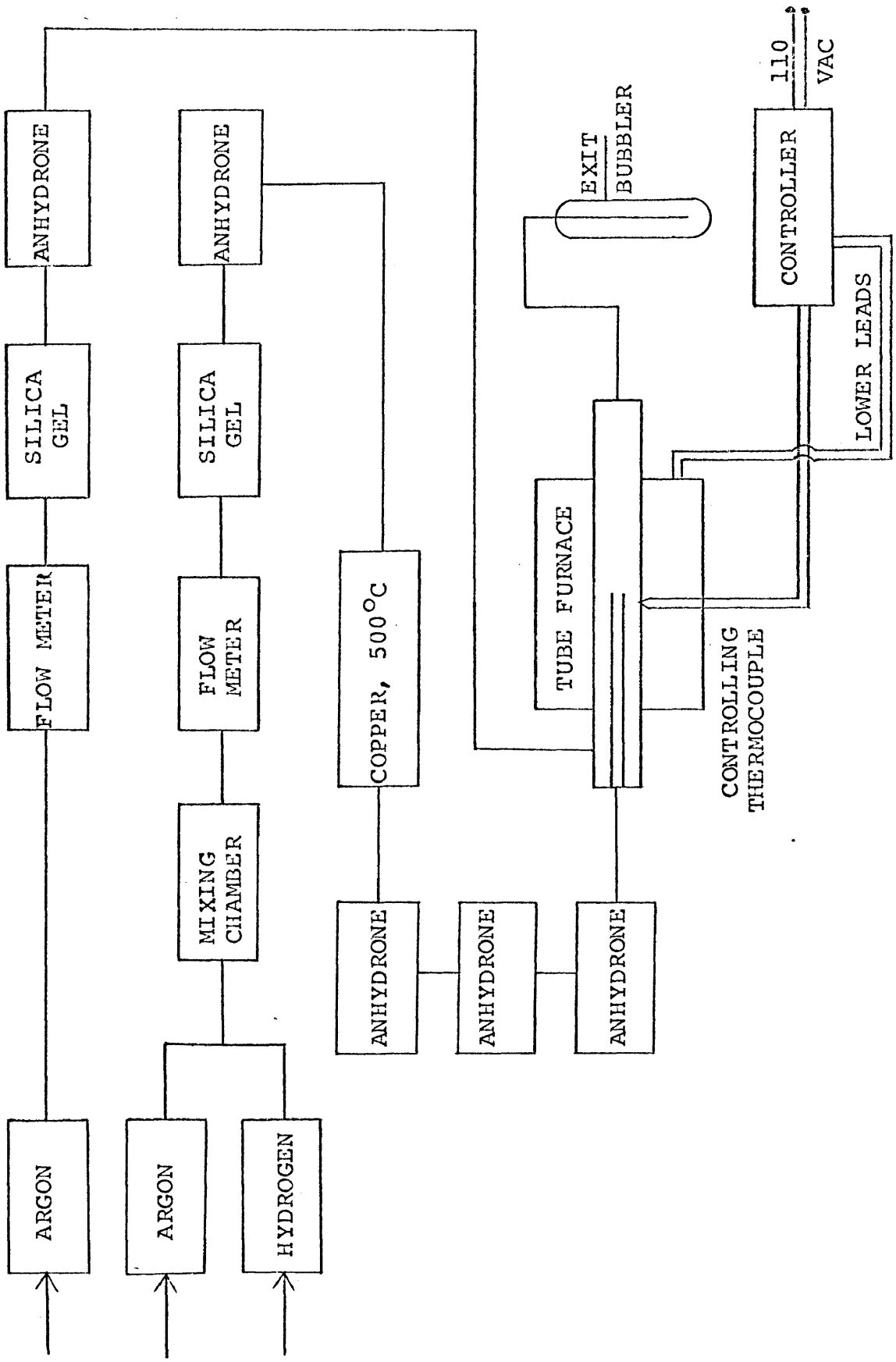

Figure 1. Schematic Diagram of Transportation System

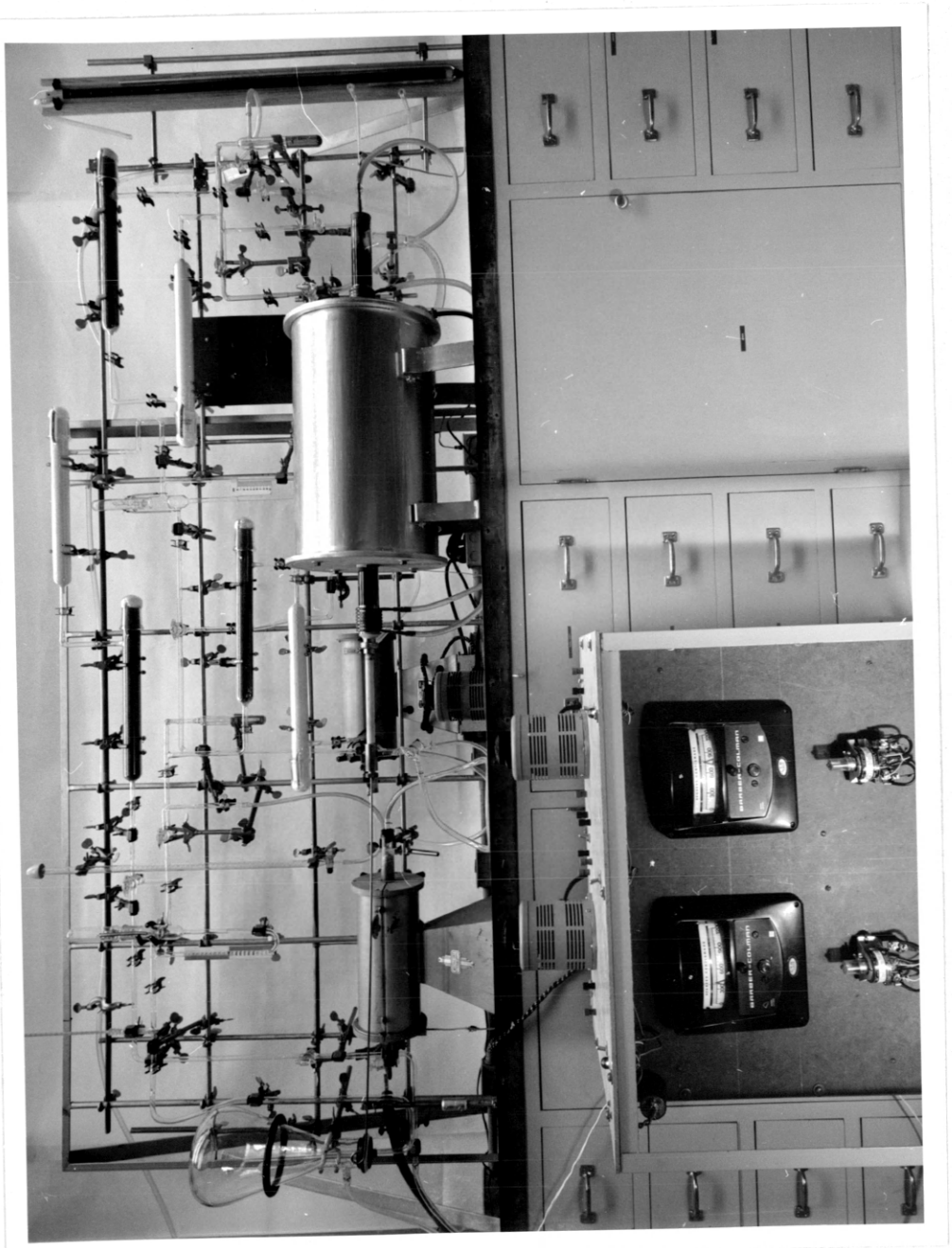

Figure 2. Photograph of Transportation System.

water vapor. A mercury pressure-relief bubbler was placed in the gas train immediately upstream from the drying chambers to protect the system from any blockage. It was found that this method of gas purification was sufficient for the experiments involving vapor-pressure determinations on oxide systems. For the experiments involving metal samples it was found that a slight amount of surface oxidation took place. In order to eliminate this oxidation, the argon was mixed with about 1% of hydrogen. This argon/-hydrogen gas mixture was metered and dried as before. The gas mixture was then passed over pure copper wool at a temperature of 500°C to convert the residual oxygen to water vapor. The remainder of the purification train consisted of three anhydrous magnesium perchlorate drying chambers arranged in series to remove the water vapor.

The second gas-purification train used for the argon flushing gas contained a flow meter and silica gel and anhydrous magnesium perchlorate drying chambers. Since this gas did not come into direct contact with the sample, a high degree of purity was not required.

The reaction system, shown schematically in Fig. 3, was connected to the purification system by means of a short length of vacuum tubing. This connection was originally made with Tygon brand plastic tubing, but it was observed that sufficient water vapor diffused through the

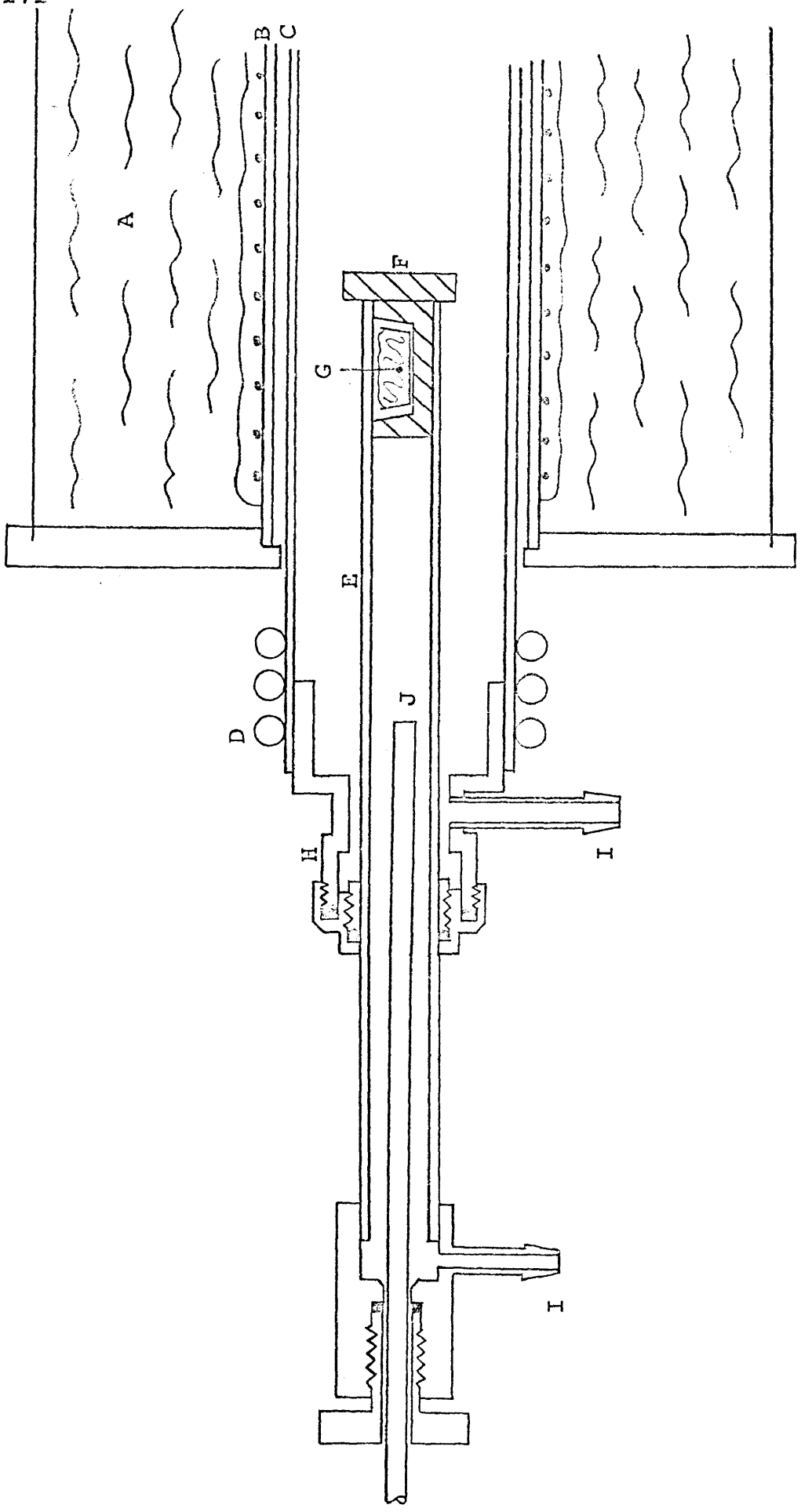

Figure 3. Schematic Diagram of Transportation Reaction System: A-Tube Furnace, B-Alumina Winding Tube, C-Vycor Tube, D-Cooling Coils, E-Alumina Reaction Tube, F-Boron Nitride Plug, G-Sample, H-Combustion Tube Breech Connector, I-Gas Inlets, J-Stainless Steel Push Rod.

walls of the tube to recontaminate the carrier gas.

The carrier gas was admitted to the reaction system through a modified brass breech connector closing one end of a 11/16-in.-OD, 7/16-in.-ID by 24-in.-long high-purity alumina reaction tube. The sample was placed in a 4-mm-wide by 25-mm-long by 4-mm-deep high-purity alumina combustion boat which fitted tightly into a plug which closed the other end of the alumina reaction tube. The plug was machined so as to provide a very close fit with the inside of the alumina reaction tube, and small channels were engraved on its surface to guide the carrier gas to the chamber containing the sample. The plug was constructed from HBR-grade boron nitride manufactured by the Union Carbide Corporation. The selection of boron nitride for the plug was made because of its inert nature, ease of machining, high-temperature dimensional stability, and resistance to thermal shock. A stainless steel pushrod was admitted through a viton O-ring seal in the modified breech connector to allow for the unloading of the reaction tube without opening the reaction system.

The reaction tube was placed inside a 45-mm-OD, 40-mm-ID by 36-in.-long Vycor brand glass tube. Closure was made, on one end, by a brass combustion-tube breech connector from which the sight glass had been removed and a Viton O-ring seal installed in its place. The breech

connector was sealed into the end of the Vycor tube with a heat-resistant epoxy resin. The O-ring seal provided for a sliding seal between the alumina reaction tube and the Vycor tube by means of which the sample could be easily positioned once it was inside the furnace. The argon flushing gas was also admitted to the reaction system through the breech connector.

Closure on the other end of the Vycor tube was achieved by means of a rubber stopper. A standardized chromel-alumel measuring thermocouple in a Vycor brand glass sheath and a gas outlet tube were positioned within the reaction tube through the rubber stopper. All furnace gases exited the transportation system through a dibutylphthalate bubbler.

The furnace used in this study was constructed from a 16-in.-diameter by 22-in.-long light-gauge, mild steel shell filled with diatomaceous earth insulation. The heating element consisted of 15 ft of 20-gauge nichrome wire and was supported by a 2½-in.-OD, 2-1/8-in.-ID by 22-in.-long mullite tube. The furnace assembly was closed on both ends by 3/8-in.-thick transite end plates held by four stainless steel tie rods. The heating element was wound nonuniformly so as to yield a 4-in.-long constant-temperature zone in which the temperature gradient did not exceed 0.5°C per linear inch in the temperature range from 250° to 750°C.

The furnace power was supplied by a Type 116 Powerstat

operating on 110 VAC. The furnace temperature was controlled by a Barber-Coleman Model 293C Capacitrol and a 20-ft chromel-alumel thermocouple. A variable resistance shunt was installed around the Capacitrol and adjusted to bypass 95% of the minimum furnace power required to maintain a given furnace temperature. The combination of the Capacitrol and the power shunt allowed for a maximum temperature variance within the furnace of ±1.5°C.

The Vacuum Distillation System. The vacuum distillation system shown schematically in Fig. 4 and pictorially in Fig. 5 allowed for the distillation of volatile oxides from 500 gm of PbO-SiO_2-oxide slag in an inert atmosphere at reduced pressure at a controlled, elevated temperature.

The distillation experiments were carried out in a 3¼-in.-OD, 2-3/4-in.-ID by 4¼-in.-deep Type 416 stainless steel crucible. It was found that only the 400 series stainless steels would withstand the highly corrosive action of the slags at sustained high temperatures. Type 446 stainless steel was later found to be particularly resistant due to its ferritic rather than martensitic structure at high temperatures. The crucible was placed on an insulating firebrick pedestal located in the bottom of a vertically mounted 4-in.-ID, 4¼-in.-OD by 18-in.-long fused-silica reaction tube which was closed on the bottom end. A condenser section composed of a 3½-in.-ID, 3-3/4-in.-OD by 12-in.-long fused-silica tube, open on both ends,

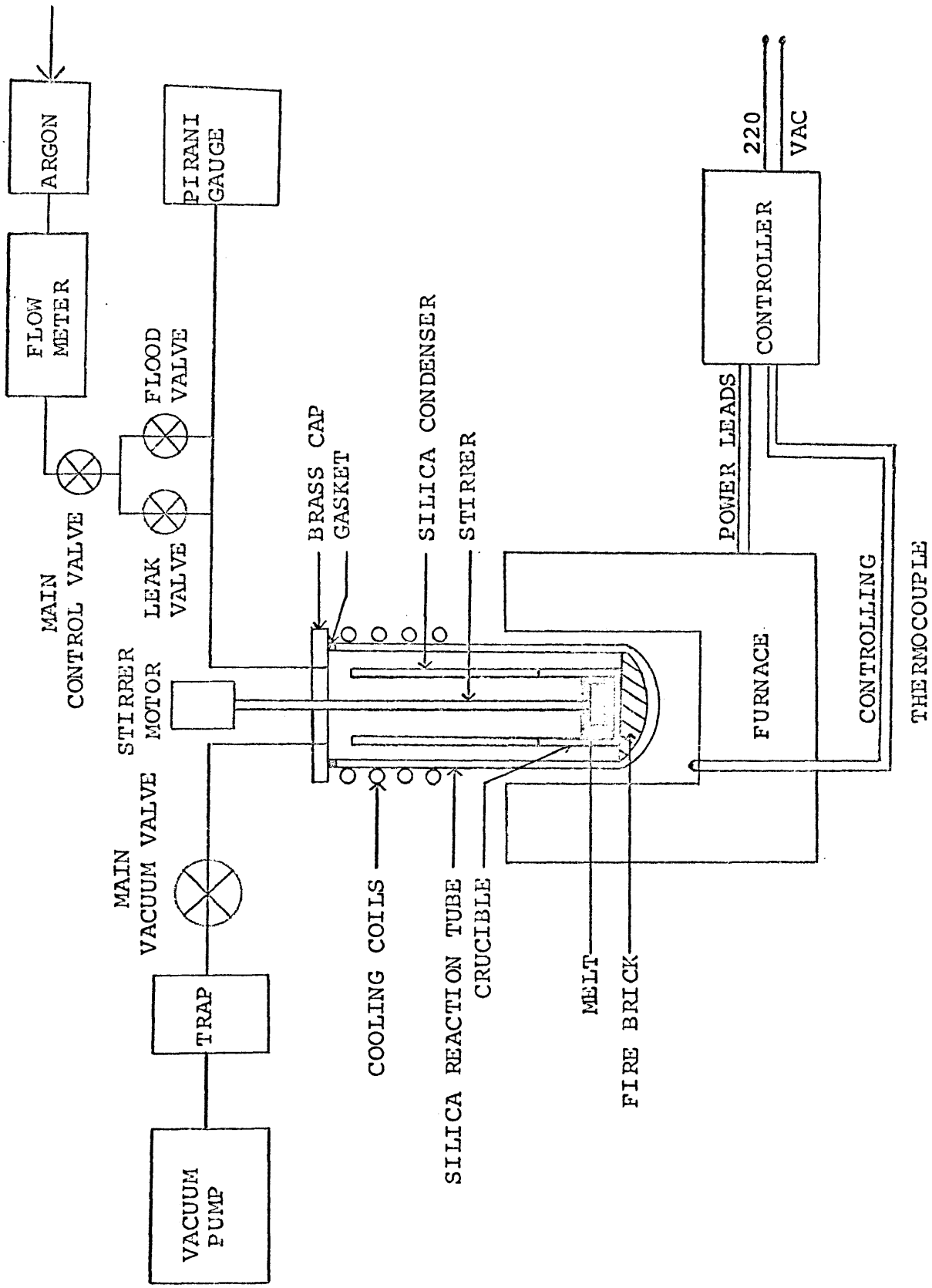

Figure 4. Schematic Diagram of Vacuum Distillation System

Figure 5. Photograph of Vacuum Distillation System

rested on an annular flange around the top of the stainless steel crucible. The condenser served to collect the products of volatilization and prevented any of the slag splashed out of the crucible from coming into contact with the fused-silica reaction tube. The reaction tube was closed on the open end by a water-cooled brass cap sealed by an annular silicone rubber gasket and an adjustable collar clamp. Connected to the brass cap were a sampling port, a takeoff for the introduction of inert gas, a takeoff to the vacuum pump, and a port housing a Teflon vacuum feed-through gland. A Type 416 stainless steel, motor-driven paddle stirrer was introduced into the reaction tube through the vacuum feed-through gland.

A Lindberg Model 56622 crucible furnace with a 5-in.-ID by 8-in.-deep heating chamber was used as the source of heat. The furnace was capable of attaining a maximum temperature of 1210°C and maintaining a constant temperature zone of 4½ in. in the temperature range from 500° to 800°C. The furnace power was supplied by a Type 236 Powerstat operating on 220 VAC. A Barber-Coleman Model 293C Capacitrol and a 20-ft chromel-alumel thermocouple provided furnace temperature control to within ±3°C. The slag-melt temperature was calibrated with the temperature scale on the controller to avoid having the thermocouple protection tube remain in contact with the highly corrosive slag for sustained periods

of time. The slag-melt temperature was periodically checked with a calibrated chromel-alumel thermocouple enclosed in a protective Vycor tube to insure that significant temperature variations did not go unnoticed.

For the experiments operated at reduced pressure, a Duo-Seal Model 1402B mechanical pump capable of producing a vacuum of 1μ Hg was used to produce a vacuum in the reaction tube. The vacuum level was periodically monitored by means of a McLeod gauge. The vacuum was controlled at the desired level by the introduction of argon through a modified reverse-taper Teflon stopcock. This method provided a control of ±15μ Hg on the vacuum level.

For the experiments operated at atmospheric pressure, argon at 1 psig was allowed to flood the reaction tube through a valve in the inert-gas introduction system. Any leaks in the reaction system could be detected by observing the flow meter in the inert-gas introduction system.

Periodic sampling of the slag and metal phases was accomplished by inserting 7-mm Vycor tubes into the melt. The slags were sampled by inserting a sealed Vycor tube into the melt and immediately raising it. Approximately 1 gm of slag solidified on the tube and was scraped off and retained for chemical analysis. Samples of the metal phase were collected with a similar Vycor tube which had a small hole 3/8 in. above the sealed end. The sample tube was

lowered into the metal phase, allowed to fill, and quickly raised. The metal was then poured into cold water and the sample dried and retained for chemical analysis.

The X-ray Diffraction System. The X-ray analysis of the slag and condensate phases was accomplished by means of standard diffractometer procedures at room temperature. All diffraction patterns were made with Cu K_α radiation at 45 kv and 35 ma with appropriate rate-meter settings.

Procedure

Three basically different types of experiments were conducted in this investigation: 1) vapor-pressure determinations on pure metals, alloys, pure oxides, and oxide slags, 2) rate-of-distillation experiments in an inert atmosphere at reduced pressure, and 3) slag-metal equilibrations in an inert atmosphere at atmospheric pressure. The samples collected during the experiments were analyzed to determine the composition of the slag and condensate phases and the impurity content of the metal.

Vapor-Pressure Determinations. The sample whose vapor pressure was to be determined was placed in the alumina combustion boat so as to fill it as completely as possible. The combustion boat was then inserted into the boron nitride plug which, in turn, was inserted into the open end of the alumina reaction tube. All loading operations were performed

against a strong flow of argon to prevent air from entering the system. A bypass line was installed in the flushing gas train to permit the introduction of argon from either end of the Vycor tube. The end of the reaction tube was positioned in the cold end of the Vycor tube for five minutes while a current of argon flushed away any air that might be present in the combustion boat. The reaction tube was then slid into the furnace and the cap of the combustion-tube breech connector securely fastened. As soon as closure was effected, the argon bypass line was removed from the system by a pair of 3-way stopcocks and the flushing gas allowed to resume its normal flow. The final positioning of the sample within the furnace was effected by sliding the reaction tube through the O-ring seal in the cap of the breech connector. After the sample was in position, the carrier gas was turned off until the sample attained the proper temperature. When the sample had reached thermal equilibrium with the furnace, the carrier gas was turned up to the desired flow rate. This time was recorded as time zero for the experiment.

The time required for the sample to reach thermal equilibrium with the furnace varied as the character of the sample changed from metal to oxide and as the temperature of the experiments was increased. The amount of time required for the sample to heat up was determined separately

for each sample material at each temperature by embedding a standardized chromel-alumel thermocouple inside of a dummy sample. For the alloys and slags studied, weight losses during heat-up times were always negligible with respect to the total weight loss occurring during the experiment.

When a sufficient time had elapsed, the stainless steel push rod was used to slide the plug device to the end of the Vycor tube where the sample was cooled as rapidly as possible by a strong blast of air on the outside of the tube. Lead alloys originally at 700°C were observed to solidify within 30 seconds after unloading. The end of the experiment was recorded as the moment the plug was pushed out of the reaction tube.

After cooling for 5 minutes, the plug was removed from the Vycor tube and placed on a brass cooling block inside a dessicator. When the sample had reached room temperature, the combustion boat was weighed on a Mettler semimicro balance to determine its loss in weight during the experiment. The Mettler balance was capable of measuring weight changes of 1 mg accurately to 1%.

Sampling of the alloys and slags studied in this investigation was unnecessary due to the large differences in vapor pressure for the various components of the samples. In all cases, the observed weight losses could be attributed to only one volatile species.

The Pb-As alloys were prepared by melting the required amounts of lead and arsenic together under carbon powder in a graphite crucible in an inert atmosphere. (Reagent analyses are given in Appendix I.) The resulting alloy was then quickly cast into rods in a graphite mold and the mold quenched in cold water. The $PbO-SiO_2-Sb_2O_3$ slags were prepared by melting together the required amounts of PbO, SiO_2, and Sb_2O_3 in a Type 446 stainless steel crucible in the vacuum distillation apparatus under an inert atmosphere at atmospheric pressure. When the slag had been thoroughly mixed, the reaction system was quickly opened and the slag cast into a cast-iron mold which was then quenched in cold water. The alumina combustion boats were brought to constant weight by heating for 12 hours in a strong current of argon at 750°C.

Rate-of-Distillation Experiments. The rate-of-distillation experiments were performed primarily on 500-gm samples of the $PbO-Sb_2O_3$ and $PbO-SiO_2-Sb_2O_3$ slags in the vacuum-distillation apparatus under an inert atmosphere at reduced pressure. Reagents were mixed in the desired amounts and placed in the stainless steel crucible; the crucible was placed inside the fused silica reaction tube; and the condenser was placed on the crucible. The stirring assembly was adjusted to a raised position in the brass cap, the cap was placed over the end of the reaction tube

and clamped securely. After the vacuum line and the inert gas introduction line was connected by means of ball-and-socket joints, the system was evacuated to 50μ Hg and flushed with argon eight times. After the last evacuation, argon at 1 psig was allowed to flood the system. The furnace, which had to be set at the desired temperature, was then raised into position around the reaction tube by means of a counter-weight system.

When the slag had reached the desired temperature, the stirrer was lowered into the melt and switched on, and the argon flow was turned off. The vacuum pump was turned on and the vacuum level adjusted by means of the Teflon leak-valve. This time was recorded at time zero for the experiment. A vacuum of 200μ Hg could be attained in about 30 seconds, and a level of 25μ Hg required about 2 minutes.

Sampling of the slag was carried out at appropriate time intervals. When the last sample had been taken, the stirrer was switched off and raised out of the melt. The slag was then allowed to furnace cool under an inert atmosphere at atmospheric pressure to allow crystallization of the slag. When the solidification process was complete, the furnace was lowered, and the reaction system was allowed to air-cool to room temperature. After the entire system had cooled to room temperature, the argon flow was stopped; the brass cap and stirring assembly were

disconnected and removed; and the condenser and crucible were removed from the reaction tube. The condensate was chipped out of the condenser, weighed, and sampled; and the slag was sampled for X-ray diffraction analysis. The remaining slag was melted out of the crucible and cast into cakes.

Slag-Metal Equilibrations. The same general procedure as was described in the preceding section was used for the slag-metal equilibrations, with the exception that the experiments were carried out at atmospheric pressure. Approximately 18 hr were required for the establishment of equilibrium, and therefore sampling was carried out at 2-hr intervals after 18 hr until the analyses of two consecutive samples of both the slag and metal phases showed no significant change.

Analysis of the Slag, Condensate, and Metal Phases. Analyses of the slag and metal phases were performed by ASTM standard wet methods. The following methods of chemical analysis were used and are described in Appendix II:

1) Sb and As in oxide slags --
   ASTM Standard Analysis E46-56, Arsenic and Antimony by the Distillation-Bromate Method.
2) Sb dissolved in Pb -- same as 1).
3) Sn in oxide slags -- ASTM Standard Analysis E57-60, Tin by the Iodimetric Titration Method.

All Sb_2O_3 condensate analyses were furnished through the courtesy of the St. Joseph Lead Co., Monaca, Pennsylvania. An outline of their atomic absorption procedure is included in Appendix II. As was previously mentioned in the discussion of apparatus, the slags and condensates were analyzed by standard X-ray diffraction procedures using Cu K_α radiation at room temperature.

EXPERIMENTAL RESULTS

The experimental results of this investigation are classified in four separate categories according to the type of experiment involved: 1) vapor-pressure determinations for Cd, Sb_2O_3, $PbO-Sb_2O_3$ and $PbO-SiO_2-Sb_2O_3$ slags, and Pb-As alloys, 2) rate-of-volatile-oxide-distillation experiments in the $PbO-Me_xO_y$ and $PbO-SiO_2-Me_xO_y$ systems at 750° and 850°C, 3) slag-metal equilibrations in the $Pb-(PbO+SiO_2+SbO_3)$ system at 700° and 750°C, and 4) results of X-ray diffraction analyses on slags and condensates produced in experiments 2) and 3).

Results from Vapor-Pressure Determinations for Cd, Sb_2O_3, $PbO-Sb_2O_3$ and $PbO-SiO_2-Sb_2O_3$ Slags, and Pb-As Alloys

The experimental results obtained from this portion of the investigation were obtained by determining the weight loss of a sample when a measured volume of inert gas at constant flow rate was passed over the sample in a known time at a known temperature. Due to large differences in the vapor pressures of the various components of the sample, the observed losses in weight of the sample could be

attributed solely to As for the Pb-As alloys and to Sb_2O_3 for the $PbO-SiO_2-Sb_2O_3$ and $PbO-Sb_2O_3$ slags. A sample calculation for p_{Cd} above pure Cd is given in Appendix III.

The standard deviation, normalized against the mean, for each vapor-pressure measurement was calculated and found to lie within the limits $0.00374<\sigma'<0.0433$.

Cadmium. In order to provide a check on the accuracy and reliability of the transportation apparatus constructed for this investigation, a brief vapor-pressure study was first made on a well known system. The results from the vapor-pressure determination experiments for Cd are shown in tabular form in Table 1 and graphically in Fig. 6. The experimental data for these experiments are presented in tabular form in Appendix IV.

Table 1. Vapor Pressure of Cadmium as a Function of Temperature

Temperature, °C	p_{Cd}, mm Hg
254	0.00534
297	0.0364
346	0.223
393	1.014

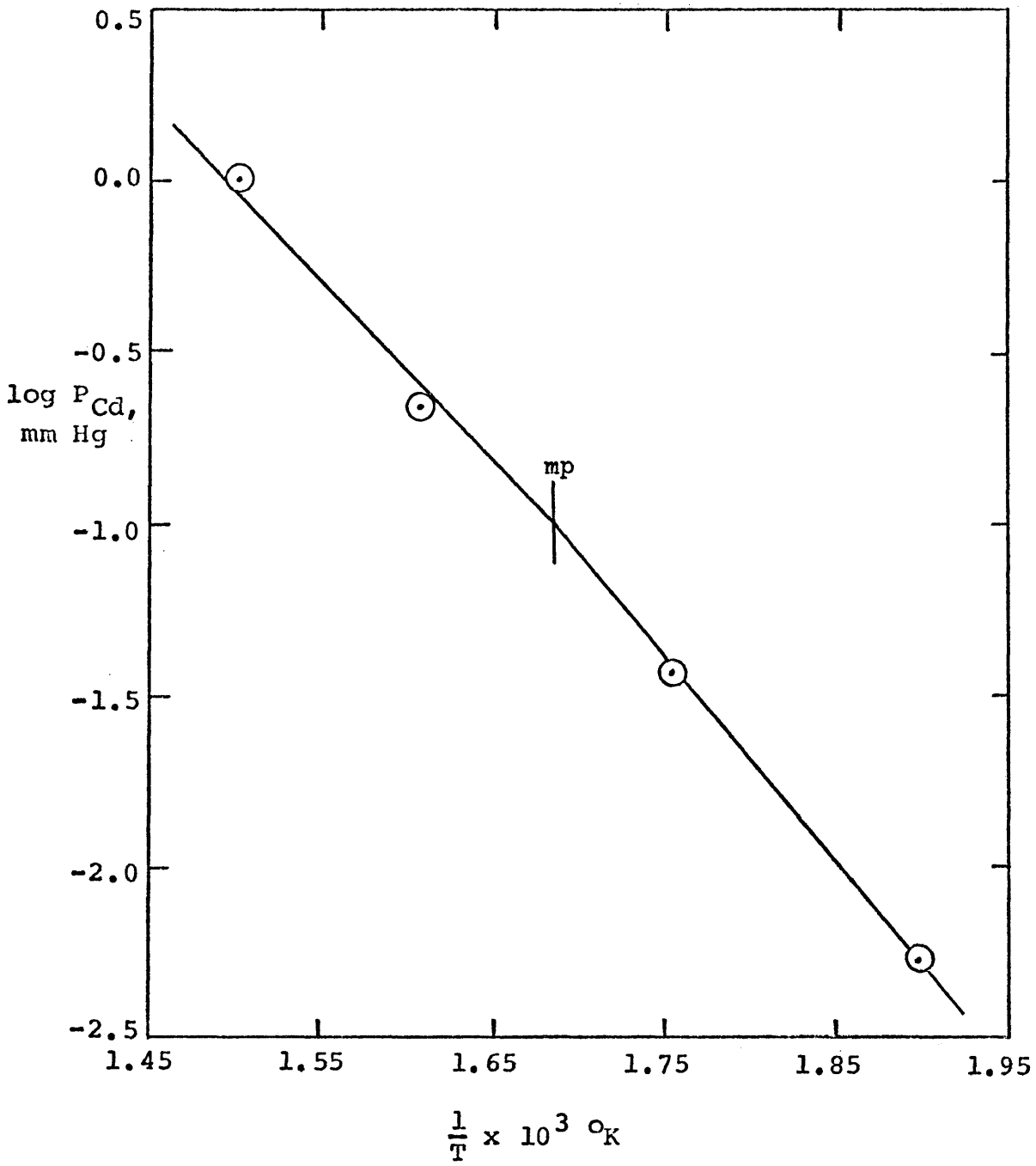

Figure 6. Variation of log P_{Cd} above Pure Cd with Reciprocal Temperature

Sb_2O_3. The results for this portion of the investigation are presented in tabular form in Table 2 and shown graphically in Fig. 7. The predominant vapor species has been shown to be Sb_4O_6 by Norman and Staley (1964, p. 1503). The vapor pressure of Sb_4O_6 above pure, solid, cubic Sb_2O_3 was determined in the temperature range from 422° to 599°C.

Table 2. Vapor Pressure of Sb_4O_6 as a Function of Temperature

Temperature, °C	$p_{Sb_4O_6}$, mm Hg
422	0.00162
454	0.00772
485	0.0277
514	0.0934
547	0.330
568	0.689
599	1.752

PbO-Sb_2O_3 Slags. The results for this portion of the investigation are presented in tabular form in Table 3 and shown graphically in Fig. 8. The vapor pressure of Sb_4O_6 was determined above PbO-Sb_2O_3 slags in the range from $X_{Sb_2O_3}$ = 0.0442 to 0.495 at 700°C. X-ray diffraction analysis of the condensates produced in these experiments did not reveal the presence of any chemical species other

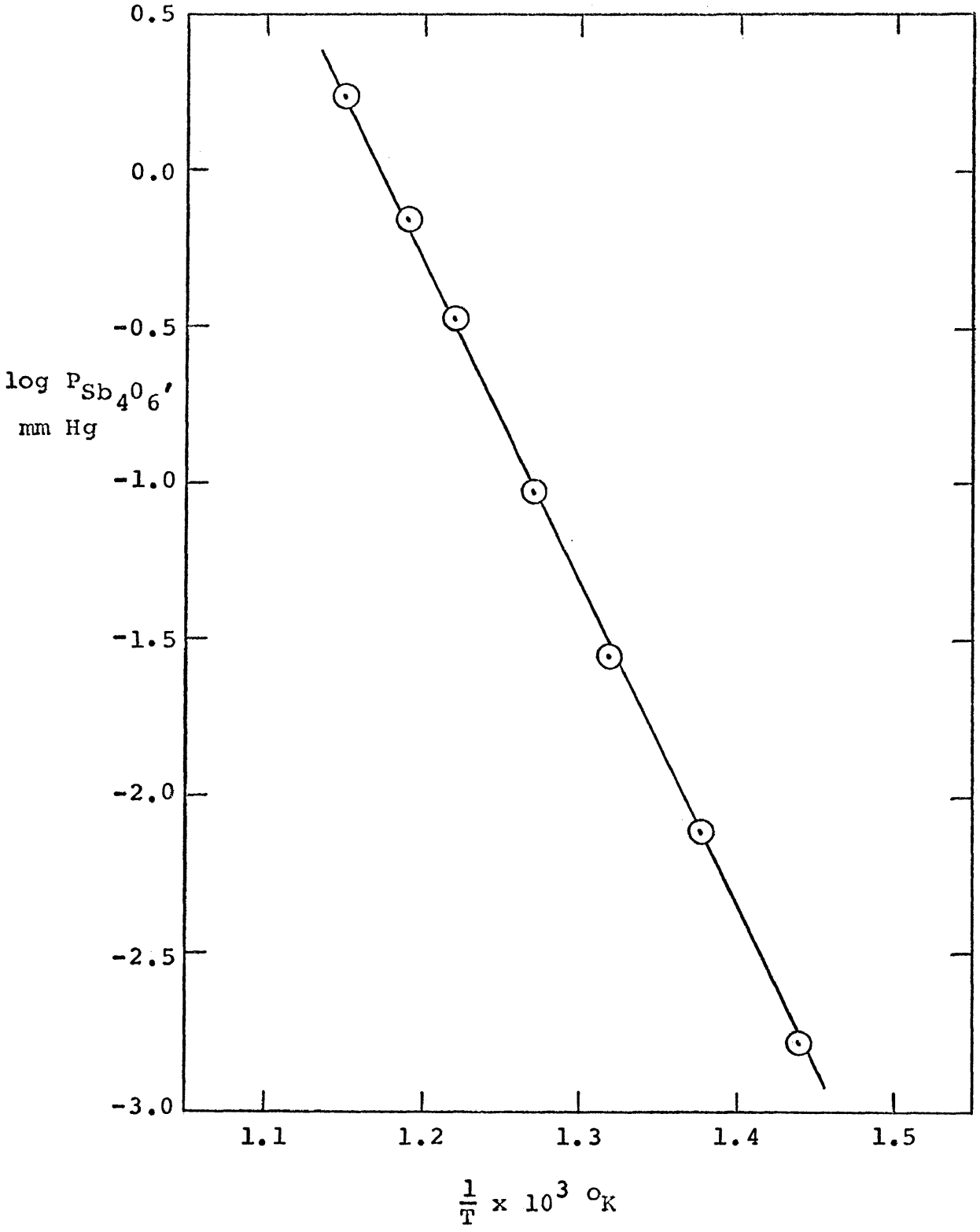

Figure 7. Variation of log $P_{Sb_4O_6}$ above Cubic Sb_2O_3 with Reciprocal Temperature

than Sb_2O_3.

Table 3. Vapor Pressure of Sb_4O_6 above $PbO-Sb_2O_3$ Slags at 700°C

$X_{Sb_2O_3}$ in slag	$P_{Sb_4O_6}$, mm Hg
0.0442	0.0304
0.108	0.0293
0.137	0.0290
0.176	0.0380
0.212	0.0560
0.280	0.126
0.495	1.235

$PbO-SiO_2-Sb_2O_3$ Slags. The experimental results for this portion of the investigation are presented in tabular form in Table 4 and shown graphically in Fig. 9. The vapor pressure of Sb_4O_6 above $PbO-SiO_2-Sb_2O_3$ slags was determined for the composition range from $X_{Sb_2O_3}$ = 0.0296 to 0.246 at 700°C. In order to keep this portion of the investigation within reasonable limits, a molar ratio corresponding to $\frac{PbO}{SiO_2}$ = 2 was selected and held constant throughout the experiments. X-ray diffraction analysis of the condensates produced in these experiments did not reveal the presence of any chemical species other than Sb_2O_3.

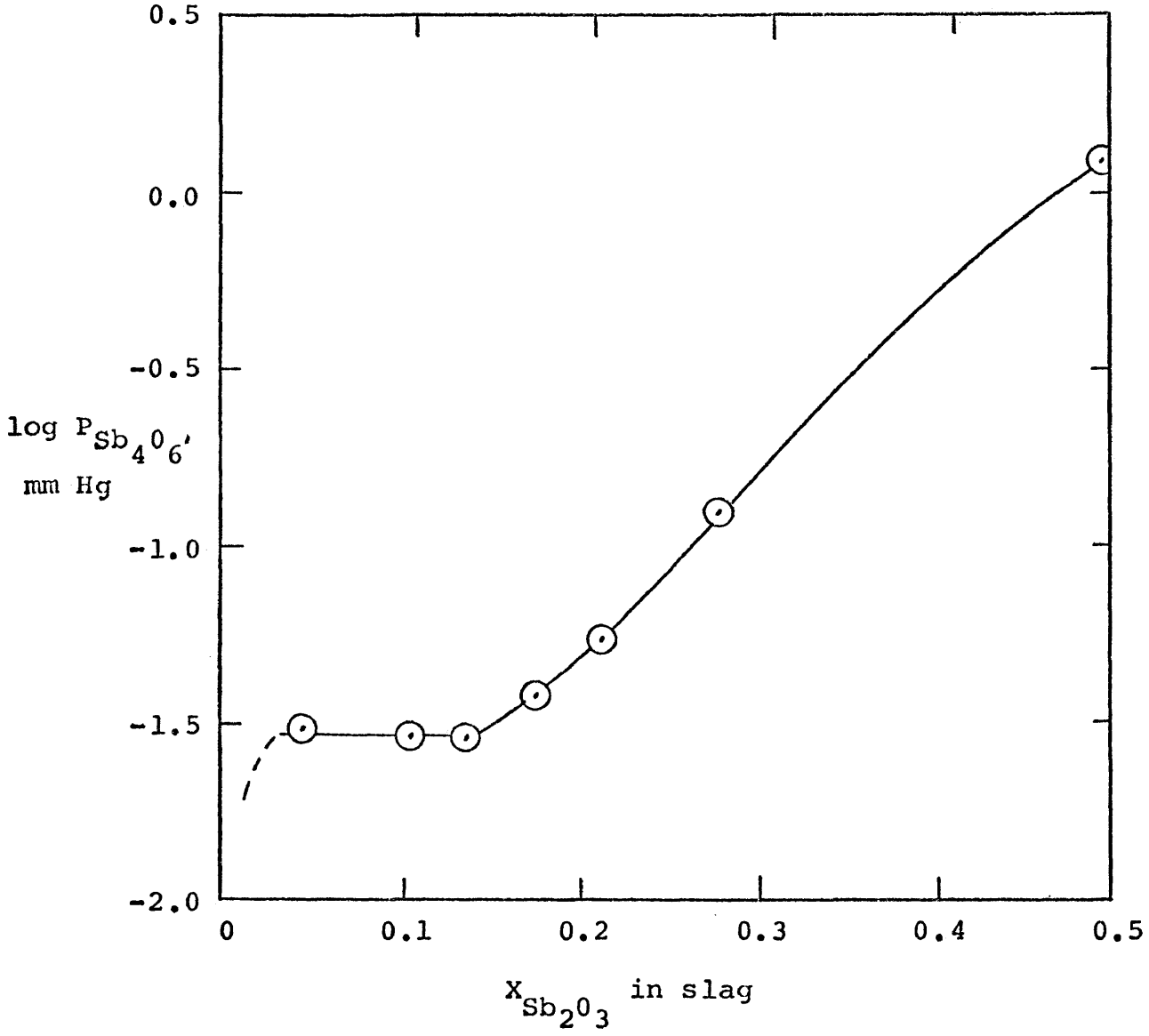

Figure 8. Variation of log $P_{Sb_4O_6}$ above $PbO-Sb_2O_3$ Slags with Composition at 700°C

Table 4. Vapor Pressure of Sb_4O_6 above $PbO-SiO_2-Sb_2O_3$ (PbO/SiO_2 = 2) Slags at 700°C

$X_{Sb_4O_6}$ in slag	$P_{Sb_4O_6}$, mm Hg
0.0296	0.000537
0.0634	0.00275
0.0945	0.00766
0.130	0.0265
0.167	0.0804
0.206	0.204
0.246	0.441

Pb-As Alloys. The results from this portion of the investigation are presented in tabular form in Table 5 and shown graphically in Fig. 10. The composition range covered was 0.01 to 0.09 mole fraction As dissolved in Pb at 703°C. Due to very small losses in weight for the samples containing 0.01425 mole fraction As, the calculated vapor pressure of arsenic above an alloy of this composition is only an approximation.

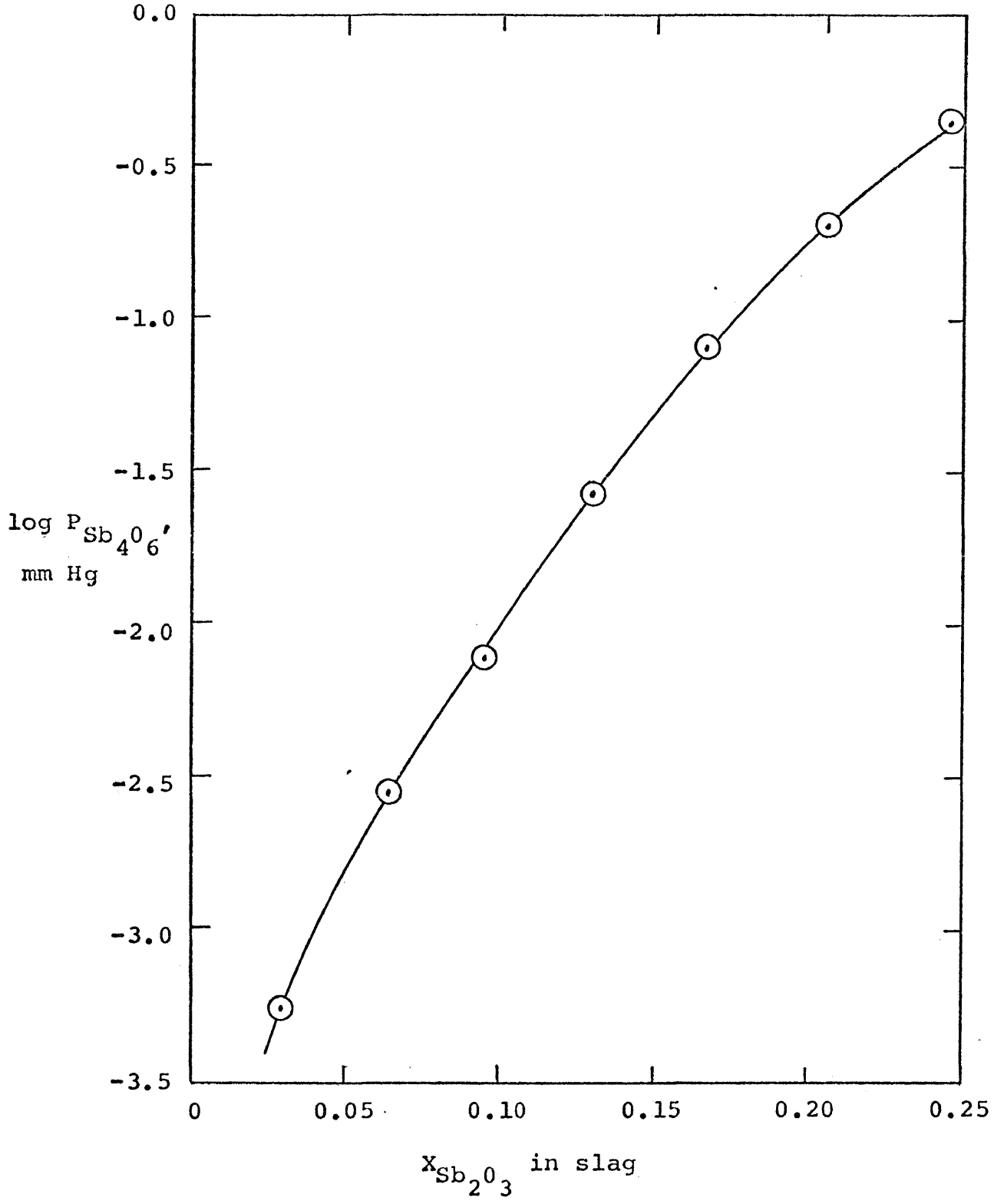

Figure 9. Variation of log $P_{Sb_4O_6}$ above $PbO-SiO_2-Sb_2O_3$ $\left(\frac{PbO}{SiO_2}\right) = 2$ Slags with Composition at 700°C

Table 5. Vapor Pressure of As_4 above Dilute Pb-As Alloys at 703°C

X_{As} in alloy	P_{As_4} above alloy, mm Hg
0.01425	0.00781
0.02794	0.0147
0.03805	0.0351
0.05265	0.0821
0.06901	0.238
0.08575	0.563

Results from Rate-of-Volatile-Oxide-Distillation Experiments in the $PbO-Me_xO_y$ and $PbO-SiO_2-Me_xO_y$ Systems

The results from this portion of the investigation were obtained by chemical analysis of the slags and condensates produced by treating $PbO-Me_xO_y$ and $PbO-SiO_2-Me_xO_y$ slag-forming mixtures under various conditions of temperature and pressure. The slag-phase analyses can be considered to be accurate to ±0.02 wt %.

$PbO-Me_xO_y$ Systems. Artificial lead-softening slags containing approximately 3 wt % As_2O_3-97 wt % PbO, 3 wt % As_2O_3 - 30 wt % Sb_2O_3 - 67 wt % PbO, 30 wt % Sb_2O_3 - 70 wt % PbO, and 3 wt % As_2O_3 - 10 wt % SnO_2 - 30 wt % Sb_2O_3 - 57 wt % PbO were prepared and treated under various conditions of temperature and pressure. All experiments were

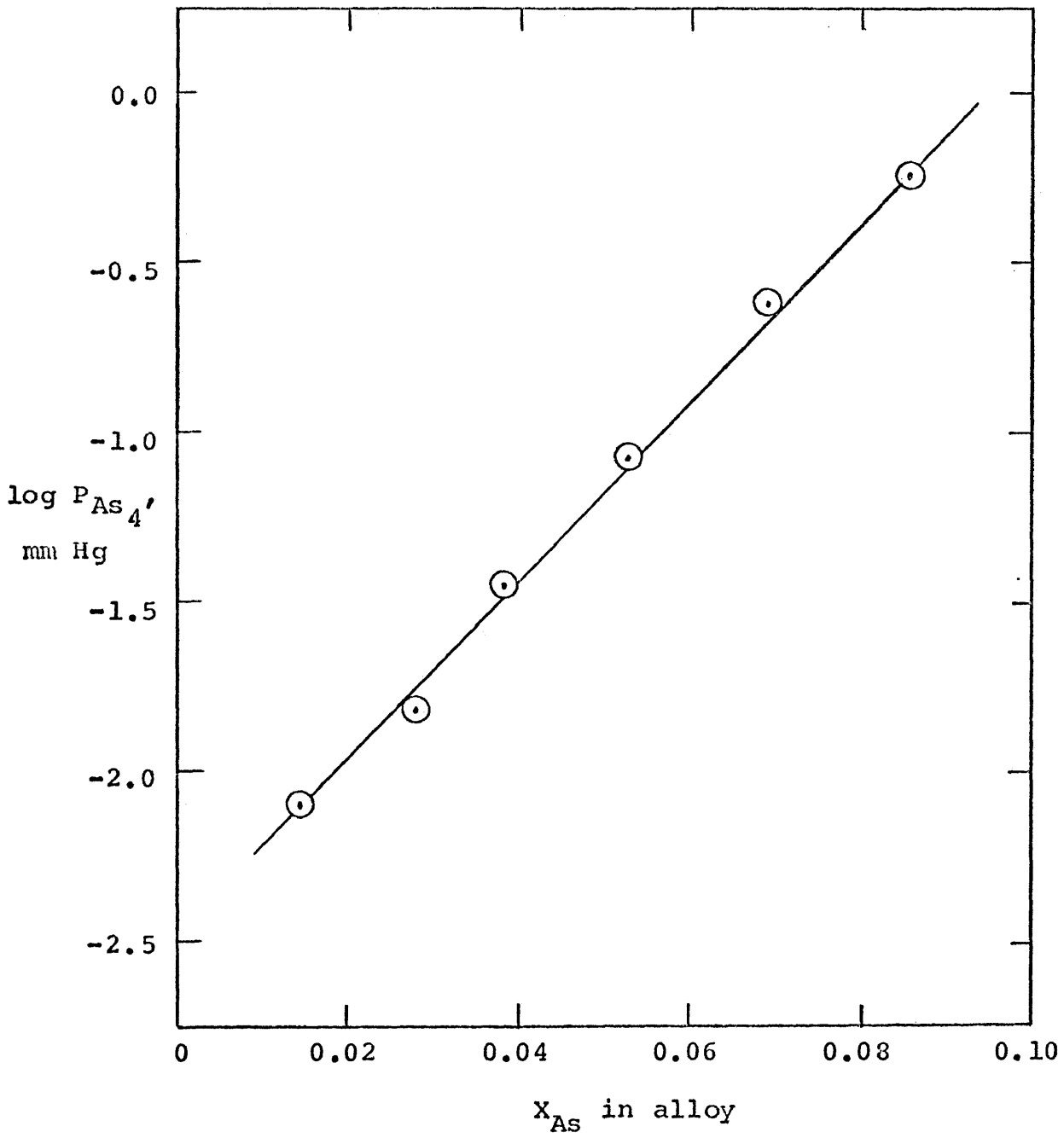

Figure 10. Variation of log P_{As_4} above Dilute As-Pb Alloys with Composition at 703°C

carried out under an argon atmosphere. The results from these experiments are given in Table 6.

PbO-SiO_2-Me_xO_y Systems. Based on the results of vacuum distillation experiments on the above PbO-Me_xO_y systems, a decision was made to limit experimental investigation of silica additions to the PbO-SiO_2-Sb_2O_3 system. Artificial lead-softening slags containing approximately 30 wt % Sb_2O_3 and varying amounts of PbO and SiO_2 were prepared and treated under various conditions of temperature and pressure. All experiments were carried out under an argon atmosphere. The results of these experiments are given in Table 7.

Results from Slag-Metal Equilibrations in the Pb-(PbO+SiO_2+Sb_2O_3) System at 700° and 750°C

Selected slag compositions in the PbO-SiO_2-Sb_2O_3 system were equilibrated with Pb-Sb alloys at 700° and 750°C. The results from this portion of the investigation were obtained from the chemical analysis of the equilibrium metal and slag phases produced in each experiment. The experimental results are shown in Table 8. The metal-phase analyses can be considered to be accurate to wt % Sb = ± 0.002.

Results from X-ray Diffraction Analysis of the Slags and Condensates

The various slags and condensates produced in a portion of the experiments in this investigation were analyzed by

Table 6. Vacuum Distillation of As_2O_3, Sb_2O_3, and SnO_2 from $PbO-Me_xO_y$ Artificial Lead Softening Slags

Test	Temp. °C	Pressure	Time, hr	Wt % Sb_2O_3 in slag	Wt % As_2O_3 in slag	Wt % SnO_2 in slag	Wt of Condensate, gm	Analysis of Condensate
F	750	200μ	0	27.35	--	--		
			1	26.51	--	--		
			3	24.18	--	--		
			4	23.76	--	--	25.4	95.76% Sb_2O_3 2.26% PbO
G	750	atm	0	29.39	--	--		
			1	29.11	--	--		
			2	29.02	--	--		
			3	27.94	--	--		
			4	27.35	--	--	~2	74.87% Sb_2O_3 22.37% PbO
H	500	200μ	0	--	1.80	--		
			4	--	1.32	--	0	none
J	650	200μ	0	--	1.80	--		
			4	--	0.96	--	0	none
P	750	200μ	0	27.47	2.93	--		
			1	25.38	2.88	--		
			2	21.24	2.87	--		
			3	20.13	2.90	--		
			4	19.41	2.85	--	43.9	95.64% Sb_2O_3 3.07% As_2O_3 1.04% PbO

Table 6. Cont'd

Test	Temp. °C	Pressure	Time, hr	Wt % Sb_2O_3 in slag	Wt % As_2O_3 in slag	Wt % SnO_2 in slag	Wt of Condensate, gm	Analysis of Condensate
E	650	200μ	0	27.24	--	--		
			1	24.91	--	--		
			2	24.55	--	--		
			3	22.34	--	--		
			4	19.49	--	--	4.5	92.29% Sb_2O_3 4.42% PbO
U	700	200μ	0	23.32	2.70	12.68		
			2	21.25	2.10	12.42		
			6	21.13	2.07	12.04	26.7	95.28% Sb_2O_3 2.96% As_2O_3 2.34% SnO_2 0.99% PbO
AA	750	200μ	0	26.58	--	--		
			3	22.14	--	--		
			12	18.12	--	--	43.0	98.27% Sb_2O_3 1.72% PbO
BB	850	200μ	1	28.89	--	--		
			3	22.34	--	--		
			6	21.68	--	--		
			9	19.12	--	--		
			12	15.70	--	--	105.7	94.44% Sb_2O_3 5.28% PbO

Table 6. Cont'd

Test	Temp. °C	Pressure	Time, hr	Wt % Sb_2O_3 in slag	Wt % As_2O_3 in slag	Wt % SnO_2 in slag	Wt of Condensate, gm	Analysis of Condensate
CC	800	200μ	0	30.71	2.49	--		
			3	22.00	2.43	--		
			6	20.01	2.53	--		
			9	19.41	3.13	--		
			12	16.94	3.27	--	115.0	95.16% Sb_2O_3 2.58% As_2O_3 1.83% PbO
DD	800	200μ	0	--	2.91	--		
			3	--	2.64	--		
			6	--	2.14	--		
			9	--	1.89	--		
			12	--	1.75	--	8.0	38.66% As_2O_3 54.50% PbO
GG	850	200μ	0	30.49	--	--		
			1	25.81	--	--		
			1.8	24.98	--	--		
			4	22.75	--	--		
			8.5	21.74	--	--		
			12	19.82	--	--	122.0	96.60% Sb_2O_3 6.46% PbO
HH	775	200μ	0	37.02	--	--		
			1	36.09	--	--		
			2	34.25	--	--		
			4	31.37	--	--		
			8	29.30	--	--		
			12	26.06	--	--	105.0	102.70% Sb_2O_3 1.51% PbO

Table 6. Cont'd

Test	Temp. °C	Pressure	Time, hr	Wt % Sb_2O_3 in slag	Wt % As_2O_3 in slag	Wt % SnO_2 in slag	Wt of Condensate, gm	Analysis of Condensate
II	700	200μ	0	35.24	--	--		
			1	34.40	--	--		
			2	33.73	--	--		
			4	30.12	--	--		
			8	27.56	--	--		
			12	24.09	--	--	39.4	102.82% Sb_2O_3
								0.58% PbO
JJ	775	200μ	0	32.14	--	--		
			1	30.69	--	--		
			2	29.80	--	--		
			4	29.13	--	--		
			8	26.22	--	--		
			11	25.35	--	--	65.2	102.58% Sb_2O_3
								1.29% PbO
LL	700	200μ	0	30.04	--	--		
			7.75	23.68	--	--	28.2	102.10% Sb_2O_3
MM	700	200μ	0	22.02	--	--		
			8	21.22	--	--	7.0	99.47% Sb_2O_3
								3.39% PbO
NN	700	200μ	0	26.95	--	--		
			8	7.40	--	--	56.0	102.34% Sb_2O_3
								1.40% PbO

Table 7. Vacuum Distillation of Sb_2O_3 from $PbO-SiO_2-Sb_2O_3$ Artificial Lead Softening Slags

Test	Temp, °C	Pressure	Time, hr	Wt % Sb_2O_3 in slag	Wt % Sb_2O_3 in slag	Wt of Condensate, gm	Analysis of Condensate
RR	750	200μ	0	4.30	32.91		
			1		29.20		
			2		26.74		
			4		23.67		
			8		21.36	80.5	101.27 % Sb_2O_3 1.29 % PbO
SS	850	200μ	0	4.30	33.75		
			1		22.43		
			2.25		20.52		
			4		18.16		
			8		16.04	119.0	97.32 % Sb_2O_3 6.14 % PbO
VV	750	200μ	0	5.60	32.72		
			1		31.49		
			2		27.56		
			4		24.21		
			8		20.91	84.0	100.79 % Sb_2O_3 0.55 % PbO
WW	850	200μ	0	5.60	29.61		
			1		21.01		
			2		17.81		
			4		14.83		
			8		13.81	115.0	100.07 % Sb_2O_3 1.83 % PbO

Table 7. Cont'd.

Test	Temp, °C	Pressure	Time, hr	Wt % SiO_2 in slag	Wt % Sb_2O_3 in slag	Wt of Condensate, gm	Analysis of Condensate
PP	750	200μ	0	8.20	31.20		
			1		24.31		
			2		21.26		
			4		18.23		
			8		15.70	99.0	102.46 % Sb_2O_3 1.02 % PbO
QQ	850	200μ	0	8.20	31.14		
			1.25		18.84		
			2.50		14.90		
			4		14.05		
			8		11.16	134.0	101.63 % Sb_2O_3 1.94 % PbO
XX	750	200μ	0	10.50	31.79		
			1		24.59		
			2		21.66		
			4		17.33		
			8		14.50	91.0	100.30 % Sb_2O_3 0.89 % PbO
YY	850	200μ	0	10.50	30.27		
			1		17.67		
			2		14.13		
			4		11.93		
			8		9.42	126.0	98.75 % Sb_2O_3 1.29 % PbO

Table 7. Cont'd.

Test	Temp, °C	Pressure	Time, hr	Wt % SiO_2 in slag	Wt % Sb_2O_3 in slag	Wt of Condensate, gm	Analysis of Condensate
TT	750	200μ	0	14.70	29.74		
			1.25		27.14		
			2		25.52		
			4		21.78		
			8		19.35	73.0	99.71 % Sb_2O_3 0.50 % PbO
UU	850	200μ	0	14.70	29.08		
			1		21.43		
			2		16.93		
			4		13.85		
			8		12.06	107.0	99.53 % Sb_2O_3 0.75 % PbO
AB	750	25μ	0	8.20	31.88		
		5μ	1		17.46		
		5μ	2		13.77		
		5μ	4		10.17		
		5μ	8		8.54	140.0	95.64 % Sb_2O_3 4.36 % PbO
AC	850	25μ	0	8.20	31.49		
		5μ	1		12.76		
		5μ	2.10		9.29		
		5μ	4		6.74		
		5μ	8		5.35	161.0	95.64 % Sb_2O_3 5.48 % PbO

Table 8. Equilibrium Sb Contents for Pb-Sb Alloys in Contact with $PbO-SiO_2-Sb_2O_3$ Slags at 700° and 750°C

Test	Temperature, °C	PbO/SiO_2 molar ratio	$X_{Sb_2O_3}$ in slag	Wt % Sb in alloy	Remarks
BD	700	1.48	0.0643	0.501	Single-phase slag
BF		2.00	0.0683	0.175	Single-phase slag
BB		2.92	0.0621	0.082	Single-phase slag
BC	750	1.48	0.0587	0.679	Single-phase slag
BE		2.00	0.0648	0.215	Single-phase slag
BA		2.92	0.0658	0.148	Single-phase slag

standard x-ray diffraction techniques to determine the compounds present. The x-ray diffraction analysis data are presented in Table 9, together with the compounds responsible for the diffraction peaks. The x-ray diffraction data for the pure compounds was taken from the ASTM Powder Data Index and are presented in tabular form in Appendix V.

Table 9. X-ray Diffraction Analysis of Slags and Condensates Using Cu K_α Radiation at Room Temperature

Test	2 θ, °	Relative Intensity	Source of Peak
Condensate typical of the type produced where % Sb_2O_3>95%	13.84	w	Sb_2O_3
	27.88	vs	Sb_2O_3
	28.30	m	Sb_2O_3
	28.53	w	Sb_2O_3
	32.19	m	Sb_2O_3
	35.17	w	Sb_2O_3
Condensate typical of the type produced where 90% %Sb_2O_3<95%	13.84	w	Sb_2O_3
	27.88	vs	Sb_2O_3
	28.30	m	Sb_2O_3
	28.53	w	Sb_2O_3
	28.67	vw	PbO
	31.35	w	Pb
	32.19	m	Sb_2O_3
	35.17	w	Sb_2O_3
Condensate Test DD	13.91	vs	As_2O_3
	22.81	vw	As_2O_3
	28.02	vs	As_2O_3
	28.75	m	PbO
	31.35	vs	Pb
	32.40	m	As_2O_3
	35.41	s	As_2O_3
	36.35	m	Pb

Table 9. Cont'd

Test	2 θ, °	Relative Intensity	Source of Peak
Slag - Test F	27.52	m	($PbO \cdot Sb_2O_3$)*
	28.30	vs	PbO, Sb_2O_3
	29.38	w	($PbO \cdot Sb_2O_3$), PbO
	31.30	w	PbO, Pb
	32.58	s	PbO
	33.29	w	($PbO \cdot Sb_2O_3$)
	34.10	vw	($PbO \cdot Sb_2O_3$)
	35.40	vw	PbO
	36.21	vw	PbO
Slag - Test G	27.74	m	($PbO \cdot Sb_2O_3$)
	28.20	vs	Pbo, Sb_2O_3
	29.48	w	($PbO \cdot Sb_2O_3$), PbO
	29.83	vw	- - -
	31.37	vw	PbO, Pb
	32.53	s	PbO
	33.48	w	($PbO \cdot Sb_2O_3$)
	36.14	vw	PbO
Slag - Test P	27.65	m	($PbO \cdot Sb_2O_3$), As_2O_3
	28.35	vs	PbO, Sb_2O_3
	29.31	vw	($PbO \cdot Sb_2O_3$), PbO
	29.72	vw	($PbO \cdot Sb_2O_3$)
	30.02	vw	- - -
	31.28	w	PbO, Pb
	32.67	s	PbO, As_2O_3
	33.38	w	($PbO \cdot Sb_2O_3$)
	34.00	vw	($PbO \cdot Sb_2O_3$)
	35.43	vw	PbO, As_2O_3
Slag - Test E	27.78	s	($PbO \cdot Sb_2O_3$)
	28.32	vs	PbO, Sb_2O_3
	29.59	m	($PbO \cdot Sb_2O_3$)
	30.50	w	PbO
	31.59	m	PbO, Pb
	32.80	m	PbO
	34.29	m	($PbO \cdot Sb_2O_3$)
	36.32	w	PbO

*No standard pattern available in ASTM Powder Data Index, see Appendix VI.

Table 9. Cont'd

Test	2 θ, °	Relative Intensity	Source of Peak
Slag - Test U	26.60	vw	SnO_2
	28.27	s	PbO, Sb_2O_3
	29.38	vw	($PbO \cdot Sb_2O_3$), PbO
	31.38	m	PbO, Pb
	32.88	m	PbO
	34.02	m	($PbO \cdot Sb_2O_3$)
	36.32	w	PbO
Slag - Test AA	27.45	vw	($PbO \cdot Sb_2O_3$)
	27.97	s	- - -
	29.67	vs	($PbO \cdot Sb_2O_3$), PbO
	31.42	w	PbO, Pb
	33.67	m	($PbO \cdot Sb_2O_3$)
	34.40	m	($PbO \cdot Sb_2O_3$)
	36.69	vw	PbO
Slag - Test BB	27.62	s	($PbO \cdot Sb_2O_3$)
	28.31	s	PbO, Sb_2O_3
	29.58	m	($PbO \cdot Sb_2O_3$), PbO
	30.30	w	PbO
	31.40	w	PbO, Pb
	32.10	vw	Sb_2O_3, ($PbO \cdot Sb_2O_3$)
	32.87	m	PbO
	33.30	w	($PbO \cdot Sb_2O_3$)
	34.29	w	($PbO \cdot Sb_2O_3$)
	35.58	w	PbO
	36.40	w	PbO
Slag - Test CC	28.22	vw	PbO, Sb_2O_3
	28.62	vs	PbO, Sb_2O_3
	29.73	w	($PbO \cdot Sb_2O_3$)
	30.38	vw	PbO
	31.50	vw	PbO, Pb
	33.17	m	Sb_2O_3, ($PbO \cdot Sb_2O_3$)
	34.50	vw	($PbO \cdot Sb_2O_3$)
	35.75	w	PbO
Slag - Test DD	28.12	s	- - -
	28.88	s	PbO
	29.27	w	PbO
	30.28	m	PbO
	31.17	m	Pb
	31.40	w	- - -
	32.00	w	PbO
	33.45	m	- - -
	35.70		PbO

Table 9. Cont'd

Test	2 θ, °	Relative Intensity	Source of Peak
Slag - Test GG	26.80	vw	($PbO \cdot Sb_2O_3$)
	27.60	s	($PbO \cdot Sb_2O_3$)
	28.33	vs	PbO, Sb_2O_3
	29.38	w	($PbO \cdot Sb_2O_3$)
	30.10	vw	PbO
	31.30	w	Pb
	32.87	m	PbO
	33.20	w	($PbO \cdot Sb_2O_3$)
	34.10	vw	($PbO \cdot Sb_2O_3$)
	35.50	vw	PbO
	36.28	vw	($PbO \cdot Sb_2O_3$)
Slag typical of Tests HH, II, JJ, LL, MM, and NN	27.77	m	($PbO \cdot Sb_2O_3$)
	28.30	vs	PbO, Sb_2O_3
	31.40	variable	Pb
	32.80	m	PbO
	33.30	w	($PbO \cdot Sb_2O_3$)
	35.60	vw	PbO
	36.38	vw	($PbO \cdot Sb_2O_3$)
Slag - Tests RR and SS	28.08	s	Sb_2O_3
	28.58	vs	γ-$4PbO \cdot SiO_2$
	29.60	w	γ-$4PbO \cdot SiO_2$
	30.00	w	γ-$4PbO \cdot SiO_2$
	30.81	w	γ-$4PbO \cdot SiO_2$
	31.50	m	γ-$4PbO \cdot SiO_2$
	32.54	w	Sb_2O_3
	33.18	m	γ-$4PbO \cdot SiO_2$
	33.50	w	γ-$4PbO \cdot SiO_2$
	36.50	vw	PbO
Slag - Tests VV and WW	21.67	w	$2\ PbO \cdot SiO_2$
	23.12	w	$2\ PbO \cdot SiO_2$
	25.72	w	$2\ PbO \cdot SiO_2$
	28.50	vs	γ-$4PbO \cdot SiO_2$, Sb_2O_3, $2PbO \cdot SiO_2$
	29.72	m	γ-$4PbO \cdot SiO_2$, $2PbO \cdot SiO_2$
	30.44	m	γ-$4PbO \cdot SiO_2$, $2PbO \cdot SiO_2$
	31.60	m	γ-$4PbO \cdot SiO_2$
	31.80	m	$2PbO \cdot SiO_2$
	32.58	m	γ-$4PbO \cdot SiO_2$, Sb_2O_3
	33.05	m	γ-$4PbO \cdot SiO_2$, Sb_2O_3
	33.72	m	γ-$4PbO \cdot SiO_2$, Sb_2O_3
	34.40	m	$2PbO \cdot SiO_2$

Table 9. Cont'd

Test	2 θ, °	Relative Intensity	Source of Peak
Slag - Tests PP, QQ, AB, and AC	21.43	w	$2PbO \cdot SiO_2$
	22.95	w	$2PbO \cdot SiO_2$
	25.60	w	$2PbO \cdot SiO_2$
	28.20	vs	$2PbO \cdot SiO_2$, Sb_2O_3
	29.63	w	$2PbO \cdot SiO_2$
	30.18	m	$2PbO \cdot SiO_2$
	31.58	m	$2PbO \cdot SiO_2$
	32.60	variable	Sb_2O_3
Slag - Test XX and YY	20.83	w	$PbO \cdot SiO_2$
	23.92	w	- - -
	25.19	w	$PbO \cdot SiO_2$
	27.27	m	$PbO \cdot SiO_2$
	27.61	s	$PbO \cdot SiO_2$
	28.30	m	$2PbO \cdot SiO_2$, Sb_2O_3
	29.25	m	$2PbO \cdot SiO_2$, $PbO \cdot SiO_2$
	30.10	m	$2PbO \cdot SiO_2$, $PbO \cdot SiO_2$
	31.10	s	$PbO \cdot SiO_2$
	31.40	vs	$PbO \cdot SiO_2$
	31.85	s	$PbO \cdot SiO_2$
Slag - Tests TT and UU	These slags produced diffraction patterns typical of vitreous materials. They consisted of one broad, low peak extending approximately from 24° to 34° 2θ.		
Slag - Tests BA and BB	27.83	m	$2PbO \cdot SiO_2$
	28.71	w	$2PbO \cdot SiO_2$
	29.91	w	$2PbO \cdot SiO_2$
	31.33	w	$2PbO \cdot SiO_2$
	32.17	w	$2PbO \cdot SiO_2$
	The diffraction peaks were nearly masked by a broad, low peak extending approximately from 24° to 34° 2θ indicating non-crystallization of $PbO \cdot SiO_2$		

Table 9. Cont'd

Test	2 θ, °	Relative Intensity	Source of Peak
Slag - Tests BC and BD	21.32	w	$2PbO \cdot SiO_2$
	22.87	w	- - -
	24.00	w	$2PbO \cdot SiO_2$
	25.50	w	$2PbO \cdot SiO_2$
	27.82	vs	$2PbO \cdot SiO_2$, Sb_2O_3
	28.22	vs	γ-$4PbO \cdot SiO_2$
	29.50	s	γ-$4PbO \cdot SiO_2$, $2PbO \cdot SiO_2$
	30.02	m	γ-$4PbO \cdot SiO_2$, $2PbO \cdot SiO_2$
	31.50	w	$2PbO \cdot SiO_2$
	32.27	w	- - -
	32.75	w	γ-$4PbO \cdot SiO_2$
	33.40	w	- - -
	33.80	w	γ-$4PbO \cdot SiO_2$
	34.77	w	$2PbO \cdot SiO_2$
Slag - Tests BE and BF	21.12	w	$2PbO \cdot SiO_2$
	22.80	w	- - -
	24.03	w	$2PbO \cdot SiO_2$
	25.48	w	$2PbO \cdot SiO_2$
	27.75	w	$2PbO \cdot SiO_2$, Sb_2O_3
	28.00	m	- - -
	28.74	vs	$2PbO \cdot SiO_2$
	29.70	w	$2PbO \cdot SiO_2$
	31.28	w	$2PbO \cdot SiO_2$
	31.80	w	$2PbO \cdot SiO_2$
	32.40	w	- - -
	33.27	w	- - -
	34.75	w	$2PbO \cdot SiO_2$

CALCULATIONS AND INTERPRETATION OF RESULTS

The discussion of the experimental results obtained in this investigation is presented in six sections: 1) the use of the transportation technique for the measurement of vapor pressures, 2) the vapor pressure of Sb_2O_3 in the range from 422° to 599°C, 3) the evaluation of vapor-pressure data for the determination of thermodynamic data for PbO-Sb_2O_3 and PbO-SiO_2-Sb_2O_3 slags at 700°C, 4) the application of vacuum techniques to the removal of As_2O_3, Sb_2O_3, and SnO_2 from lead-softening slags, 5) selected slag-metal equilibria in the PbO-SiO_2-Sb_2O_3 system, and 6) the vapor pressure of As_4 above dilute Pb-As alloys at 703°C.

Use of the Transportation Technique for the Measurement of Vapor Pressures

The transportation technique, or inert-gas saturation method, for the measurement of vapor pressures has been in general use for many years. The published literature contains accounts of a great many experimental investigations using this technique, investigations which are far too numerous to list here. In the past, the design of the

apparatus and the size of the sample to be studied have been largely the choice of the individual worker. Not until the work of Alcock and Hooper (1959, p. 325-340) has there been any attempt to establish criteria by which the accuracy and reliability of the method could be estimated.

The design of the experimental apparatus used in this investigation is based largely on the apparatus used by Alcock and Hooper. Certain modifications were made in the basic design to provide more thorough carrier-gas purification and to provide greater ease in sample handling. The sample geometry is essentially the same as that used by Alcock and Hooper. Figure 3, p. 13, illustrates the conditions under which the experiments were made. A sample, weighing between 1 and 5 gm, is held in a small combustion boat which rests in a recess in a plug device. The recess in the plug was machined to conform to the outside contours of the combustion boat in order to reduce the dead volume between the boat and the plug to a minimum. For reasons to be explained later, the sample must be made to fill the space between the boat and the reaction tube as completely as possible. The plug containing the sample is then placed in the open end of the reaction tube. It is necessary to provide as tight a seal as possible between the plug and the reaction tube. Careful lapping of the inside surface of the reaction tube can result in a nearly air-tight seal

at room temperature. Small channels were engraved on the top surface of the up-stream end of the plug to provide an entrance to the sample chamber for the carrier gas. A single channel provided the necessary exit at the other end of the plug.

When the above precautions are taken, it can be reasonably assumed that the carrier gas passes over the sample to be studied and not around the sides and/or bottom of the plug. In passing over the sample, the carrier gas accumulates the vapor of the sample and carries it out of the reaction system. The amount of volatile matter removed from the sample is determined as the loss in weight of the sample and is normalized against a unit volume of carrier gas. By plotting the normalized weight-losses measured at different flow rates against flow rate, a curve similar to that shown in Figure 11 is obtained.

The curve shown in Figure 11 represents a somewhat idealized case. It can be readily divided into three separate sections whose slope is controlled by three different phenomena. Section I shows a smooth decrease in the normalized weight loss from very small carrier-gas flow rates up to some given value, say f_1. Section II shows that the normalized weight-loss remains constant at all values of carrier-gas flow rate between the limits f_1 and f_2. This portion of the curve corresponds to the true

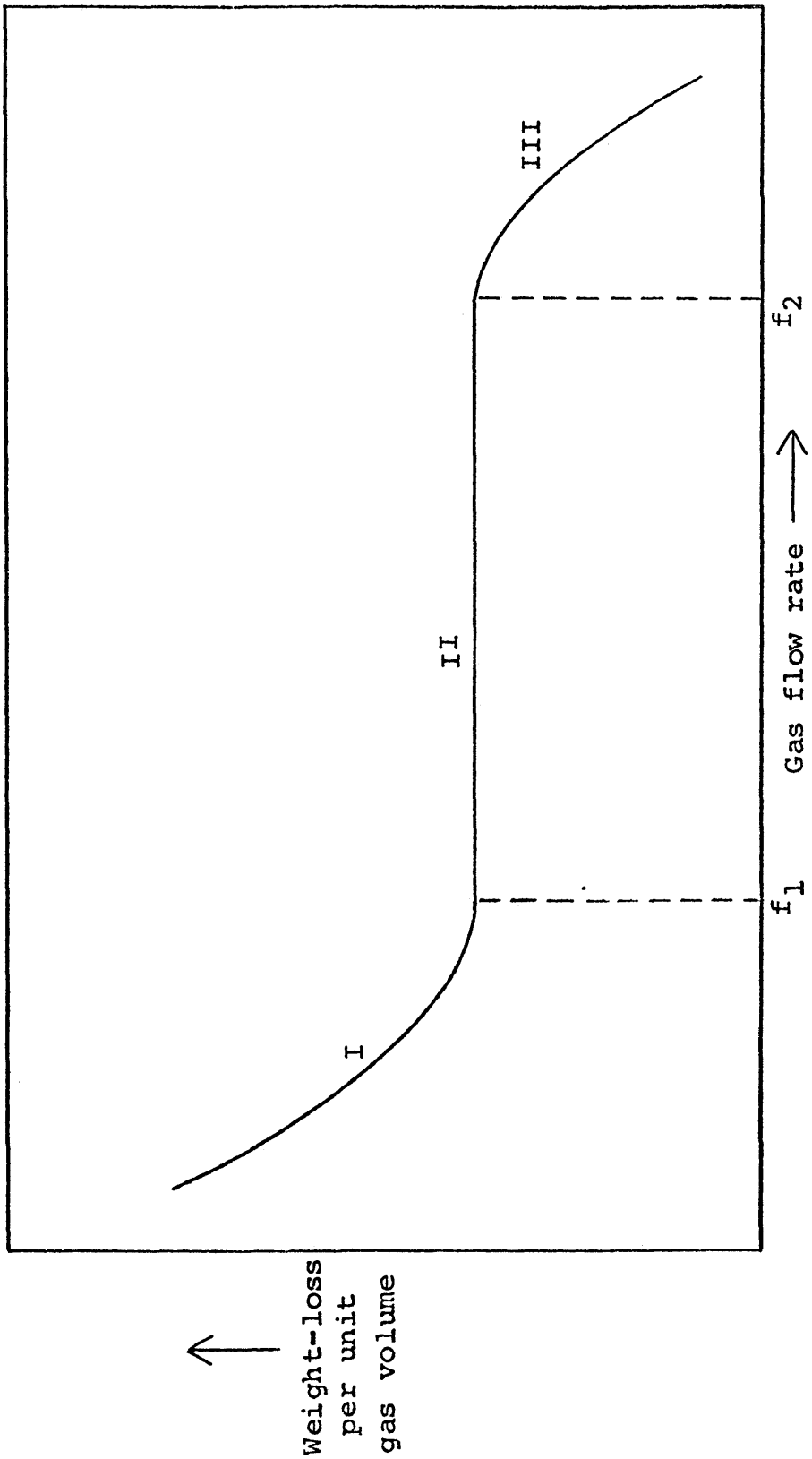

Figure 11. Schematic Weight-loss Versus Flow Rate Curve

vapor pressure of the sample. Section III shows an increasingly rapid decrease in the normalized weight-loss as the carrier-gas flow rate is increased above the value represented by the point f_2 in Figure 11.

The cause of the abnormally high weight losses at low flow rates can be thought of as being three-fold: 1) a large difference in molecular weight between the volatile species and the inert carrier gas provides for a tendency for the various molecular species to segregate from one another, 2) the existing thermal gradients on either side of the sample will result in a mass flux of one of the vapor species relative to the other as a result of thermal diffusion, and 3) the concentration gradients set up on either side of the sample will give rise to a diffusive mass flux of one of the vapor species relative to the other.

In the first case, actual physical segregation of the vapor species due to differences in molecular weight can be neglected for two reasons: 1) the carrier gas is moving over the sample with a relatively high velocity so that the retention time above the sample is small and 2) obstacles such as the uneven surface of solid samples, or artificial baffles in the case of liquid samples, serve to provide a maximum amount of turbulence in the gas phase.

Thermal diffusion, as a rule, provides for only a minimal degree of vapor segregation unless the thermal

gradient is quite large. Such large differences in temperature in the vicinity of the sample are not to be expected under normal conditions. In order to illustrate the magnitude of this contribution, a calculation will be made for the binary vapor system argon-Sb_4O_6.

A temperature gradient in the system will give rise to a mass flux of Sb_4O_6 given by:

$$j^{(T)}_{Sb_4O_6,\,z} = -\frac{c^2}{\rho} M_{Sb_4O_6} M_A D_{Sb_4O_6-A} \frac{k_T}{T} \frac{dT}{dz} \qquad (1)$$

where: $j^{(T)}_{Sb_4O_6,\,z}$ = mass flux of Sb_4O_6, gm/sec-cm^2

c = total molar concentration, mols/cm^3

M_i = molecular weight of species i, gm/mol

$D_{Sb_4O_6,A}$ = binary diffusivity for system Sb_4O_6-A, cm^2/sec

k_T = thermal diffusion ratio

T = temperature, ^oK

ρ = fluid density, gm/cm^3

dT/dz = temperature gradient, ^oK/cm

This mass flux will set up a concentration gradient which will result in an opposing mass flux:

$$j^{(x)}_{Sb_4O_6,\,z} = \frac{c^2}{\rho} M_{Sb_4O_6} M_A D_{Sb_4O_6-A} \frac{dx_{Sb_4O_6}}{dz} \qquad (2)$$

In this case $dx_{Sb_2O_3}/dz$ refers to the concentration gradient expressed in mols/cm. When steady-state conditions have been attained, the two opposing mass fluxes will

nullify one another:

$$0 = j^{(t)}_{Sb_4O_6,\ z} + j^{(x)}_{Sb_4O_6,\ z} = \frac{c^2}{\rho} M_{Sb_4O_6} M_A D_{Sb_4O_6-A} \left[\frac{dx_{Sb_4O_6}}{dz} + \frac{k_T}{T} \frac{dT}{dz} \right] \tag{3}$$

from which,

$$dx_{Sb_4O_6} = - \frac{k_T}{T} dT \tag{4}$$

From Equation (4) it is seen that, when k_T is positive, Sb_4O_6 will move towards increasingly lower temperatures; and when k_T is negative, Sb_4O_6 will move towards increasingly higher temperatures. In order to integrate Equation (4) it will be assumed that k_T is constant with composition if the mass flux is small. Also, since k_T varies in a complex manner with temperature, it will be assumed to be independent of temperature for small temperature gradients. By use of these assumptions, then, Equation (4) can be integrated as follows:

$$\int_{X'_{Sb_4O_6}}^{X''_{Sb_4O_6}} dX_{Sb_4O_6} = -k_T \int_{T_1}^{T_2} \frac{dT}{T} \tag{5}$$

from which,

$$X''_{Sb_4O_6} - X'_{Sb_4O_6} = k_T \ln \frac{T_2}{T_1} \tag{6}$$

Before Equation (6) can be solved, it is necessary to evaluate the thermal diffusion ratio, k_T. Gillespie (1939, p. 530-5) has derived an expression for k_T in terms of the square roots of the molecular weights, m_i, and the mole fractions, X_i, of the species in a binary system with the result that:

$$k_T = \frac{\frac{1}{2}\left(\frac{M_A}{M_{Sb_4O_6}} - 1\right) X_A}{1 + \frac{M_A}{M_{Sb_4O_6}} \cdot \frac{X_A}{X_{Sb_4O_6}}} \qquad (7)$$

For purposes of calculation, the mole fraction of Sb_4O_6 is chosen as $X_{Sb_4O_6} = 1.6 \times 10^{-3}$, and the total pressure of the system is taken to be 1 atm. This value for $X_{Sb_4O_6}$ corresponds to a partial pressure of Sb_4O_6 of 1 mm Hg. Substitution of this data together with the appropriate molecular weights into Equation (7) yields $k_T = -2.8 \times 10^{-3}$. Since k_T is negative, it is readily seen from Equation (6) that Sb_4O_6 will tend to diffuse to a region of higher temperature under the influence of a temperature gradient. Thermal diffusion, then, cannot be responsible for the abnormally high weight losses observed at low flow rates. The negative value of k_T would tend to cause abnormally low weight losses rather than higher.

The significance of this back diffusion, however, is of little importance. At a mean temperature of 700°C, a

temperature gradient of 2° to 3°C from the sample to the mouth of the reaction tube would result in a concentration difference, $X''_{Sb_4O_6} - X'_{Sb_4O_6}$, of only 8.4×10^{-6} mole fraction, which is less than 0.1% of $X_{Sb_4O_6}$.

The third possible explanation for the abnormally high weight losses observed at low flow rates involves the concentration gradients established in the vicinity of the sample. If the gas phase is assumed to be stationary, it can be reasoned that very steep concentration gradients exist between the space immediately above the sample and the gas film surrounding the plug at the beginning of the experiment. Before this mass flux is calculated by means of Equation (2), it is necessary to estimate the binary diffusivity, $D_{Sb_4O_6}$, for the system Sb_4O_6-argon.

Several methods are available for estimating binary diffusivities. The most accurate method is based on the Chapman-Enskog kinetic theory. The resulting equation can be represented as follows:

$$D_{Sb_4O_6\text{-}A} = 1.858 \times 10^{-3} \sqrt{\frac{T^3\left(\frac{1}{M_{Sb_4O_6}} + \frac{1}{M_A}\right)}{p\,\sigma^2_{Sb_4O_6\text{-}A}\,\Omega_{D,Sb_4O_6\text{-}A}}} \qquad (8)$$

where: p = pressure of the system, atm

$\sigma_{Sb_4O_6\text{-}A}$ = collision diameter, Å

$\Omega_{D,Sb_4O_6\text{-}A}$ = dimensionless function of the temperature and of the intermolecular potential field for one molecule of each species

The collision diameter, $\sigma_{Sb_4O_6\text{-}A}$, must be approximated by the sum of the molecular radii. Norman and Staley (1964, p. 1503-4) have shown that Sb_4O_6 is composed of tetrahedrally-located Sb atoms, with each oxygen atom associated with an edge of the tetrahedron. The Sb-Sb distance is 3.61 Å and will be used as the approximate molecular diameter. The atomic diameter of argon, as calculated from the Van der Waal's equation, is 2.94 Å. By the assumption that the molecules behave as elastic, hard spheres, $\Omega_{D,Sb_4O_6\text{-}A}$ can be set equal to unity.

Substitution of the appropriate values into Equation (8) using p = 1 atm and T = 973°K yields:

$$D_{Sb_4O_6\text{-}A} = 0.861 \text{ cm}^2/\text{sec}$$

Therefore, using the above values for $X_{Sb_4O_6}$, $M_{Sb_4O_6}$, M_A, and $D_{Sb_4O_6\text{-}A}$ Equation (2) becomes,

$$j^{(x)}_{Sb_4O_6,z} = -6.18 \times 10^{-3} \frac{dx_{Sb_4O_6}}{dz} \qquad (9)$$

Integrating Equation (9) over the limits $X''_{Sb_4O_6} = 0$ to $X'_{Sb_4O_6} = 2 \times 10^{-3}$ and z" = 0.25 cm to Z' = 0.0 cm yields 4.94×10^{-5} gm/sec-cm^2, initially. This mass flux will of course decrease with time towards some steady-state value. If the total cross-sectional area between the plug and the reaction tube is taken to be 0.2 cm^2, the mass flux due to diffusion can be shown to be as much as 20% of the weight

losses observed in experiments made with a carrier-gas flow rate of 100 cm^3/min where $p_{Sb_4O_6}$ = 1 mm Hg. At the point represented by flow rate f_1, in Figure 11, the carrier gas is flowing over the sample at the minimum rate capable of sweeping away all of the diffusional mass flux of Sb_4O_6 produced by the zero-time concentration gradient. By use of the above calculated flux, this minimum flow rate is calculated to be 50 cm^3/min. The actual flow rate at which the normalized weight-loss versus flow-rate curve becomes horizontal for $p_{Sb_4O_6}$ approximately equal to 1 mm Hg is slightly above this value for the experiments performed in this investigation.

Considering the assumptions and approximations made in calculating the diffusional mass flux of Sb_4O_6, it would appear that this flux is of the correct order of magnitude to cause the abnormally high normalized weight losses observed at low carrier gas flow rate.

Referring again to Figure 11, it is seen that Section II of the curve has zero slope. This condition is explained by the fact that at all flow rates between f_1 and f_2 the carrier gas is able to become saturated with the volatile species from the sample. The diffusional mass flux of the volatile species is not sufficiently rapid to affect the removal of these species from the reaction zone by the rapidly moving carrier-gas stream.

Section III of the curve in Figure 11 is due to the carrier gas moving at too rapid a rate over the sample to allow for complete saturation. As the carrier gas flow rate increases from f_2, the degree of undersaturation increases and the normalized weight-loss of the sample falls to lower values.

As mentioned earlier, the curve shown in Figure 11 represents a somewhat idealized case. In order to obtain a curve of the required form, i.e. a curve showing the normalized sample weight-loss to be independent of carrier-gas flow rate over a range of flow rates, it is necessary to reduce the dead volume above the sample to a minimum. When this condition is not met, the horizontal segment of the normalized weight-loss versus flow-rate curve will either assume a finite slope or disappear altogether. Figure 12 illustrates this phenomenon for 2 series of experiments made on pure Sb_2O_3at 514°C. In one case, the sample extended above the top of the combustion boat to insure a small dead volume in the reaction system and a curve of the desired form was obtained.

For the experimental results represented by the second curve, the sample extended to slightly above the center of the combustion boat, resulting in a relatively large dead volume above the sample. It can readily be seen that the curve shows a smoothly decreasing normalized weight-loss

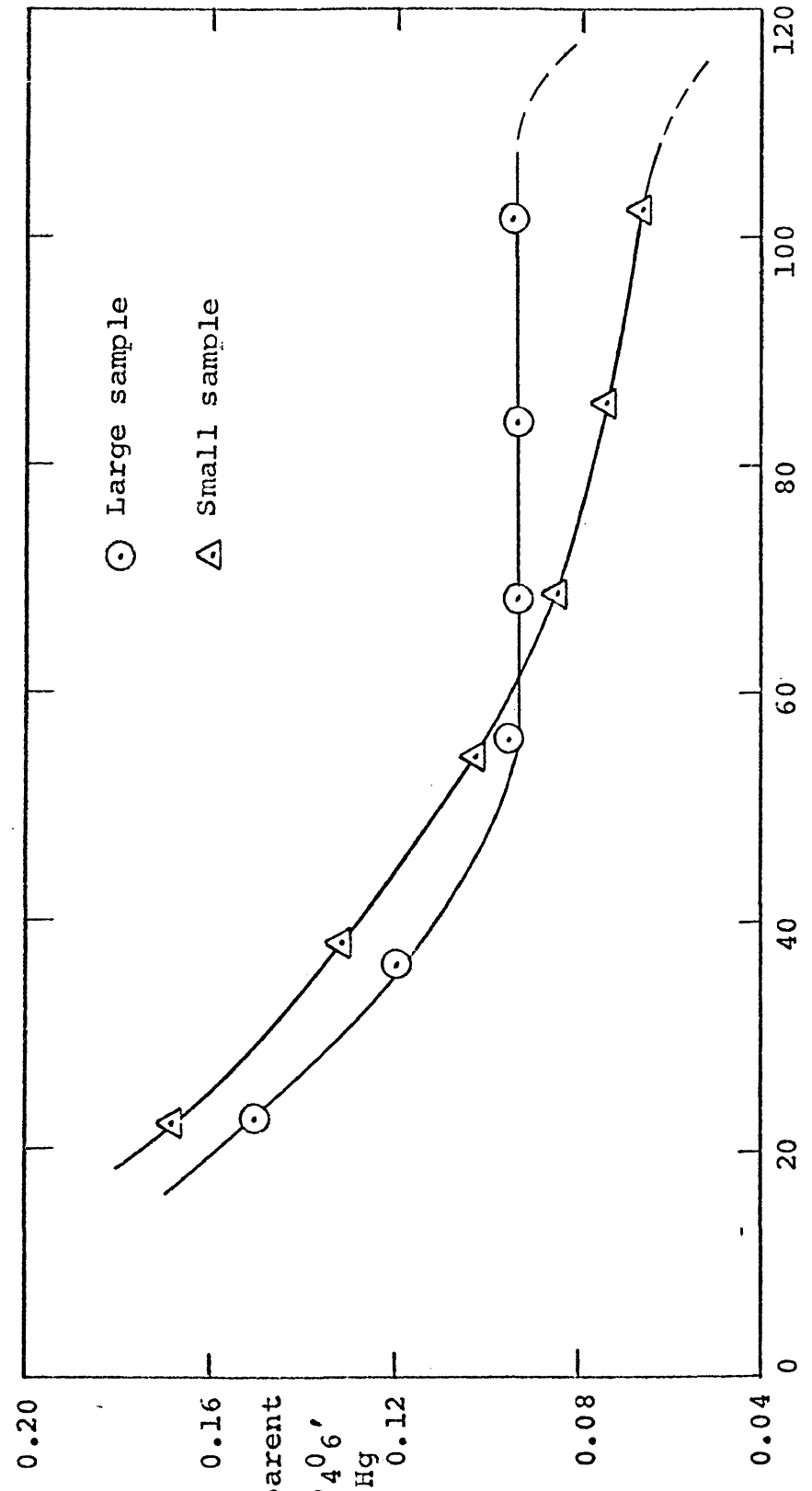

Figure 12. Apparent $P_{Sb_4O_6}$ above Cubic Sb_2O_3 as a Function of Carrier-Gas Flow Rate at 514°C

with increasing carrier-gas flow rate over the entire range of flow rates studied. The true vapor pressure of the sample cannot even be estimated from these data.

In order to provide a check on the accuracy and reliability of the transportation apparatus constructed for this investigation, a brief vapor-pressure study was first made on a well known system. Cadmium was chosen for the reference study for three primary reasons: 1) the literature contains a large number of vapor-pressure studies on Cd which are in good agreement with one another; 2) Cd possesses a vapor pressure in the range expected in the other studies reported in this investigation (10^{-3} - 10^{-6} atm); and, 3) Cd is readily available in very pure form.

A total of four vapor-pressure measurements were made on Cd in this investigation; two for the vapor pressure above solid Cd, and two for the vapor pressure above liquid Cd. The results of these measurements are shown graphically in Figures 13 and 14. Two factors concerning the shape of these curves are readily apparent. Firstly, the length of the horizontal portion of the curves decreases with an increase in the absolute magnitude of the vapor pressure. This is to be expected since saturation of the gas phase at high flow rates becomes more difficult as the total mass of volatile species increases. The second observation to be made is that the horizontal portion of the curves shifts to

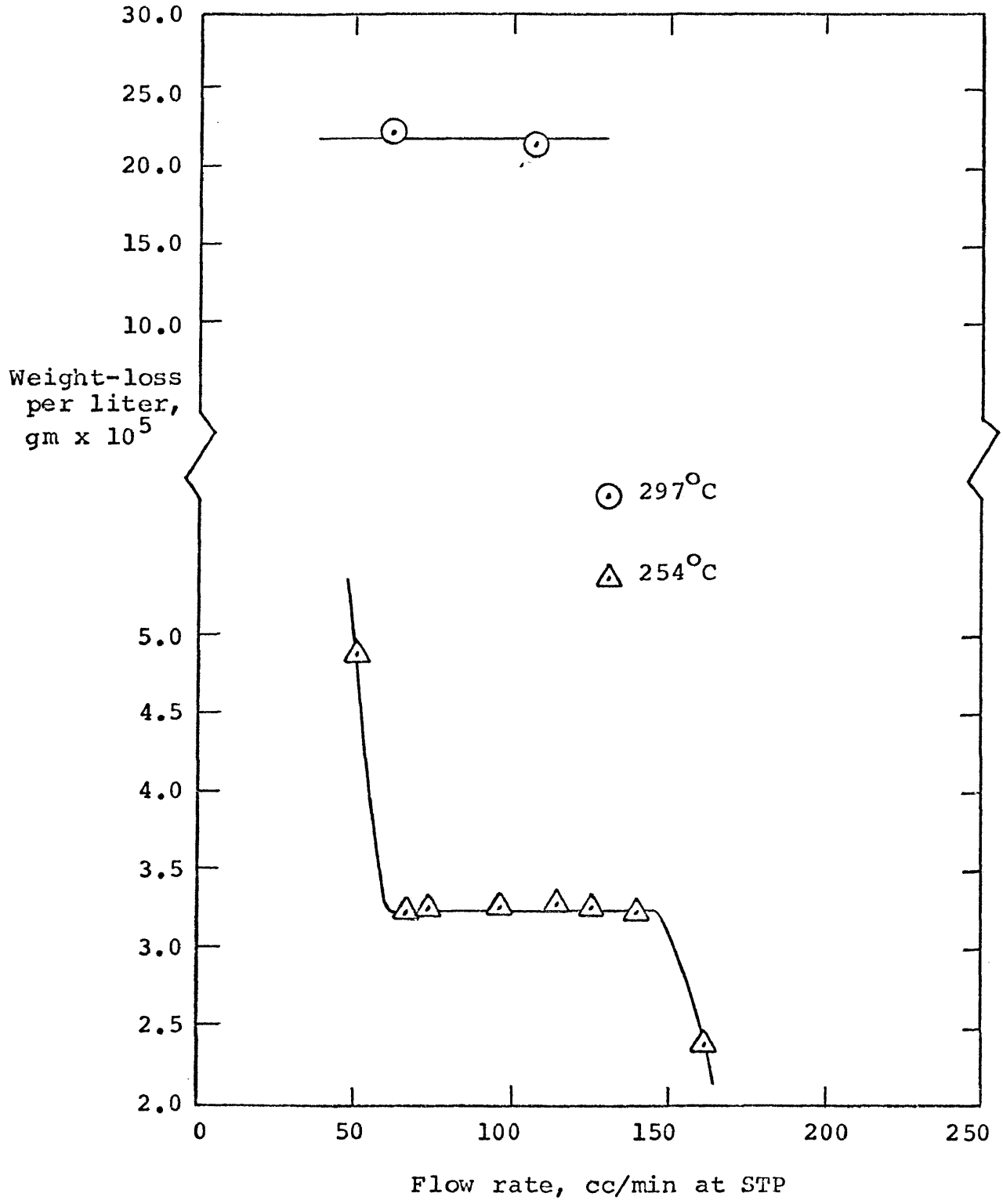

Figure 13. Weight of Cd Lost per Liter of Carrier Gas as a Function of Flow Rate at 254° and 297°C

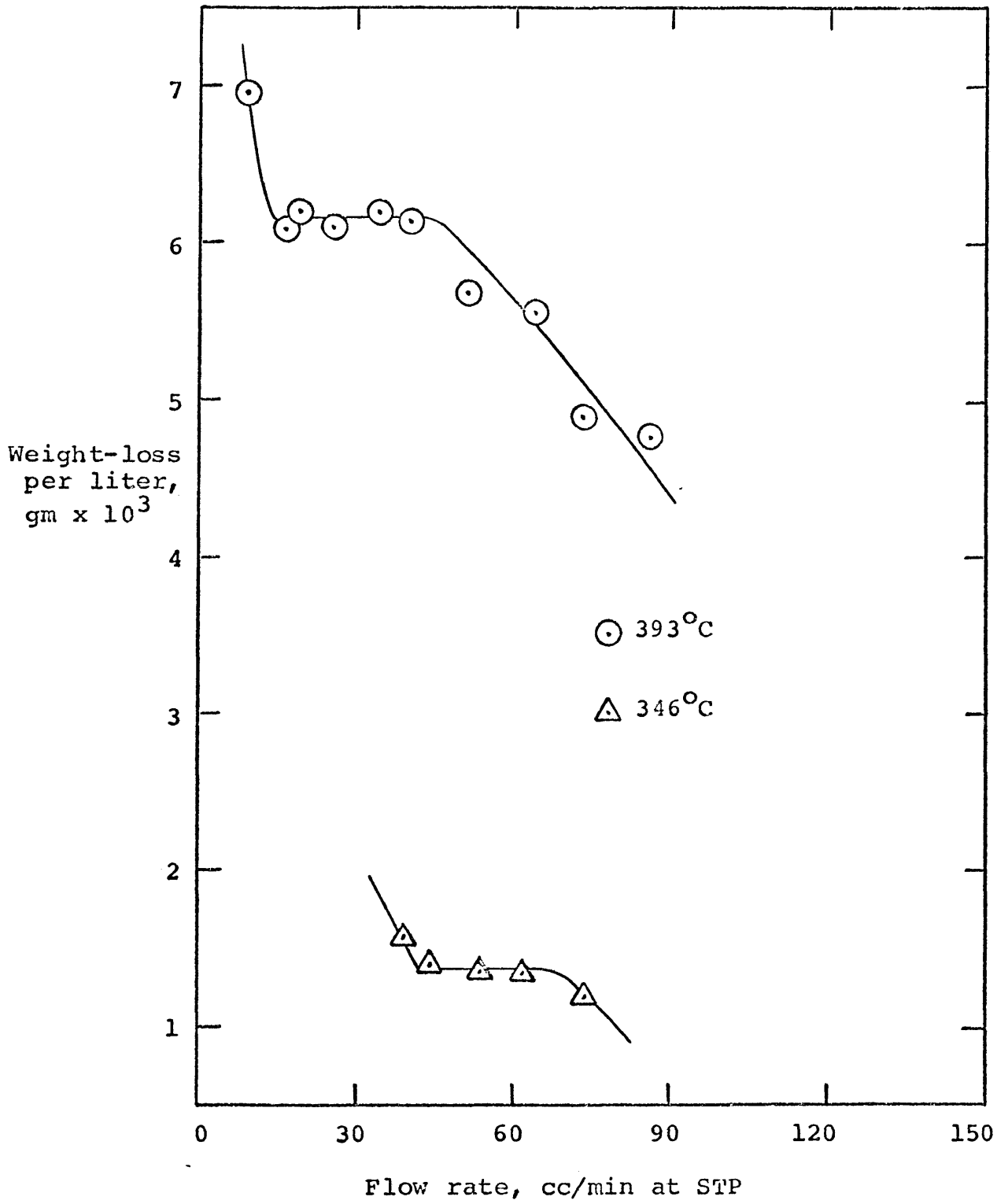

Figure 14. Weight of Cd lost per Liter of Carrier Gas as a Function of Flow Rate at 346° and 393°C

lower flow rates as the magnitude of the vapor pressure increases. This type of behavior is explained by the fact that the effects of mass diffusion are more easily overcome at higher mass densities of the volatile species.

The vapor pressures of Cd at various selected temperatures, as calculated from the data of Figures 13 and 14, are presented in Figure 15 together with a portion of the literature data for the vapor pressure of Cd. All available data have not been included in Figure 15 for the purpose of clarity. The agreement for the vapor pressure of Cd at temperatures above the melting point of Cd with the literature is seen to be quite good. The results obtained in this investigation at temperatures below the melting point of Cd agree favorably with those tabulated by Kubaschewski and Evans (1958, p. 328) but are somewhat lower than the values tabulated by Elliot and Gleiser (1960, p. 29-30).

In the experiments performed in this investigation at temperatures below the melting point of Cd, a tarnish of CdO was formed on the surface of the samples. This thin oxide film can reduce the value of the apparent vapor pressure in either or both of two ways: 1) by providing a barrier to the sublimation of Cd from the surface of the sample; and, 2) by adding oxygen to the sample, thereby reducing the observed weight loss. No oxidation was

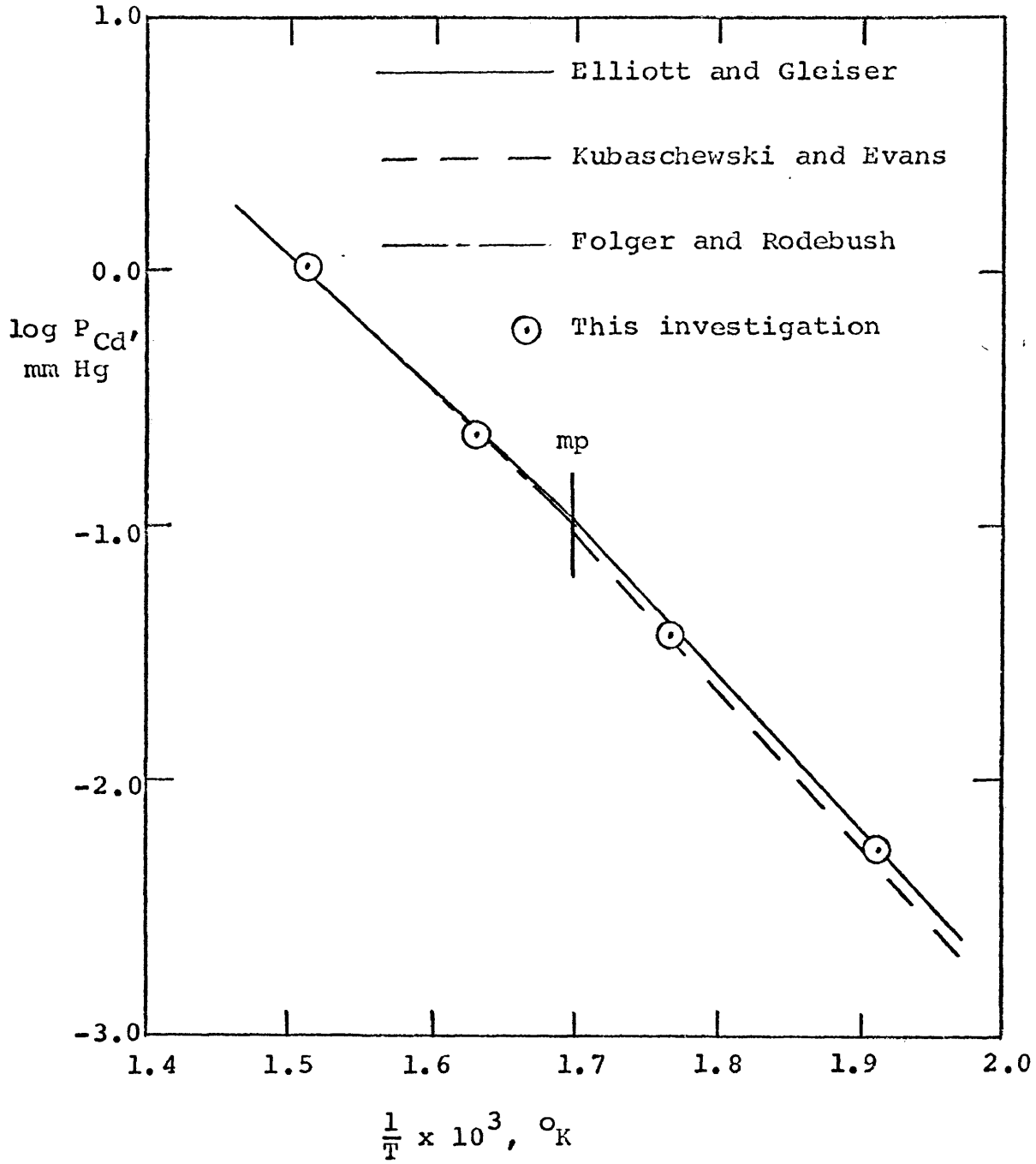

Figure 15. Variation of log P_{Cd} above Pure Cd with Reciprocal Temperature

observed in any of the other experiments.

In view of the fairly good agreement between the vapor pressure of Cd as determined in this investigation and the results found in the literature, it was decided that the apparatus and experimental technique used in this investigation provided for sufficiently accurate vapor-pressure measurement.

Vapor Pressure of Sb_2O_3 in the Range from 422° to 599°C

The vapor-pressure studies performed on PbO-based slags, to be discussed later in this section, require that the vapor pressure of Sb_4O_6 above pure Sb_2O_3 be accurately known before the experimental data can be converted into activities. Very few Sb_4O_6 vapor-pressure data have been reported in the published literature. Hincke (1930, p. 2869) using a modified version of the inert gas saturation method, has determined the vapor pressure of Sb_4O_6 above cubic, orthorhombic, and liquid Sb_2O_3 in the temperature range from 470° to 800°C. Myzenkov and Klushin (1965, p. 1709), using the boiling-point method, have determined the vapor pressure of Sb_4O_6 above liquid Sb_2O_3 in the temperature range from 715° to 1025°C.

The two investigations mentioned above show a large discrepancy between the data for liquid Sb_2O_3. In the investigation by Hincke, silica crucibles were used to contain the Sb_2O_3, whereas Myzenkov and Klushin used pure

alumina crucibles. At high temperatures, above the melting point of Sb_2O_3, it is to be expected that Sb_2O_3 would dissolve SiO_2 from the crucibles with a resultant lowering of the vapor pressure of Sb_4O_6. This increased lowering of the vapor pressure with temperature is seen as an increasing degree of curvature in the plot of $p_{Sb_4O_6}$ vs $\frac{1}{T}$ shown in Figure 16. Also included in Figure 16 are the results of Myzenkov and Klushin. Since the data of Hincke for liquid Sb_2O_3 are somewhat doubtful, it was decided to use the data of Myzenkov and Klushin to refer the slag vapor-pressure data determined in this investigation to pure liquid Sb_2O_3. Their data for the vapor pressure above pure, liquid Sb_2O_3 in the temperature range from 656° to 1025°C are represented by the formula:

$$\log p_{Sb_4O_6,\ \text{mm Hg}} = 5.775 - \frac{4341}{T} \qquad (10)$$

The vapor-pressure data of Hincke are the only data reported in the literature for solid Sb_2O_3. Since there is some question as to the accuracy of his data for liquid Sb_2O_3, it was decided to redetermine the vapor pressure above cubic Sb_2O_3 in order to ascertain whether these data were in significant error.

The Sb_2O_3 was prepared for study by resubliming it in argon at a temperature of 480°C, well below the cubic-orthorhombic transition temperature of 570°C. The cubic

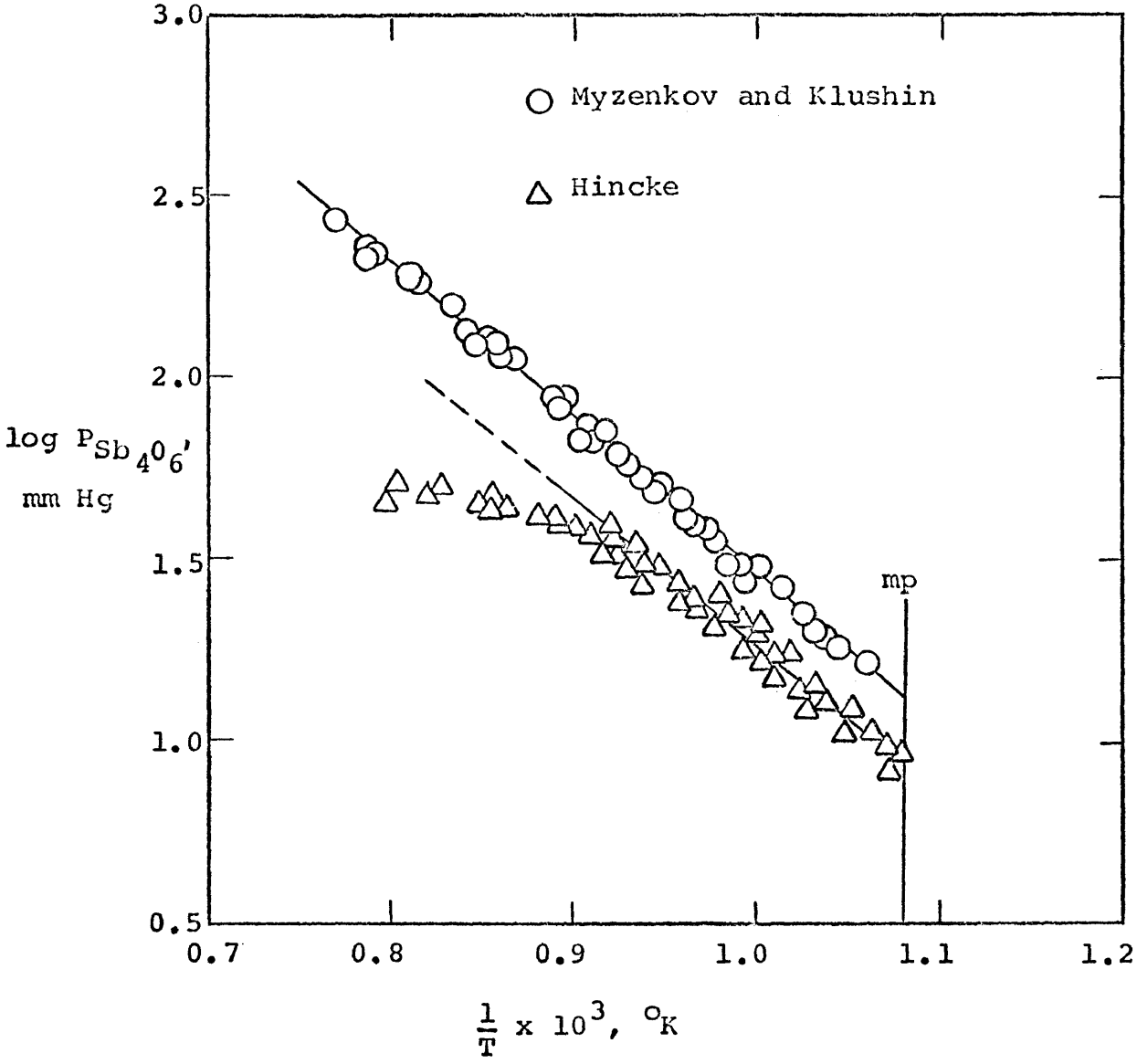

Figure 16. Variation of log $P_{Sb_4O_6}$ above Liquid Sb_2O_3 with Reciprocal Temperature

crystal modification of Sb_2O_3 thus produced was verified by x-ray diffraction analysis. The results of these experiments are shown in Figure 17 together with the data of Hincke. It is apparent from the figure that no errors have been introduced by using silica crucibles at temperatures below the melting point of Sb_2O_3. Hincke's data are somewhat high because of his extrapolation of weight-loss versus flow-rate data to zero flow rate.

A linear regression analysis of the vapor-pressure data for cubic Sb_2O_3, as determined in this investigation, has been made with the result that,

$$\log p_{Sb_4O_6,\ \text{mm Hg}} = 12.239 - \frac{10,441}{T} \qquad (11)$$

for the temperature range from 422° to 599°C. The molar heat of vaporization calculated from Equation (11) is given in Table 10 together with the values given in the literature.

Table 10. Heats of Sublimation and Vaporization of Sb_4O_6

Crystal modification	ΔH, cal	Source
cubic	47,780±1,330	This investigation
cubic	47,320	Hincke
orthorhombic	44,080	Hincke
liquid	17,830	Hincke
liquid	19,430	Myzenkov and Klushin

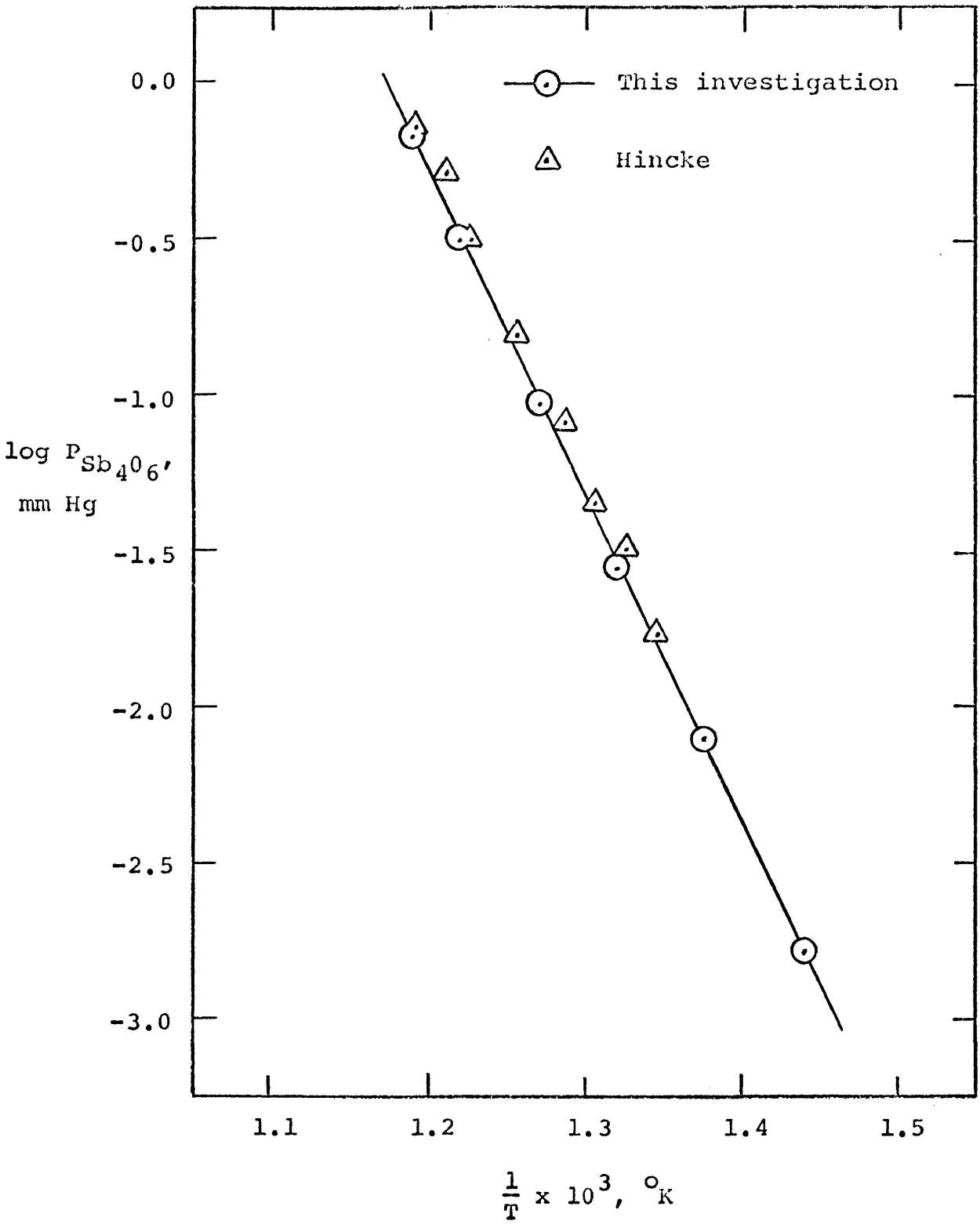

Figure 17. Comparison of Data for log $P_{Sb_4O_6}$ above Cubic Sb_2O_3 as a Function of Reciprocal Temperature

Evaluation of Vapor-Pressure Data for the Determination of Thermodynamic Data for $PbO-Sb_2O_3$ and $PbO-SiO_2-Sb_2O_3$ Slags at 700°C

The vapor-pressure data obtained in this investigation can be used to calculate the thermodynamic activity of Sb_2O_3 in the two slag systems studied. By means of a Gibbs-Duhem integration, the thermodynamic activity of PbO can be obtained for the $PbO-Sb_2O_3$ slags at 700°C. No further calculation of activities can be made for the $PbO-SiO_2-Sb_2O_3$ slags since only the activity of Sb_2O_3 was determined in this investigation.

Determination of Thermodynamic Data for $PbO-Sb_2O_3$ Slags at 700°C. The vapor-pressure determinations for the $PbO-Sb_2O_3$ system at 700°C made in this investigation are given in Table 3. Using the pressure above pure liquid Sb_2O_3 as 20.59 mm Hg, as determined by Myzenkov and Klushin (1965, p. 1715), the individual activities of Sb_2O_3 have been calculated. The results of these calculations are shown in Table 11. Maier and Hincke (1932, p. 3-12) have made a limited number of vapor-pressure measurements in the $PbO-Sb_2O_3$ system at 697°C using the inert gas saturation method. Their measurements were converted to Sb_2O_3 activities using the somewhat low value of 13.0 mm Hg for the pressure above pure Sb_2O_3, as determined by Hincke (1930, p. 3876). A

recalculation of their data using 20.59 mm Hg rather than 13.0 mm Hg as the pressure above pure Sb_2O_3 is included in Table 11 for comparative purposes. All activities are relative to pure, liquid Sb_2O_3 at the respective temperature. It is evident that the agreement is rather poor at low concentrations of Sb_2O_3 although their data are not extensive enough for an accurate comparison to be made.

Table 11. Activities of Sb_2O_3 in the PbO-Sb_2O_3 System Determined from Vapor-Pressure Measurements in the PbO-Sb_2O_3 System at 700°C

Temp, °C	$X_{Sb_2O_3}$	$a_{Sb_2O_3}$	$\gamma_{Sb_2O_3}$	Source
700	0.0442	0.0385	0.871	This investigation
700	0.108	0.0377	0.349	" "
700	0.137	0.0375	0.274	" "
697	0.144	0.0624	0.433	Maier and Hincke
700	0.176	0.0430	0.244	This investigation
700	0.212	0.0522	0.246	" "
700	0.280	0.0782	0.279	" "
700	0.495	0.245	0.495	" "
697	0.503	0.222	0.441	Maier and Hincke
697	0.730	0.630	0.863	" "

The somewhat peculiar behavior observed for the two-component mixtures containing 4.42, 10.8, and 13.7 mole % Sb_2O_3 is due to the fact that these compositions lie

within a two-phase region composed of solid PbO and liquid containing 14.4 mole % Sb_2O_3. The locations of these compositions relative to the phase boundaries are shown in the phase diagram for the PbO-Sb_2O_3 system presented in Figure 18, Zunkel and Larson (1967, p. 477). Since the composition of the liquid in the two-phase region is constant, the individual component activities remain equal between the solidus and liquidus compositions.

A Gibbs-Duhem integration of the activity data obtained in this investigation has been used to obtain the activities of PbO in the range from $X_{PbO} = 0.959$ to $X_{PbO} = 0.505$ at 700°C. The data for this calculation are given in Table 12. A plot of the α-function for Sb_2O_3 as a function of mole fraction of Sb_2O_3 is presented in Figure 19. Since α is not constant or linear as a function of composition, the PbO-Sb_2O_3 system is neither regular nor sub-regular in its behavior at 700°C. It is also readily apparent from Figure 19 that this system is far from being ideal due to the strong negative deviation observed.

The activities of Sb_2O_3 calculated from the vapor-pressure determinations in the PbO-Sb_2O_3 system and the activities of PbO calculated by means of the Gibbs-Duhem integration are shown graphically in Figure 20. The standard states are the real, pure liquid for Sb_2O_3 and the real, pure solid for PbO, both at 700°C. It can be

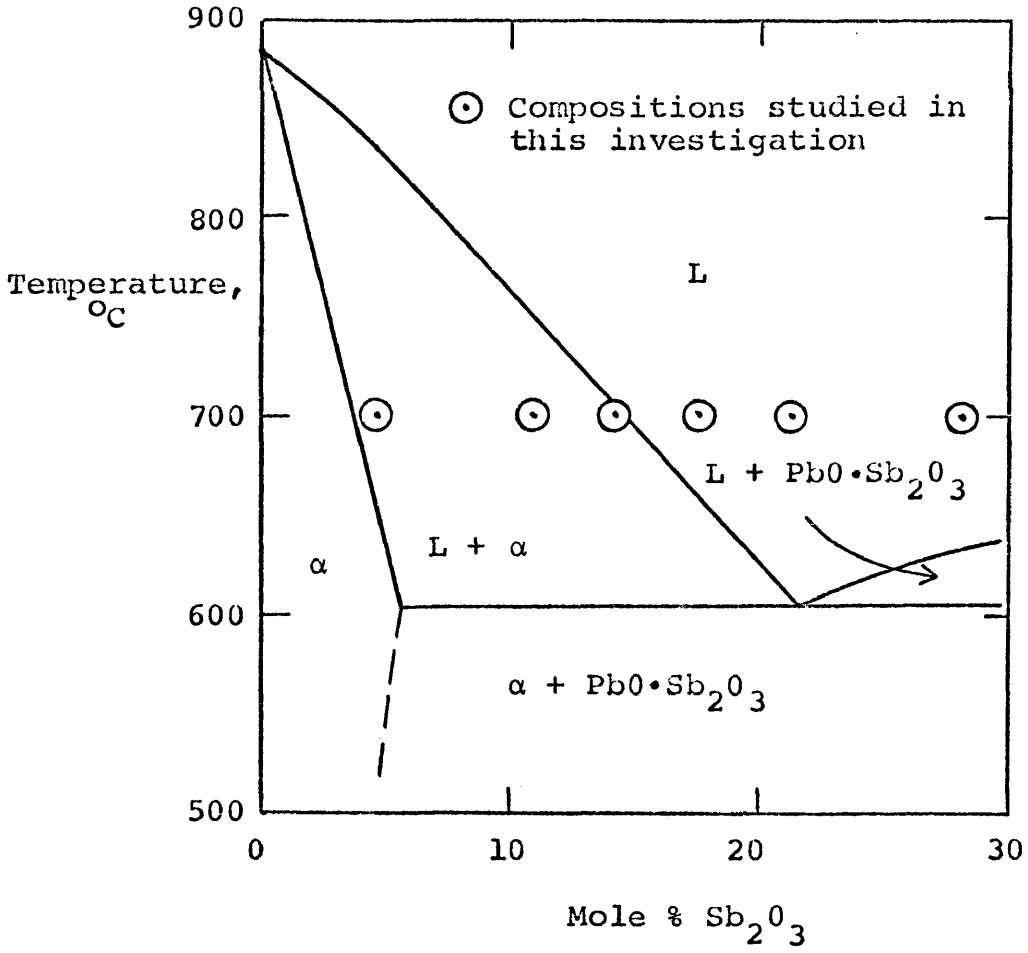

Figure 18. Phase Diagram for the PbO-rich End of the PbO-Sb_2O_3 System

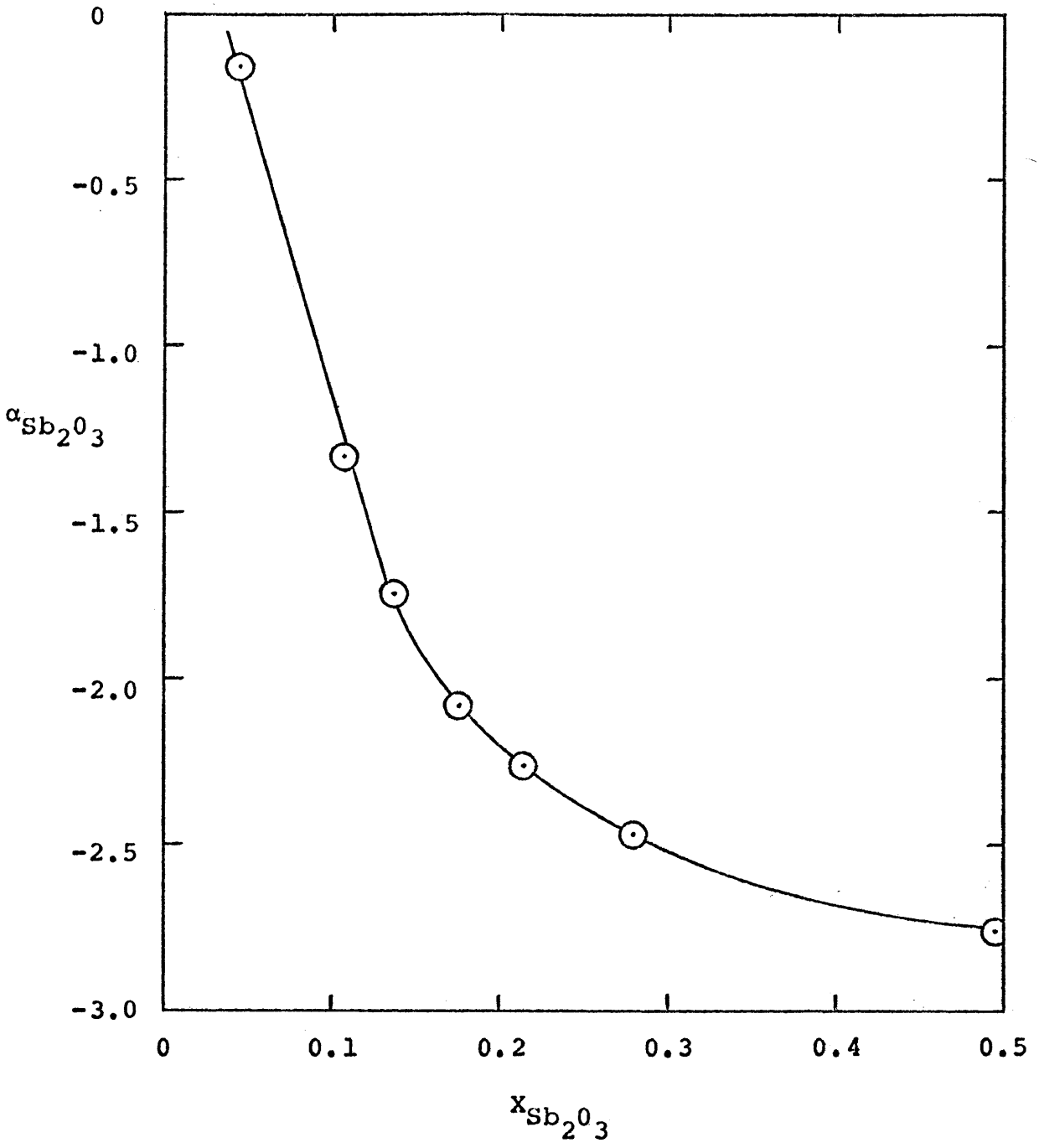

Figure 19. Variation of the Sb_2O_3 α-function with Composition for the PbO-Sb_2O_3 System at 700°C

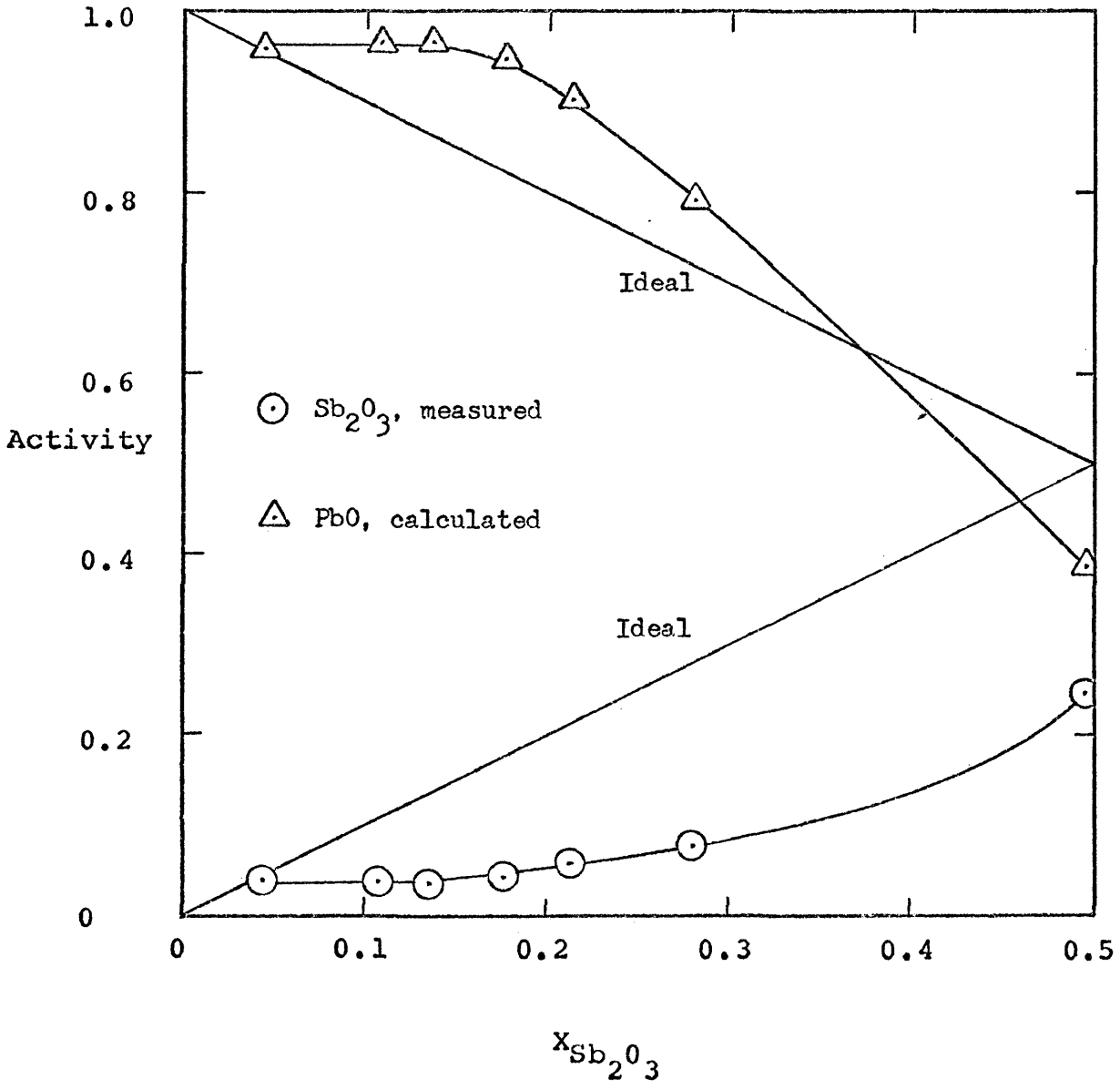

Figure 20. Activities of Sb_2O_3 and PbO in the PbO-Sb_2O_3 System at 700°C (standard states: Sb_2O_3-pure liquid, PbO-pure solid)

Table 12. Gibbs-Duhem Integration of Sb_2O_3 Activity Data Determined from Vapor-Pressure Data on the PbO-Sb_2O_3 System at 700°C

X_{PbO}	$X_{Sb_2O_3}$	$p_{Sb_4O_6}$, mm Hg	$a_{Sb_2O_3}$	$\gamma_{Sb_2O_3}$	$\ln\gamma_{Sb_2O_3}$	X^2_{PbO}	$a^*_{Sb_2O_3}$	$\ln\gamma_{PbO}$	γ_{PbO}	a_{PbO}
0.956	0.0442	0.0304	0.0385	0.871	-0.138	0.914	-0.151	0.00367	1.003	0.959
0.892	0.108	0.0293	0.0377	0.349	-1.053	0.786	-1.323	0.0803	1.083	0.966
0.863	0.137	0.0290	0.0375	0.274	-1.295	0.756	-1.738	0.116	1.122	0.968
0.824	0.176	0.0380	0.0430	0.244	-1.411	0.679	-2.078	0.137	1.147	0.945
0.788	0.212	0.0560	0.0522	0.246	-1.402	0.621	-2.259	0.134	1.143	0.901
0.720	0.280	0.126	0.0782	0.279	-1.277	0.518	-2.462	0.0963	1.101	0.793
0.505	0.495	1.235	0.245	0.495	-0.703	0.255	-2.758	-0.271	0.763	0.385
0	1	20.59	1	1	0	0				

*

$$\alpha_{Sb_2O_3} = \frac{\ln\gamma_{Sb_2O_3}}{(1-X_{Sb_2O_3})^2} = \frac{\ln\gamma_{Sb_2O_3}}{X^2_{PbO}}$$

seen that the behavior of Sb_2O_3 deviates strongly in the negative direction from ideality and appears to remain so at all compositions. The behavior of PbO, however, presents a rather interesting case which can be explained by considering the integrated form of the Gibbs-Duhem equation for a binary system:

$$\ln\gamma_1 = -\int_{X_1 = 1}^{X_1 = X_1} \frac{X_2}{X_1}\, d(\ln\gamma_2) \qquad (12)$$

If γ_2 continually increases as X_2 decreases, then γ_1 is greater than unity at all values of X_2. Also, if γ_2 continually decreases as X_2 decreases, then γ_1 is less than unity at all values of X_2. In the first case, component 1 exhibits positive deviation from the Raoult's law line over the entire composition range and in the second case, component 1 exhibits negative deviation from the Raoult's law line over the entire composition range. Close examination of the data of Table 12 reveals that $\gamma_{Sb_2O_3}$, although it is much less than unity at all compositions studied, does not continually decrease as $X_{Sb_2O_3}$ decreases. As the composition of the system enters the two-phase region (see Figure 18) where $a_{Sb_2O_3}$ becomes constant with composition, $\gamma_{Sb_2O_3}$ must of necessity begin to increase as the concentration of Sb_2O_3 continues to decrease. Thus, the fact that $\gamma_{Sb_2O_3}$ is always less than unity is not sufficient to

insure that PbO also continually deviates in the negative direction from Raoult's law line. This unusual mixed behavior is also seen to occur in some silicate systems as well as some metallic systems, e.g. Zn-Sb at 550°C, DeWitt and Seltz (1939, p. 3170).

The standard free energy of formation of liquid Sb_2O_3 has been estimated by Coughlin (1954, p. 8) using heat capacity data for the orthorhombic crystal modification of solid Sb_2O_3. By proper treatment of the Sb_2O_3 activity data determined in this investigation, together with the slag-metal equilibria data for the PbO-Sb_2O_3 system reported by Zunkel and Larson (1967, p. 475), a calculation can be made for the standard free energy of formation of Sb_2O_3 as a function of temperature. The equilibria reaction under consideration can be represented as follows:

$$2\ \underline{Sb}_{1wt\%} + 3\ PbO_{(l)} = Sb_2O_{3(l)} + 3\ Pb_{(l)} \qquad (13)$$

The equilibrium constant for this reaction is represented by the following expression:

$$K_{eq} = \frac{a_{Pb}^3 \times a_{Sb_2O_3}}{a_{PbO}^3 \times a_{\underline{Sb}}^2} \qquad (14)$$

Several assumptions can be made to simplify this expression: 1) that Henry's law is obeyed over a sufficiently wide range of both temperature and concentration for Sb dissolved in Pb, 2) that ΔCp for the reaction is zero, 3) that a_{PbO} is

unity, and 4) that Sb_2O_4 and Sb_2O_5 may be present in small amounts but do not affect the equilibrium. Assumption 1 is valid because Sb dissolved in Pb follows Henry's law up to approximately 3.9 wt % in the temperature range under consideration. Assumption 2 is valid because ΔH^o and ΔS^o are nearly independent of temperature in the range under consideration. Assumption 3 is valid since all alloys under consideration contain in excess of 99 wt % of Pb. Assumption 4 can be shown to be valid by application of the appropriate data from Table 13. As an example, if the oxygen potential in the system is assumed to be determined by the $2\ PbO_{(l)} = 2\ Pb_{(l)} + O_{2(g)}$ equilibrium, $a_{Sb_2O_4}/a_{Sb_2O_3} = 2.7 \times 10^{-3}$ and $a_{Sb_2O_5}/a_{Sb_2O_4} = 1.5 \times 10^{-9}$ at 700°C.

Using the above assumptions, Equation (14) reduces to:

$$K_{eq} = \frac{a_{Sb_2O_3}}{a_{PbO}^3\ (\%\ \underline{Sb})^2} \qquad (15)$$

Zunkel and Larson (1967, p. 476) have shown that $a_{Sb_2O_3}/a_{PbO}^3$ is a constant independent of temperature in the two-phase region in the PbO-rich end of the PbO-Sb_2O_3 system. Therefore, in the two-phase region, a plot of $\log \frac{\gamma_{Sb_2O_3}}{\gamma_{PbO}^3}$ versus $\log \frac{X_{Sb_2O_3}}{X_{PbO}^3}$ should be a temperature-independent straight line with a slope of -1.

Table 13. Thermodynamic Data for the Pb-Sb-O System at 923°, 973°, and 1023°K

Reaction	Function	Temperature, °K 923	973	1023	Reference
$2\ Pb_{(l)} + O_2 = 2\ PbO_{(s)}$	ΔG^o	-60,140	-57,800	-55,480	Wicks and Block
$PbO_{(l)} = PbO_{(s)}$	ΔG^o	-1,290	-1,030	-770	ΔH_m^o from Rodigina, Gomel'skii, and Luginina*
$2\ Sb_{(l)} + \frac{3}{2}\ O_{2(g)} = Sb_2O_{3(l)}$	ΔG^o	-109,410	-106,710	-104,010	Wicks and Block
$2\ Sb_{(l)} + 2\ O_{2(g)} = Sb_2O_{4(s)}$	ΔG^o	-127,800	-123,100	-118,400	Wicks and Block
$2\ Sb_{(l)} + \frac{5}{2}\ O_{2(g)} = Sb_2O_{5(s)}$	ΔG^o	-117,000	-111,680	-105,700	ANL - 5750
$\underline{Sb}_{1\ wt\ \%} = Sb_{(l)}$	ΔG^o	7,890	8,320	8,750	γ^o extrapolated from Hultgren et al. and Seltz and DeWitt**

* ΔH_m^o = 6,110 cal/mole. Detailed calculation given in Appendix VII

** $\gamma_{923}^o = 0.790$, $\gamma_{973}^o = 0.798$, $\gamma_{1023}^o = 0.805$. Detailed calculation given in Appendix VIII

The data for constructing the log $\frac{\gamma_{Sb_2O_3}}{\gamma^3_{PbO}}$ versus log $\frac{X_{Sb_2O_3}}{X^3_{PbO}}$ plot are given in Table 14 and the plot itself is shown in Figure 21. The data for 650° and 750°C were plotted using the assumption that $a_{PbO} = 0.96$, since insufficient data were collected to perform a Gibbs-Duhem integration for these temperatures with any degree of accuracy. Also included in Figure 21 are the slag-metal equilibria data of Zunkel and Larson plotted using the estimated values for the standard free energy of formation of Sb_2O_3 according to Coughlin. As can be seen from Figure 21, the data fall on a temperature-independent straight line with a slope of -1 for all compositions within the two-phase region. The intercept of this line has been calculated with the result that,

$$\frac{a_{Sb_2O_3}}{a^3_{PbO}} = 0.0430 \qquad (16)$$

for the two-phase region.

Using the data of Zunkel and Larson,

$$\log (\%\ \underline{Sb})^2 = -\frac{4980}{T} + 2.798 \qquad (17)$$

and Equations (15) and (16), a linear equation in temperature for the variation of log K_{eq} with temperature can be obtained with the result that,

Table 14. Data for the Plot of log $\frac{\gamma_{Sb_2O_3}}{\gamma^3_{PbO}}$ versus log $\frac{X_{Sb_2O_3}}{X^3_{PbO}}$ for the PbO-Sb_2O_3 System at 650°, 700°, and 750°C

Temp, °C	$P_{Sb_4O_6}$, mm Hg	$X_{Sb_2O_3}$	X_{PbO}	X^3_{PbO}	$\frac{X_{Sb_2O_3}}{X^3_{PbO}}$	$\gamma_{Sb_2O_3}$	γ_{PbO}	γ^3_{PbO}	$\frac{\gamma_{Sb_2O_3}}{\gamma^3_{PbO}}$
650	0.0162	0.108	0.892	0.633	0.152	0.342	1.081*	1.263	0.271
	0.0160	0.176	0.824	0.461	0.315	0.209	1.170*	1.602	0.130
700	0.0304	0.044	0.956	0.846	0.051	0.871	1.003	1.009	0.863
	0.0293	0.108	0.892	0.633	0.152	0.349	1.083	1.270	0.275
	0.0290	0.137	0.863	0.555	0.213	0.274	1.122	1.412	0.194
	0.0380	0.176	0.824	0.461	0.315	0.244	1.147	1.509	0.162
	0.0560	0.212	0.788	0.386	0.433	0.246	1.143	1.493	0.165
	0.126	0.280	0.720	0.269	0.750	0.247	1.101	1.335	0.185
	1.235	0.495	0.505	0.065	3.844	0.495	0.763	0.444	1.115
750	0.0512	0.044	0.956	0.846	0.051	0.882	1.008*	1.024	0.861
	0.0510	0.108	0.892	0.633	0.152	0.359	1.081*	1.263	0.284

* a_{PbO} estimated (see p. 88)

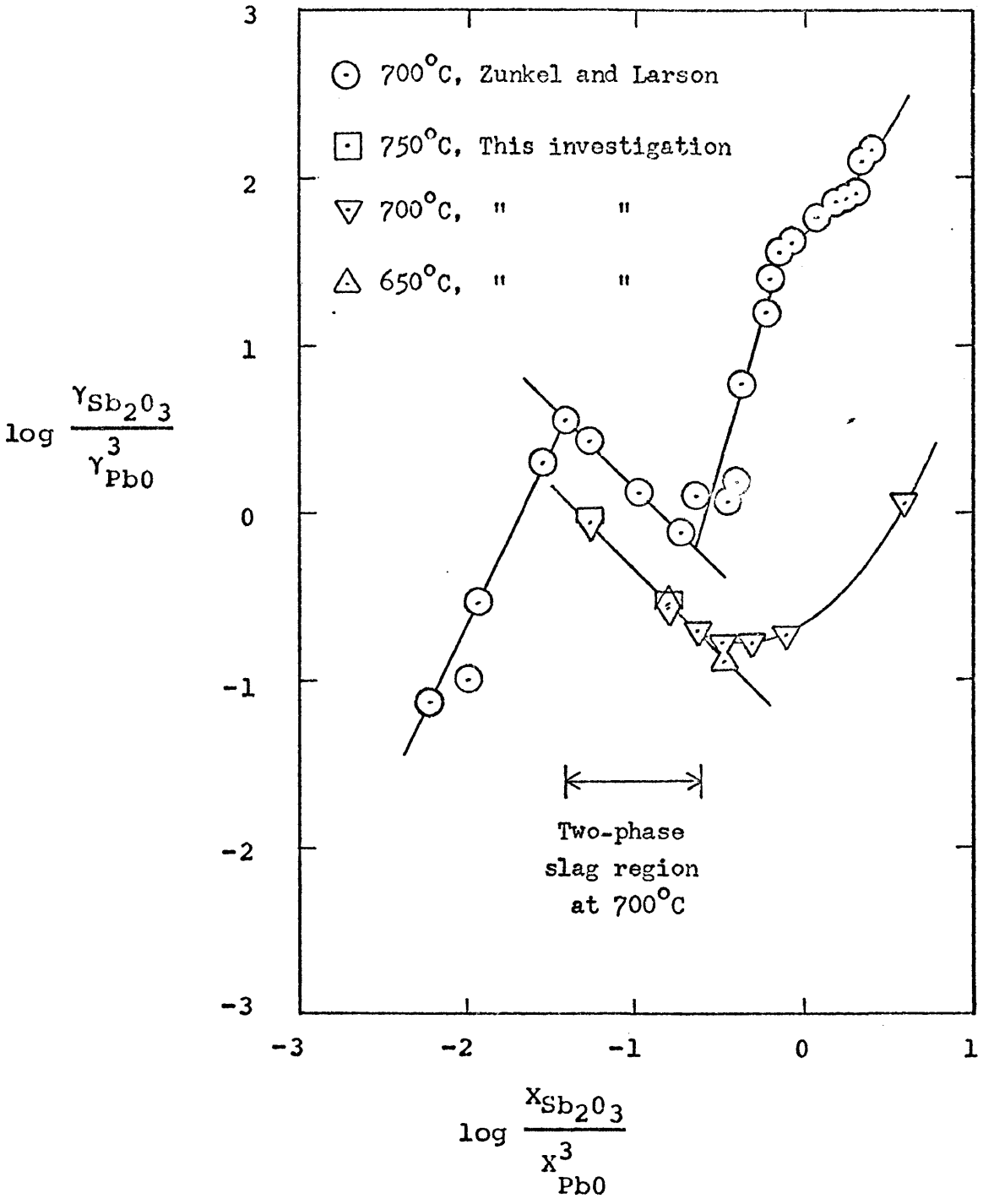

Figure 21. Log $\frac{\gamma_{Sb_2O_3}}{\gamma^3_{PbO}}$ Versus log $\frac{X_{Sb_2O_3}}{X^3_{PbO}}$ for the PbO-Sb_2O_3 System at 650°, 700°, and 750°C

$$\log K_{eq} = \frac{4980}{T} - 4.165 \qquad (18)$$

for Reaction (13).

The appropriate data from Table 13, together with Equation (18) can then be used to calculate the standard free energy of formation of $Sb_2O_{3(l)}$ according to the following reaction:

$$2\ Sb_{(l)} + \frac{3}{2}\ O_{2(g)} = Sb_2O_{3(l)} \qquad (19)$$

with the result that,

$$\Delta G_f^o = -159{,}190 + 56.20\ T \qquad (20)$$

Equation (20) was obtained from a least-squares fit of three values of ΔG_f^o calculated at 650°, 700°, and 750°C. These values are compared with the estimated values of Coughlin in Table 15. Although the correction in ΔG_f^o for Sb_2O_3 amounts to less than 3 percent, the estimated data for $\log \frac{a_{Sb_2O_3}}{a_{PbO}^3}$ are in error by approximately one-half order of magnutide. It is to be noted, however, that the application of Figure 21 to the determination of the liquidus and solidus curves in the PbO-rich end of the $PbO\text{-}Sb_2O_3$ system, as was done by Zunkel and Larson, is not affected by the correction in ΔG_f^o for $Sb_2O_{3(l)}$, since the curves are shifted only in the vertical direction.

Table 15. ΔG_f^o for $Sb_2O_{3(l)}$ as Determined from Slag-Metal Equilibria Data in the Pb-(PbO+Sb_2O_3) System and Vapor-Pressure Determinations in the PbO-Sb_2O_3 System at 650°, 700°, and 750°C

Temperature, °C	ΔG_f^o, cal (This study)	ΔG_f^o, cal (Coughlin)
650	-107,320	-109,410
700	-104,490	-106,710
750	-101,700	-104,010

The data of Table 14 can also be used to calculate the heat of vaporization of Sb_4O_6 from artificial slags whose compositions fall within the two-phase region in the PbO-rich end of the PbO-Sb_2O_3 system as shown in Figure 18. By means of a plot of log $p_{Sb_4O_6}$ versus $\frac{1}{T}$ over the temperature range from 650° to 750°C, a value of +20,830 cal/mole has been calculated. This value is seen to be somewhat larger than the corresponding value for ΔH_{vap} of pure Sb_2O_3 due to the strong negative deviation of Sb_2O_3 from the Raoult's law line as shown in Figure 20.

The phase diagram for the PbO-Sb_2O_3 system shown in Figure 18 may be used to calculate the standard free energy of formation of $PbO \cdot Sb_2O_3$. At a temperature just below the eutectic temperature, the following reaction may be considered:

$$\underline{PbO}_{(\alpha)} + \underline{Sb_2O_3}_{(\alpha)} = PbO \cdot Sb_2O_{3(s)} \quad (21)$$

The equilibrium constant for this reaction is represented by the following expression:

$$K_{eq} = \frac{a_{PbO \cdot Sb_2O_3}}{a_{\underline{PbO}} \times a_{\underline{Sb_2O_3}}} \quad (22)$$

The activity of $PbO \cdot Sb_2O_3$, referred to the pure solid, can be set equal to unity using the pure solid as the standard state. For purposes of calculation, the activity of PbO can be set equal to its mole fraction; 0.944 at 604°C. The activity of Sb_2O_3 can be obtained from the data given in Table 14 for the 2-phase slag compositions. By extrapolating log $p_{Sb_4O_6}$ versus $\frac{1}{T}$ to 604°C and dividing the resultant pressure by $p^o_{Sb_4O_6}$ = 2.203 mm Hg at 604°C (Hincke, 1930, p. 3876), $a_{Sb_2O_3}$ is calculated to be 0.0647, relative to pure, solid Sb_2O_3.

Substitution of the above values into equation (22) at 604°C yields K_{eq} =16.4 for the reaction:

$$PbO_{(s)} + Sb_2O_{3(s)} = PbO \cdot Sb_2O_{3(s)} \quad (23)$$

By use of the relation,

$$\Delta G^o = -RT \ln K_{eq} \quad (24)$$

the standard free energy change for reaction (23) can be calculated with the result that ΔG^o_{877} = -4,860 cal/mole of $PbO \cdot Sb_2O_3$.

The standard free energy of formation of $PbO \cdot Sb_2O_3$ from the elements at 604°C can be calculated by summing the following equilibria and their corresponding free energy values.

$$PbO_{(s)} + Sb_2O_{3(s)} = PbO \cdot Sb_2O_{3(s)} \quad (25)$$

$\Delta G^{o}_{877} = -4,860$ cal
(Calculated)

$$Sb_2O_{3(l)} = Sb_2O_{3(s)} \quad (26)$$

$\Delta G^{o}_{877} = -740$ cal
(Wicks and Block, 1963, p. 14)

$$2Sb_{(l)} + \frac{3}{2} O_{2(g)} = Sb_2O_{3(l)} \quad (27)$$

$\Delta G^{o}_{877} = -109,900$ cal
(Calculated)

$$Pb_{(l)} + \frac{1}{2} O_{2(g)} = PbO_{(s)} \quad (28)$$

$\Delta G^{o}_{877} = -31,080$ cal
(Wicks and Block, 1963, p. 63)

By summation of equations (25), (26), (27), and (28), and their free energies,

$$Pb_{(l)} + 2Sb_{(l)} + 2O_{2(g)} = PbO \cdot Sb_2O_{3(s)} \qquad (29)$$

$$\Delta G^{o}_{877} = -146{,}580 \text{ cal}$$

The literature does not contain any data with which this calculated value can be compared.

Determination of Thermodynamic Data for PbO-SiO_2-Sb_2O_3 Slags at 700°C. The vapor-pressure determinations for the PbO-SiO_2-Sb_2O_3 slags have been converted to Sb_2O_3 activities using the data of Table 4 by means of $p^{o}_{Sb_4O_6}$ = 20.59 mm Hg at 700°C, as determined by Myzenkov and Klushin. The results of these calculations are presented in tabular form in Table 16 and shown graphically in Figure 22. The molar ratio of PbO to SiO_2, for reasons to be explained later in this chapter, was held constant at a value of 2 for all slag compositions studied in this investigation.

Table 16. Activities of Sb_2O_3 in the PbO-SiO_2-Sb_2O_3 System ($\frac{PbO}{SiO_2}$ = 2) Determined from Vapor-Pressure Measurements in the PbO-SiO_2-Sb_2O_3 System at 700°C

$X_{Sb_2O_3}$	$a_{Sb_2O_3}$	$\gamma_{Sb_2O_3}$
0.0296	0.00511	0.173
0.0634	0.0116	0.183
0.0945	0.0193	0.204
0.130	0.0359	0.276
0.167	0.0625	0.374
0.206	0.0995	0.483
0.246	0.146	0.593

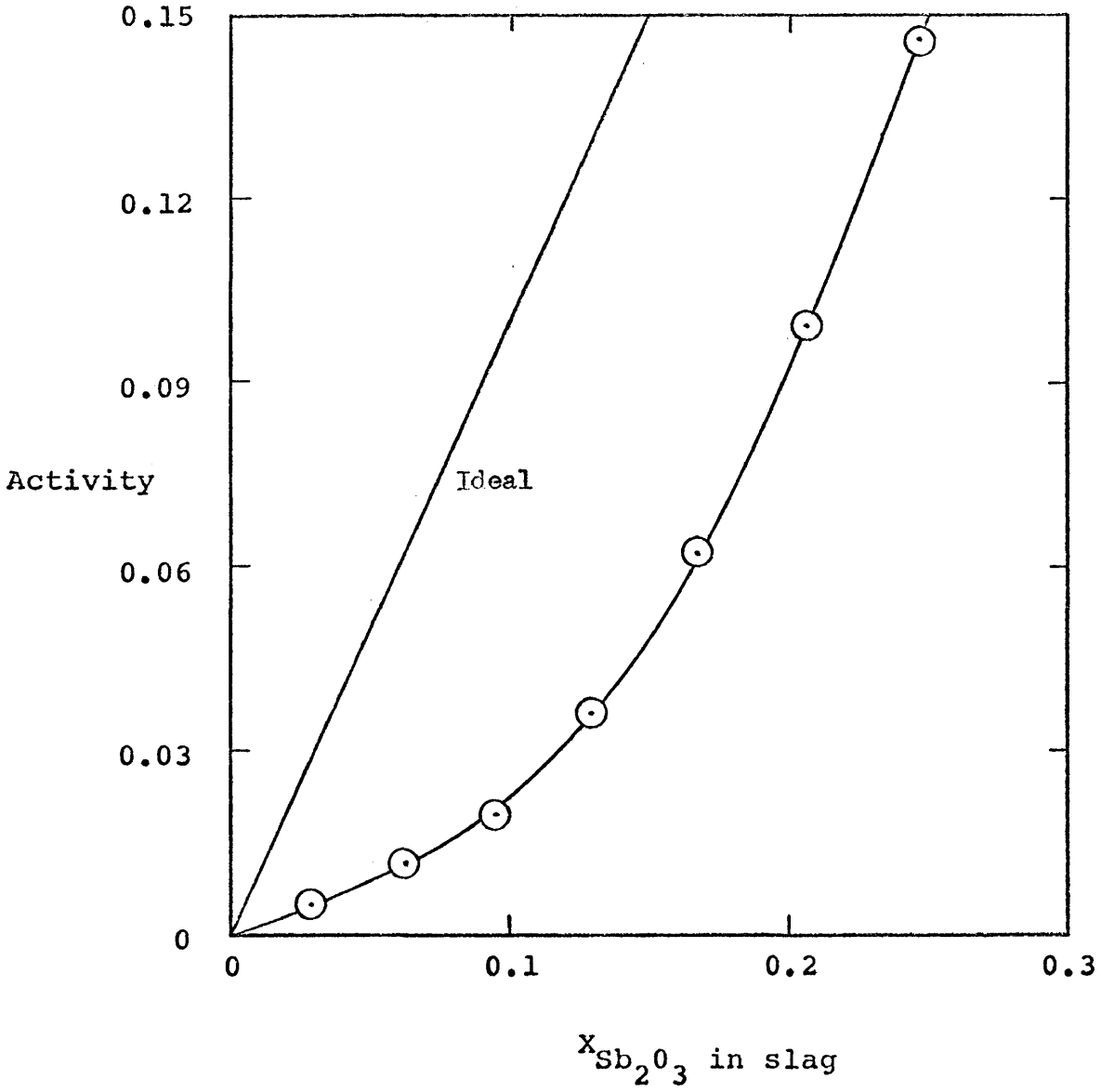

Figure 22. Activity of Sb_2O_3 in $PbO-SiO_2-Sb_2O_3$ ($\frac{PbO}{SiO_2} = 2$) Slags at 700°C (Standard state - pure liquid Sb_2O_3)

No calculation can be made for the component activities of PbO and SiO_2 in the slags studied in this investigation, since only the activity of Sb_2O_3 was determined experimentally. Some outside data source would be required before a ternary Gibbs-Duhem integration could be performed. Sridhar and Jeffes (1967, p. 44) have determined the activities of both PbO and SiO_2 in the PbO-SiO_2 system up to the limit of silica saturation at 850°, 950°, and 1050°C, and have compared their results with those of earlier workers. In all cases, it was found that both PbO and SiO_2 exhibit strong negative deviations from the Raoult's law line at compositions below approximately $X_{SiO_2} = 0.5$. For compositions containing higher silica contents, silica begins to deviate positively from the ideal Raoult's law line and continues to do so up to the saturation limit. The negative deviation shown for PbO is to be expected due to the strong tendency for PbO to form silicates.

For comparative purposes, the vapor-pressure data for both the PbO-SiO_2-Sb_2O_3 ($\frac{PbO}{SiO_2} = 2$) slags and the PbO-Sb_2O_3 slags are plotted together as a function of $X_{Sb_2O_3}$ at 700°C in Figure 23. At low concentrations of Sb_2O_3, the vapor pressure of Sb_4O_6 is highest above the binary slags. At higher concentrations, above approximately $X_{Sb_2O_3} = 0.21$, the vapor pressure of Sb_4O_6 is highest above the ternary silicate slags (on PbO+Sb_2O_3 basis). A continuous decrease

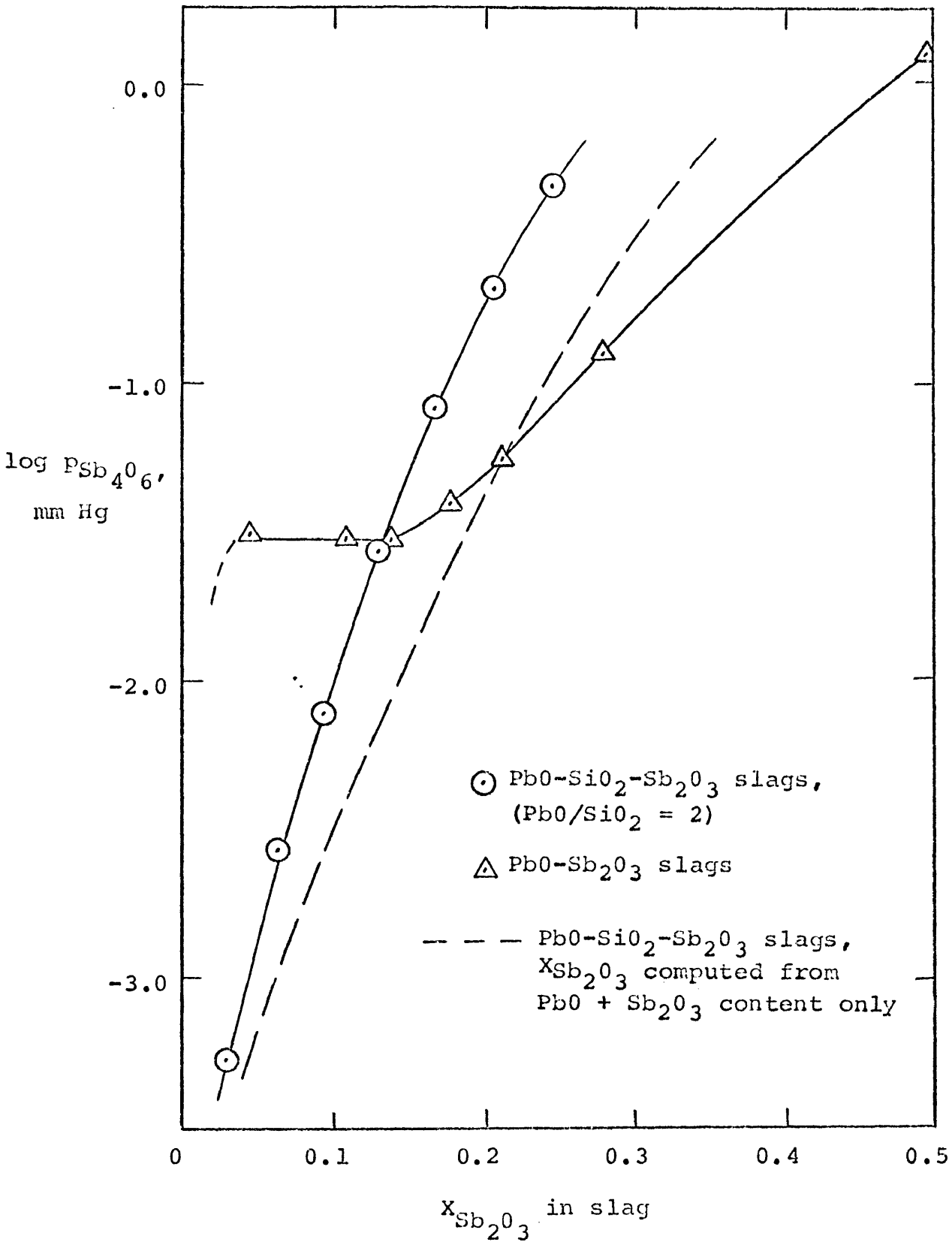

Figure 23. Variation of log $P_{Sb_4O_6}$ with Composition for PbO-SiO_2-Sb_2O_3 ($\frac{PbO}{SiO_2}$ = 2) and PbO-Sb_2O_3 Slags at 700°C

of $P_{Sb_4O_6}$ with decreasing concentration of Sb_2O_3 in the slag is observed for the silicate slags due to the fact that they are composed entirely of liquid over the composition range investigated in this study at 700°C. Further discussion of the shapes of the curves of Figure 23 and their relationship to one another will be deferred until later in this chapter.

Application of Vacuum Techniques to the Removal of As_2O_3, Sb_2O_3, and SnO_2 from Lead-Softening Slags

The primary purpose of this investigation is to determine the feasibility of removing volatile oxide impurities from the PbO-based slags produced during the softening of lead bullion by the application of vacuum techniques. Current softening practice involves a selective oxidation process in which a suitable oxidizing agent, air or PbO, is added to the lead bullion to oxidize the impurities which then dissolve in a slag composed primarily of PbO. The slag phase produced in this operation must then be recovered and separately treated to recover the oxides of the impurity metals. After reverberatory softening operations, the impurity metal oxides are recovered by fuming the slag in the presence of carbon to produce an antimonial-Pb and a fume composed primarily of the trivalent oxides of As and Sb. In kettle softening, sodium salts are added together with PbO to produce a nonvolatile liquid solution of sodium

arsenates, antimonates, and stannates which require further treatment to recover the impurity metals either as pure oxides or metals.

The results of this study propose that, provided the concentration of Sb_2O_3 in the slag is sufficiently high, slag treatment for the recovery of Sb as the trivalent oxide can be greatly simplified while, at the same time, producing a high purity product of Sb.

The experiments performed in this portion of the investigation were concerned primarily with the relative rates at which the oxides of As, Sb, and Sn could be removed from slag melts under conditions of elevated temperature and reduced pressure. This experimental investigation is intended as a feasibility study rather than a rigorous kinetic study of the various steps occurring in the overall process. A great deal of further work, not included in this study, would have to be done before any quantitative statements could be made concerning the actual rates of removal or the mechanisms by which the actual removal is effected. In view of this stated purpose, the operating variables including temperature, pressure, slag composition, and addition agents were modified in an attempt to determine the optimum conditions for the removal of volatile oxides from lead-softening slags. The vacuum-removal experiments performed in this portion of the investigation can be conveniently divided into two

separate categories: 1) those without silica additions; and, 2) those with silica additions. Each group of experiments will be discussed separately in the following sections. All x-ray diffraction phase analyses for the slags and condensates produced are presented in Table 9.

The Removal of As_2O_3, Sb_2O_3, and SnO_2 from $PbO-Me_xO_y$ Slags at Reduced Pressure and Elevated Temperature. The experimental data for the removal of As_2O_3, Sb_2O_3, and SnO_2 from $PbO-Me_xO_y$ slags are given in Table 6 and presented in graphical form in Figures 24-28. With the exception of test G, all tests were made at a reduced pressure of 200μ Hg; test G being made at atmospheric pressure.

The first tests that were run (H and J) were made to determine the feasibility of selectively distilling As_2O_3 from a 2 wt % As_2O_3-PbO slag at 500° and 650°C under a vacuum of 200μ Hg. Both slags used for these tests were first preformed, cooled, and crushed to -150 mesh before being used for the tests. In test H, the As_2O_3 content was reduced from an initial concentration of 1.80 wt % to a value of 1.32 wt % in a 4-hr period under a vacuum of 200μ Hg at 500°C. By increasing the temperature to 650°C, as in test J, the residual amount of As_2O_3 was reduced to 0.96 wt %, approximately one-half of the original amount. Due to the very high vapor pressure of As_2O_3, no measurable amount of condensate was produced in either of these tests. A

noticeable deposit was observed, however, on the inside walls of the vacuum take-off line and trap and it was noticed that the vacuum pump oil became cloudy during both tests.

Because As usually comprises only a small fraction of the impurity oxides in commercial lead softening slags, no further extensive program of experimentation was carried out to investigate the removal of As_2O_3 from binary As_2O_3-PbO slags, except for a third test made at 800°C. The results of this test (DD) are presented in Figure 24 and given in tabular form in Table 6. It is apparent that the vacuum distillation of As_2O_3 from this slag at 800°C is no more efficient than that observed for test J. The primary reason for this behaviour is due to the drastic decrease in available surface area of the slag. The enhanced volatility of As_2O_3 at the higher temperature has been nullified by virtue of the fact that the slag no longer has a high specific surface and, in addition, is composed of a very viscous, 2-phase mixture which is very difficult to stir effectively.

The second series of tests conducted in this portion of the investigation were made to determine the feasibility of selectively distilling Sb_2O_3 from binary PbO-Sb_2O_3 slags at reduced pressure over a wide variety of temperatures. Since the majority of lead softening slags contain Sb_2O_3 as the major oxide impurity, there is considerably more justification

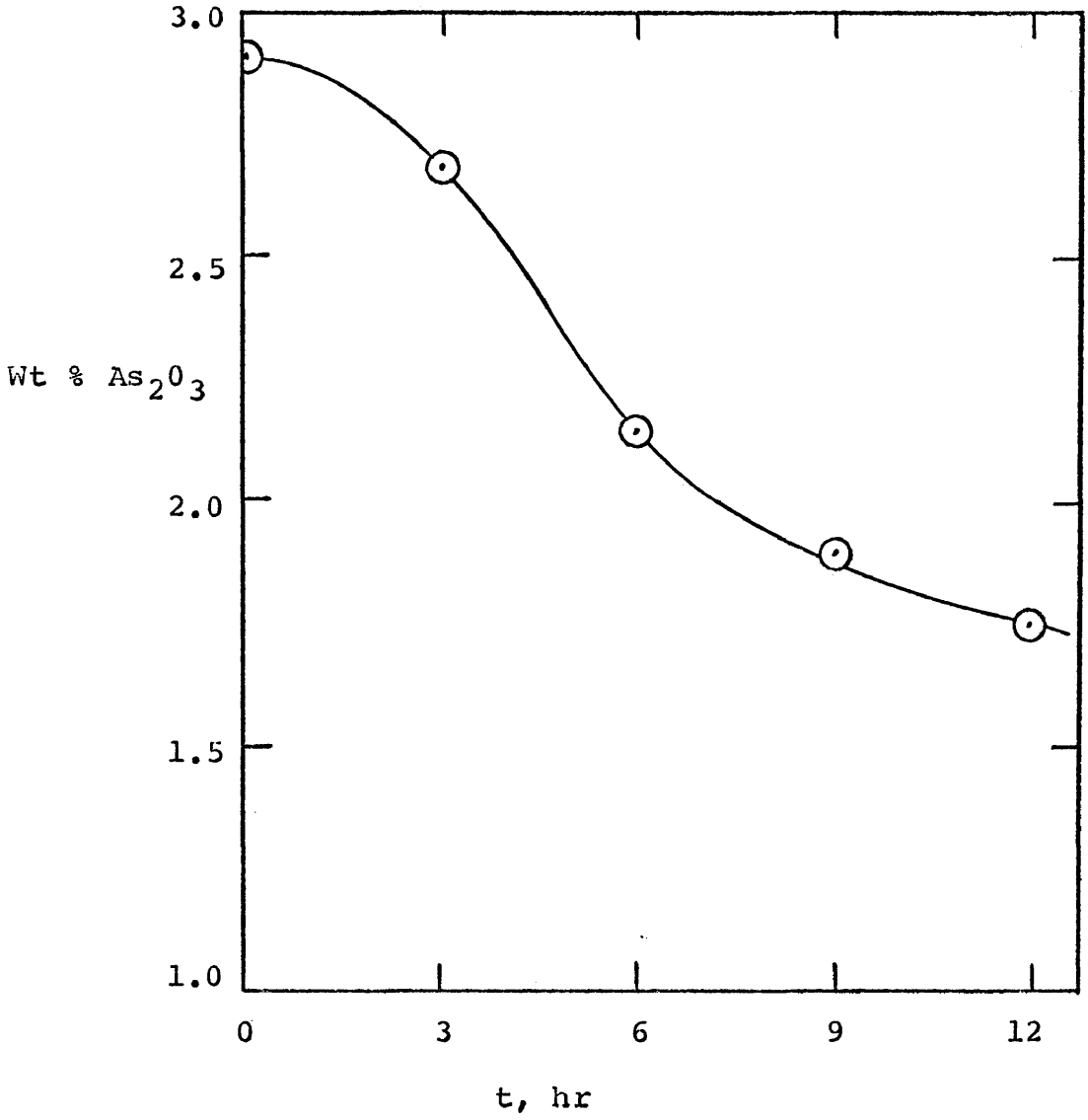

Figure 24. Removal of As from a 3 wt % As_2O_3-PbO Slag by Vacuum Distillation at 800°C: Test DD, 200μ Hg Pressure.

in investigating these binary slags than there is in the case of As.

Before any tests were made at reduced pressure, one test (G) was made at atmospheric pressure at 750°C to determine whether Sb_2O_3 could be removed from a slag without the necessity of applying a vacuum. The results of test G are included in Figure 25 and clearly indicate that no substantial reduction in the Sb content of the slag took place. Approximately 2 gm of condensate were recovered which contained 74.87 wt % of Sb_2O_3 and 22.37 wt % PbO.

The results of a series of tests made under reduced pressure at 650° and 750°C are given in Table 6 and included in Figure 25. In test E, made at 650°C, approximately 30% of the Sb was removed from the slag over a 4-hr period. Very little condensate was recovered, however, which may have been due to the nucleation of solid particles of Sb_2O_3 in the gas phase which were swept out of the reaction tube by the vacuum pump. The condensate which was recovered contained 92.29 wt % Sb_2O_3 and 4.42 wt % PbO, which is a considerable improvement in grade over the previous test (G).

The remaining two tests made at 750°C (F and AA) differ only in duration. By increasing the time from 4 hr (test F) to 12 hr (test AA), a further small reduction in the Sb_2O_3 content of the slag was achieved with a corresponding

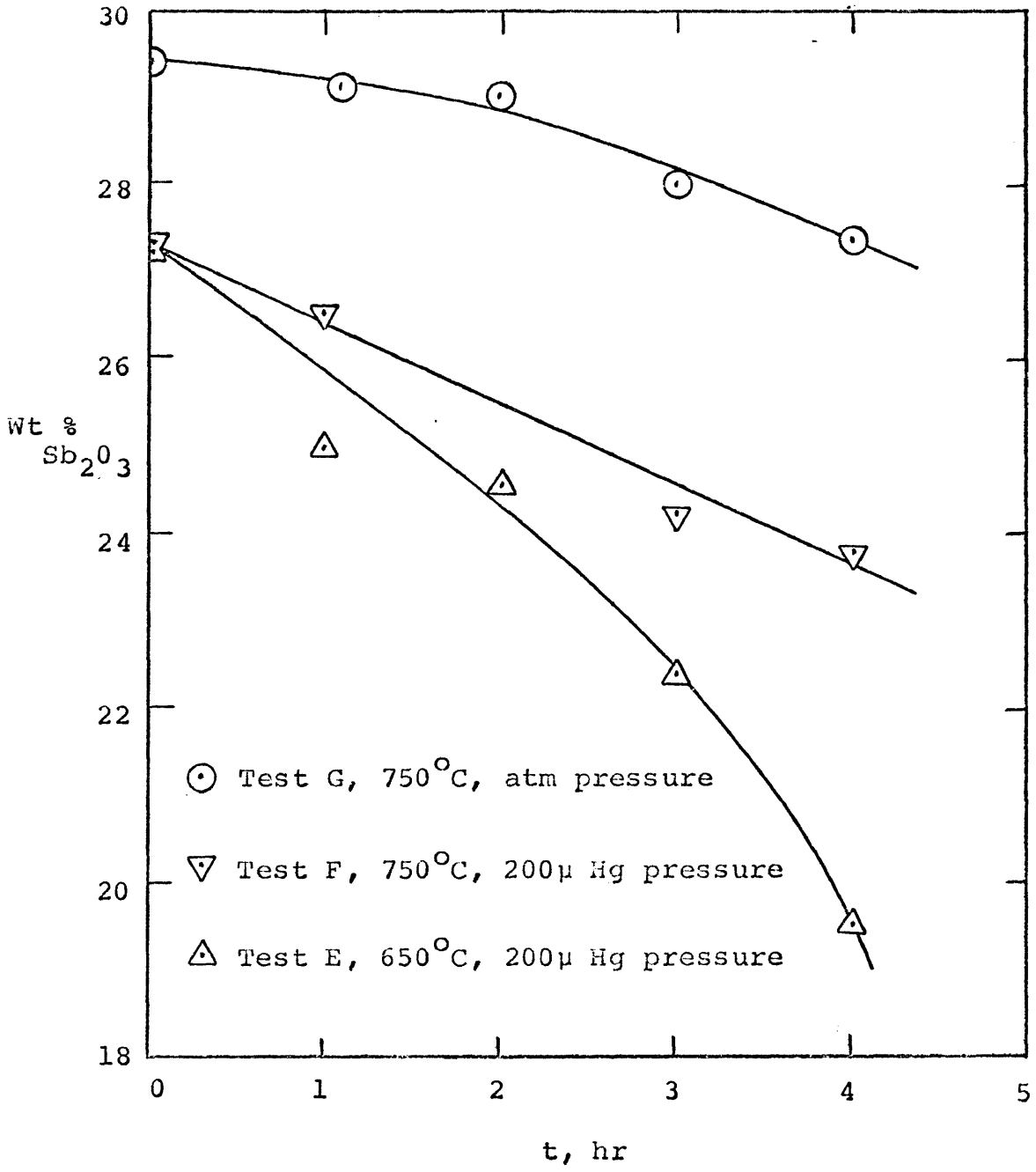

Figure 25. Removal of Sb from a 30 wt % Sb_2O_3-PbO Slag by Vacuum Distillation at 650° and 750°C

increase in the yield of condensate. Both condensates produced contained in excess of 95 wt % Sb_2O_3.

The results of a second series of tests (II, HH, JJ, BB, and GG) made on Sb_2O_3-PbO slags are given in Table 6 and shown graphically in Figures 26 and 27. The results of test II, made at 700°C, and tests HH and JJ, made at 775°C, offer little more than what has been learned from the tests already described. It is apparent that as the temperature is raised the removal of Sb_2O_3 becomes increasingly more efficient because of the increased vapor pressure of Sb_4O_6 and the decreased viscosity of the slags, which provides for more effective stirring of the melt. The analyses of the condensates produced in these tests, given in Table 6, appear to be somewhat uncertain due to the fact that they begin to show in excess of 100 wt % Sb_2O_3. By assuming that the PbO analyses are somewhat more reliable, however, the condensates appear to contain at least 98 wt % Sb_2O_3.

The disadvantage of operating at higher temperatures is shown by the results of tests BB and GG which were made at a temperature of 850°C. The results of these tests are given in Table 6 and shown graphically in Figure 26. The increased volatility of Sb_4O_6 together with the decreased slag viscosity result in more efficient removal of Sb from the slag but the higher temperature also allows for the increased volatility of PbO. In both tests the recovery of

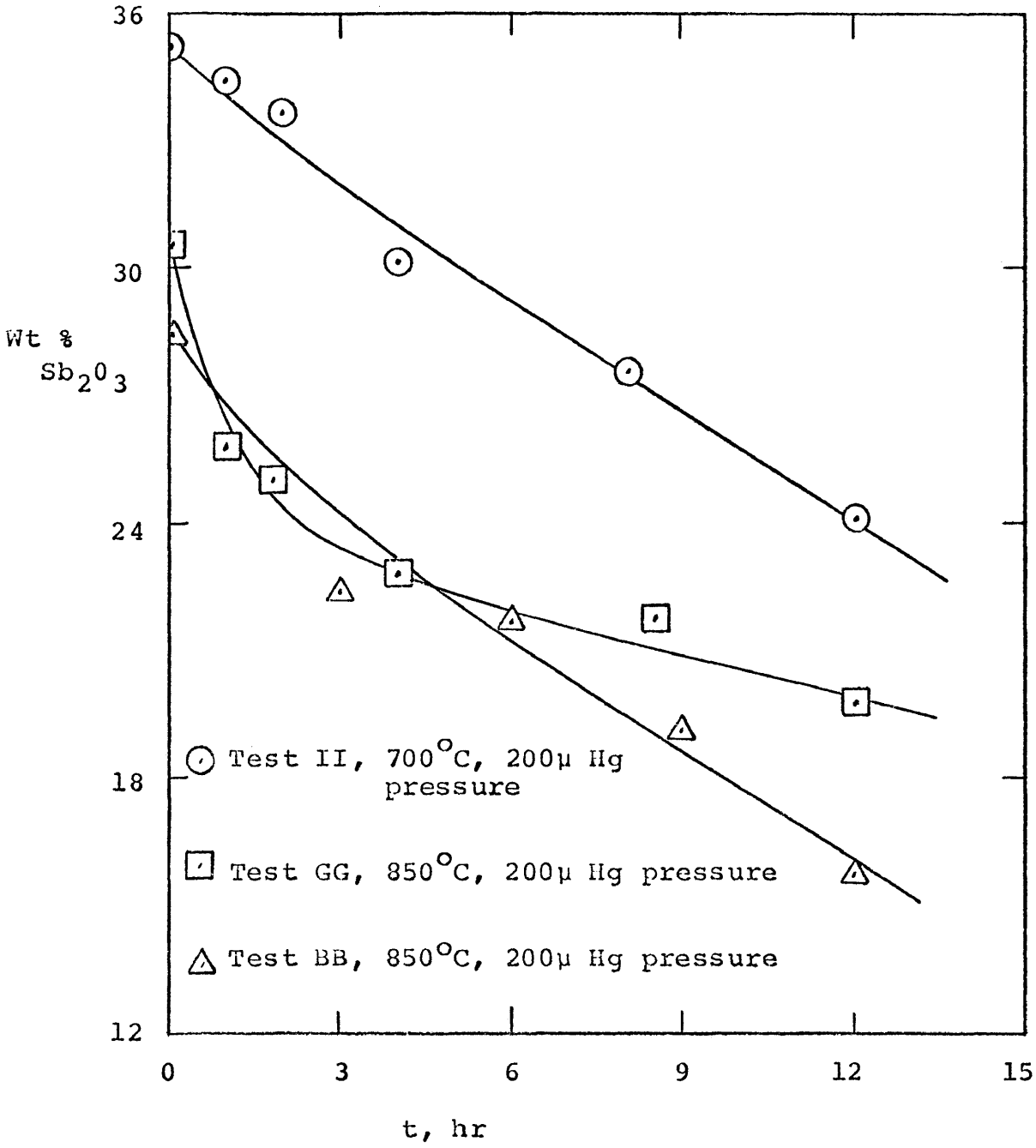

Figure 26. Removal of Sb from a 30 wt % Sb_2O_3-PbO Slag by Vacuum Distillation at 700° and 850°C

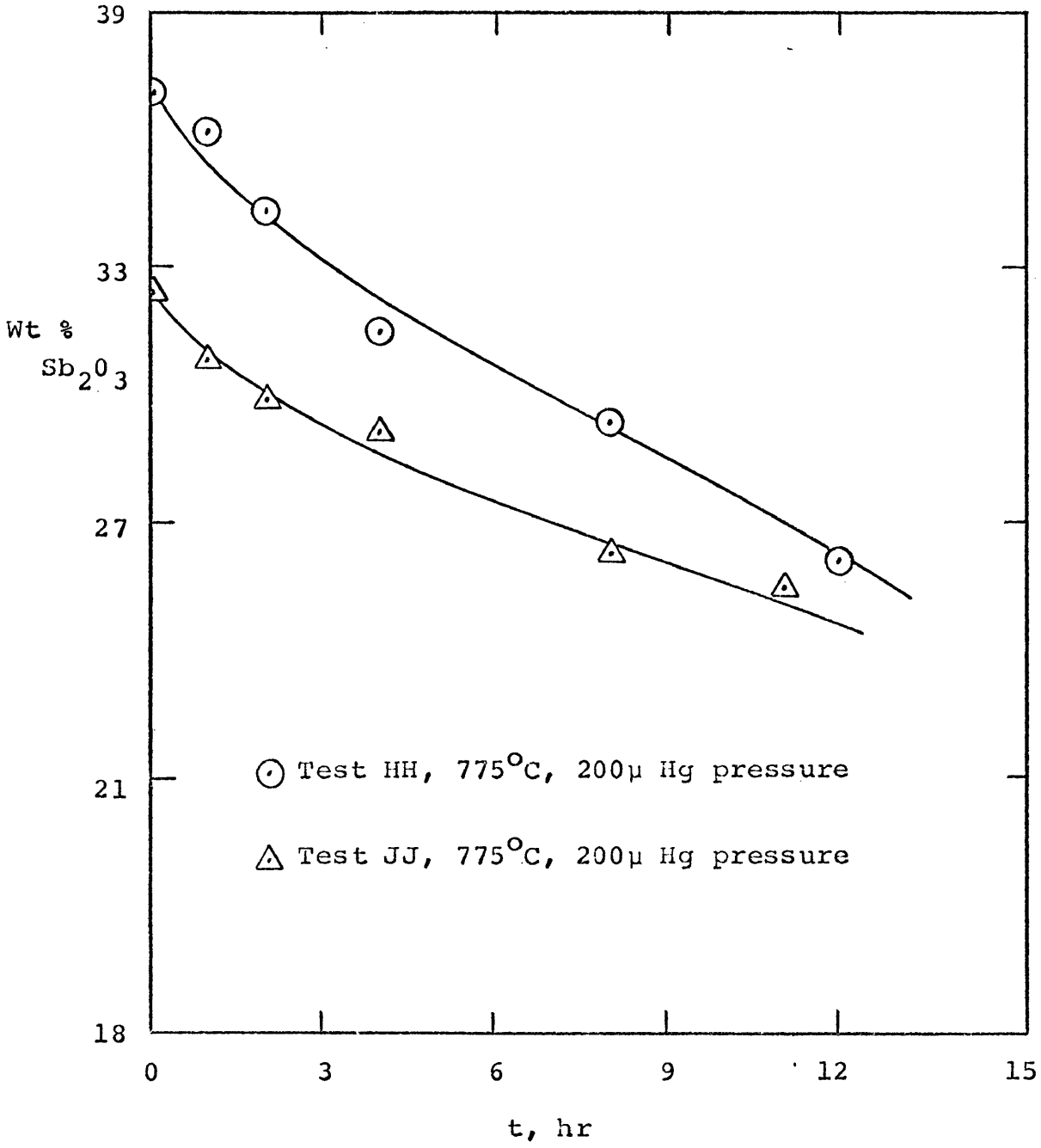

Figure 27. Removal of Sb from a 30 wt % Sb_2O_3-PbO Slag by Vacuum Distillation at 775°C

Sb as the trioxide was found to be greater than 70 wt %. The purity of the condensates produced was, however, quite a bit lower than that for tests II, HH, and JJ. The increased vapor pressure of PbO at this temperature accounted for approximately 6 wt % PbO in the condensates.

A third series of tests made on PbO-Sb_2O_3 slags was carried out at 700°C without first preforming the slags at a higher temperature to insure a completely liquid melt at the beginning of the tests. The slags used for tests LL and MM were preformed, cooled, and ground to 90%-65 mesh. In test LL the removal of Sb_2O_3 was approximately the same as that observed for test II, in which the slag was initially super-heated. The surface of the particles of slag used for this test were depleted in Sb_2O_3 during the heating-up period and prevented their coalescing into one mass. Some sintering was observed at the end of the test but the slag remained rather loosely granular. Test MM essentially duplicated test LL except that the initial Sb content of the slag was reduced to 22 wt %, approximately the composition of the slag at the end of test LL. Practically no further reduction in the Sb content of the slag was achieved in this test. Test NN was also essentially a duplication of test LL with the exception that the preformed slag was ground to 90 % -150 mesh. The Sb content of the slag decreased from 26.95 wt % Sb_2O_3 initially to 7.40 wt % Sb_2O_3

at the end of the 8-hr period. The much reduced particle size resulting in an even greater increase in the specific surface was responsible for the very low level to which Sb was removed from the slag. The condensates produced in tests LL and NN contained above 98 wt % Sb_2O_3. The condensate produced in test MM showed a somewhat lower Sb content due to the small amount of removal of Sb_2O_3.

One series of tests was made to determine the relative rates at which As and Sb could be removed from a 3 wt % As_2O_3-30 wt % Sb_2O_3-PbO slag at 750° and 800°C under a reduced pressure of 200μ Hg. The results of these tests (P and CC) are given in Table 6 and shown graphically in Figure 28. The removal of Sb from these slags compares with the results obtained in the previous tests made on the binary slags. The removal of As, however, presents an interesting phenomenon. In test P the removal of As just balances the reduction in the total slag volume caused by the distillation of relatively large amounts of Sb_2O_3. As a result, the concentration of As in the melt remains virtually constant. When the temperature is raised to 800°C, for test CC, the increased rate of removal of Sb causes the residual concentration of As in the slag to actually increase during the test. The condensates produced in these two tests contained less than 2 wt % PbO and almost equal amounts of As_2O_3; 3.07 wt % for test P and

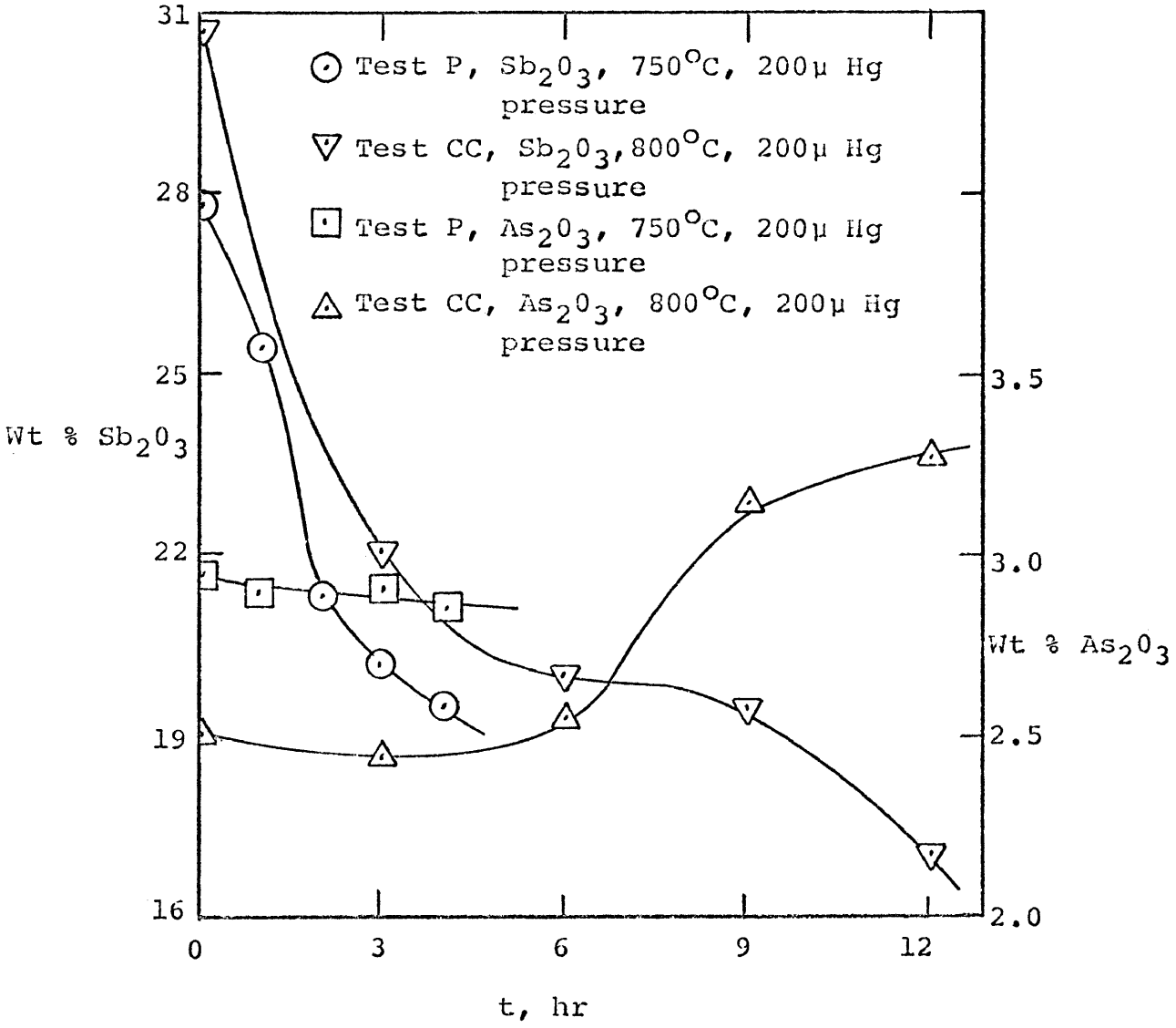

Figure 28. Removal of As and Sb from a 3 wt % As_2O_3-30 wt % Sb_2O_3-PbO Slag by Vacuum Distillation at 750° and 800°C

2.58 wt % for test CC.

Since the vapor pressure of SnO_2 is considerably less than that of either Sb_2O_3 or As_2O_3, and since lead-softening slags seldom contain more than 10 wt % SnO_2, no comprehensive series of tests was made to investigate the vacuum distillation of SnO_2 from SnO_2-PbO slags. One test (U) was made on a 3 wt % As_2O_3-25 wt % Sb_2O_3-12 wt % SnO_2-PbO slag under reduced pressure at 700°C. The results of this test are given in Table 6. Neither of the three impurity oxides present was removed from the slag to any appreciable extent. Twenty-seven gms of condensate were recovered which contained 95.28 wt % Sb_2O_3, 2.96 wt % As_2O_3, 2.34 wt % SnO_2, and 0.99 wt % PbO.

The vacuum-removal experiments briefly outlined above were performed in an attempt to determine the feasibility of removing As_2O_3, Sb_2O_3, and SnO_2, at the concentrations at which they normally occur in lead-softening slags. This procedure is not technically feasible under the conditions used in this investigation and, as a result, will not be considered further.

The vacuum distillation of Sb_2O_3 from lead-softening slags appears to be much more favorable. Two main factors contribute to the potential application of vacuum techniques to the removal of Sb_2O_3. Of primary importance is the fact that the vapor pressure of Sb_4O_6 is very much higher than

that of PbO. As a result, a near-perfect separation of Sb_2O_3 from PbO is at least theoretically possible. The second factor, of perhaps more importance than the first, is that commercially-produced lead-softening slags normally contain much higher concentrations of Sb_2O_3 than of either As_2O_3 or SnO_2. This high concentration of Sb_2O_3 allows for a sufficiently rapid rate of removal as to be of interest economically.

Several of the tests described above resulted in the removal of approximately 75% of the original Sb_2O_3 content of the slag. The time required to achieve this result, however, is much too long to be of interest on a commercial scale. Therefore, before any set of optimum conditions for the vacuum removal of Sb_2O_3 from lead softening slags can be formulated, it is necessary to reduce this time as much as possible.

The Removal of Sb_2O_3 from $PbO-SiO_2-Sb_2O_3$ Slags at Reduced Pressure and Elevated Temperature. The rate of removal of Sb_2O_3 from lead-softening slags can be achieved in either or both of two ways. The most obvious of these would be to conduct the tests at a lower reduced pressure. In doing so, however, the vaporization of PbO would also be increased which would result in an impure condensate being produced. A second alternative would be to determine suitable slag addition agents which would result in 1) an

increased activity, and hence an increased vapor pressure, of Sb_2O_3, 2) a decreased activity, and hence a decreased vapor pressure of PbO, and 3) a decreased slag viscosity. Either or all of these effects would result in an increased yield of higher purity Sb_2O_3 condensate.

It was determined that the addition of silica to the binary PbO-Sb_2O_3 slags studied in the previous section would fulfill the second objective of a desirable addition agent, as discussed above. Lead oxide has a strong tendency to form silicates in the presence of silica at elevated temperatures. The phase diagram for the PbO-SiO_2 system is shown in Figure 29. It can be seen from Figure 29 that PbO forms at least 3 stable Pb-silicates at elevated temperatures; β-$4PbO \cdot SiO_2$, $2PbO \cdot SiO_2$, and $PbO \cdot SiO_2$. In addition, at least one other Pb-silicate has been observed to occur in nature with a composition corresponding to $3PbO \cdot 2SiO_2$. In order to determine the effect of silica additions to lead-softening slags on the rate of removal of Sb_2O_3 under reduced pressure, a series of tests was conducted in which the amount of silica added was varied from 4.3 wt % to 14.7 wt % SiO_2. The relative amounts of PbO and SiO_2 contained in the slags correspond to the points labeled A, B, C, D, and E in Figure 29. In all of the tests made, the concentration of Sb_2O_3 was held constant at approximately 30 wt % initially.

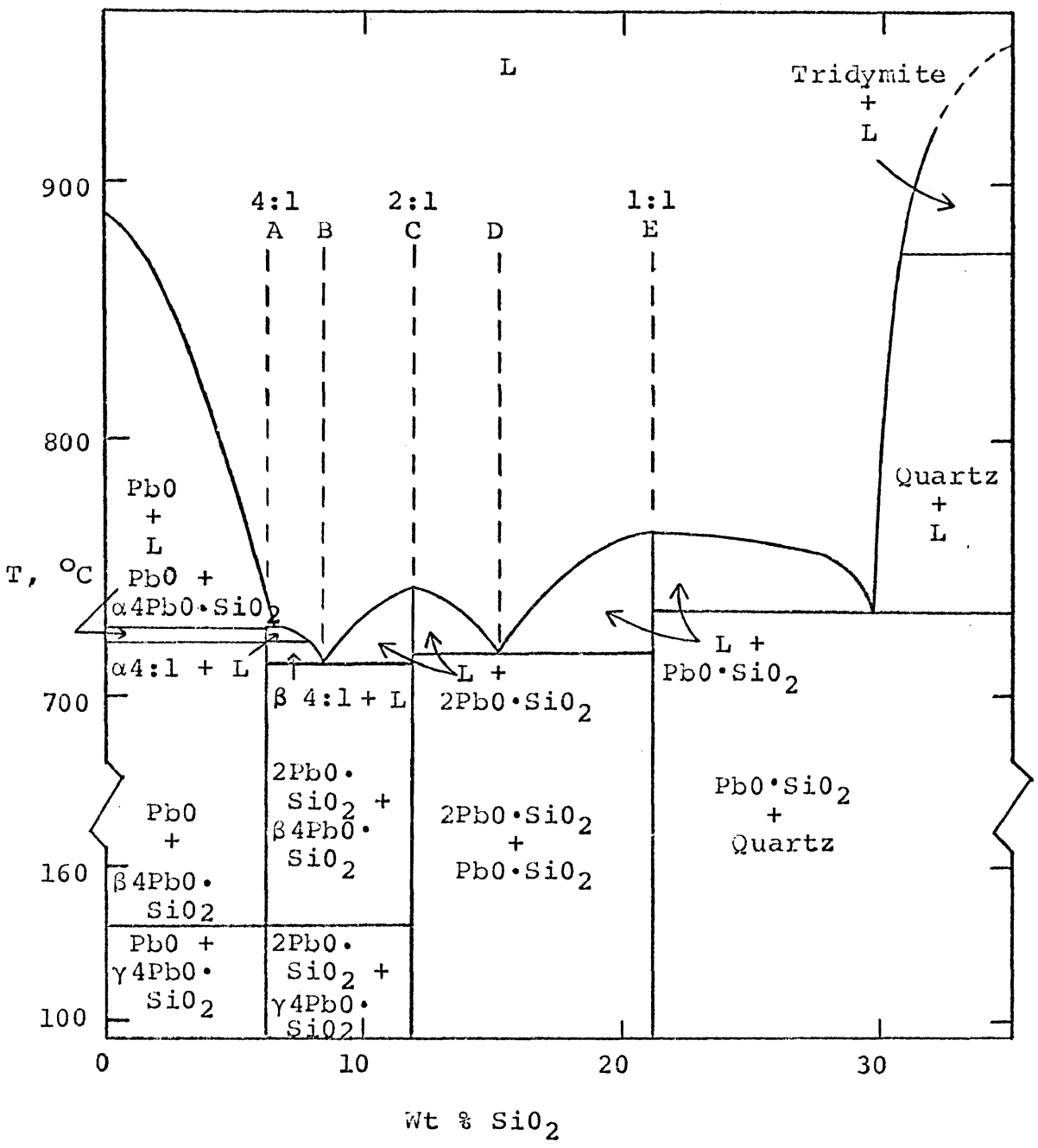

Figure 29. Phase Diagram for the Pb0-rich End of the Pb0-SiO_2 System

The results from this series of tests are presented in tabular form in Table 7 and shown in graphical form in Figures 30-34. Each test was repeated at temperatures of 750° and 850°C under a reduced pressure of 200μ Hg. In tests RR and SS the molar ratio of PbO to SiO_2 was adjusted to a value of 4, corresponding to the point A in Figure 29. It is apparent from Figure 30 that the rate of removal of Sb_2O_3 was approximately the same as that observed for the most successful test made without silica additions for test RR made at 750°C. Eighty gms of condensate were produced in this test which contained 98.71 wt % Sb_2O_3 (determined from PbO analysis). By increasing the temperature to 850°C, an increased degree of removal of Sb_2O_3 was obtained. Test SS resulted in a decrease in the Sb_2O_3 content of the slag from 33.7 wt % initially to 16.0 wt % at the end of the 8-hr period. This test produced 119 gms of condensate which contained 93.86 wt % Sb_2O_3. The decreased purity of the condensate was due to the increased volatilization of PbO at the higher temperature.

The second pair of tests (VV and WW shown in Figure 31) was made with a molar ratio of PbO to SiO_2 of 2.91, corresponding to the eutectic composition between β-$4PbO \cdot SiO_2$ and $2PbO \cdot SiO_2$ shown as point B in Figure 29. A further increase in the degree of removal of Sb_2O_3 from the slag was observed. The results of test VV, made at 750°C, are

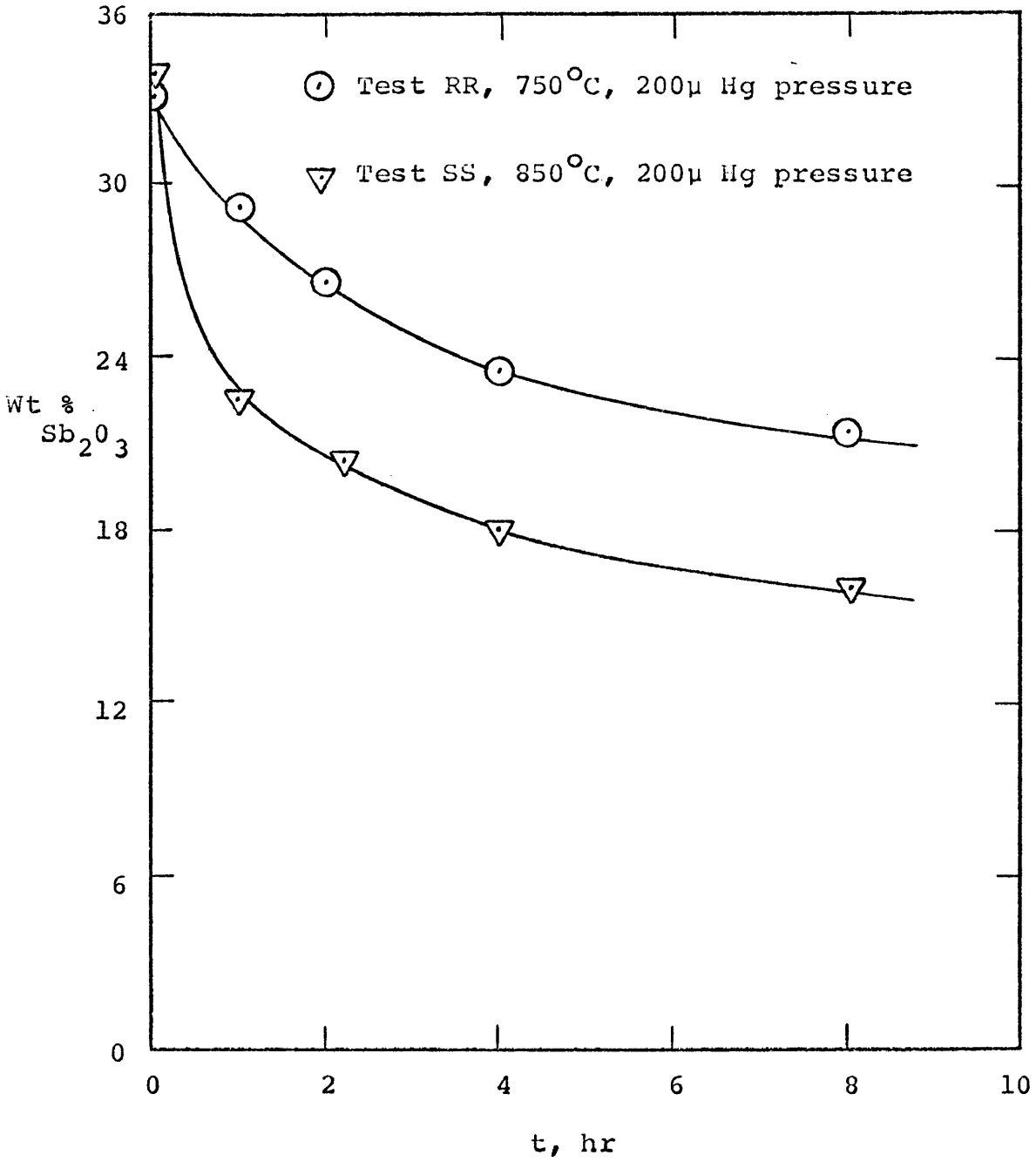

Figure 30. Removal of Sb from a 4.3 wt % SiO_2-30 wt % Sb_2O_3-PbO Slag by Vacuum Distillation at 750° and 850°C

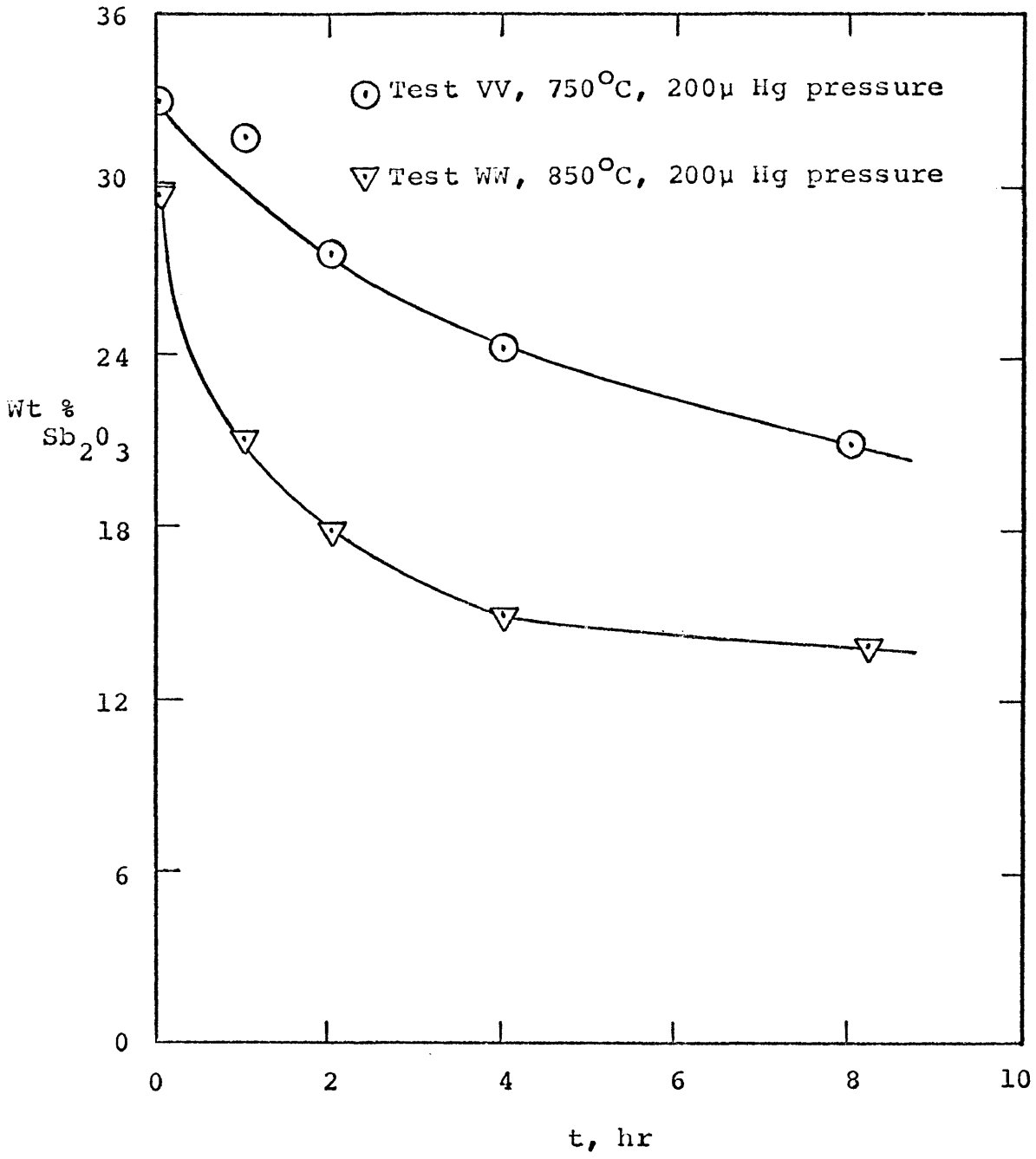

Figure 31. Removal of Sb from a 5.6 wt % SiO_2-30 wt % Sb_2O_3-PbO Slag by Vacuum Distillation at 750° and 850°C

somewhat erratic and are probably not representative. The increased efficiency of removal is well-pronounced, however, at 850°C in the results for test WW. The recovery of Sb_2O_3 in the condensate was slightly greater in these tests than what was observed for tests RR and SS. The purity of the condensates produced in these tests was also noticeably higher than was observed in tests RR and SS.

The third and fourth pairs of tests (PP and QQ shown in Figure 32 and XX and YY shown in Figure 33) were conducted on slags with a molar ratio of PbO to SiO_2 of 2 and 1.47, respectively. A further increase in the degree of removal of Sb_2O_3 was observed for these tests over that obtained for tests VV and WW. The results of these 2 pairs of tests are seen to be nearly identical at the respective temperatures and will be discussed together. The condensates produced in tests PP and XX contained approximately 70% of the original amount of Sb_2O_3 contained in the slag at a purity of 99 wt % Sb_2O_3 or higher. The condensates produced in tests QQ and YY, made at 850°C accounted for a recovery of approximately 87% of the Sb_2O_3 at a purity of greater than 98 wt % Sb_2O_3.

Because of the high degree of removal of Sb_2O_3 from slags containing 8.2 and 10.5 wt % SiO_2, tests PP and QQ were duplicated at greatly reduced pressure under the same conditions of temperature. The results of these tests (AB and AC), made at a pressure of 5μ Hg, have been included

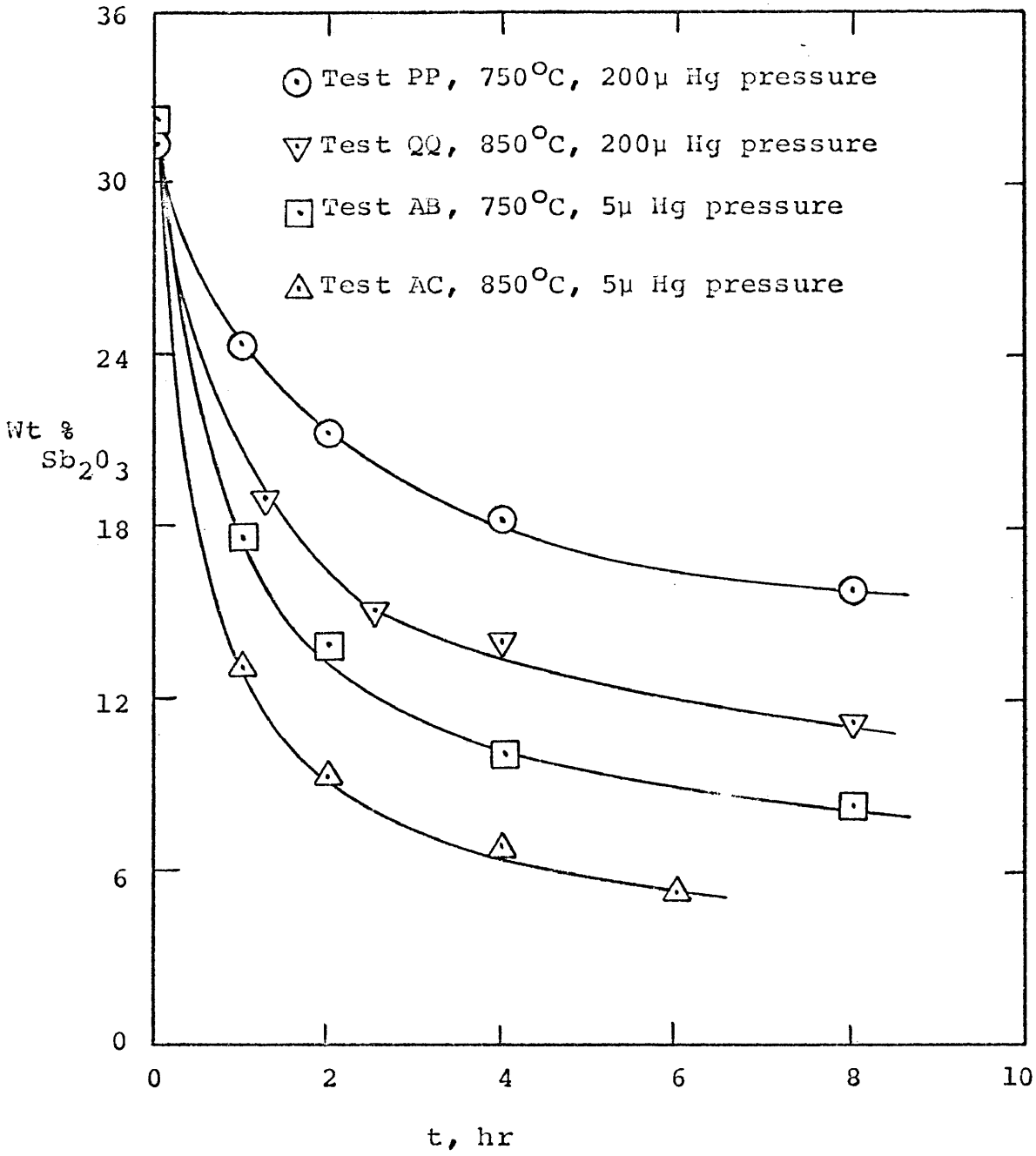

Figure 32. Removal of Sb from a 8.2 wt % SiO_2-30 wt % Sb_2O_3-PbO Slag by Vacuum Distillation at 750° and 850°C

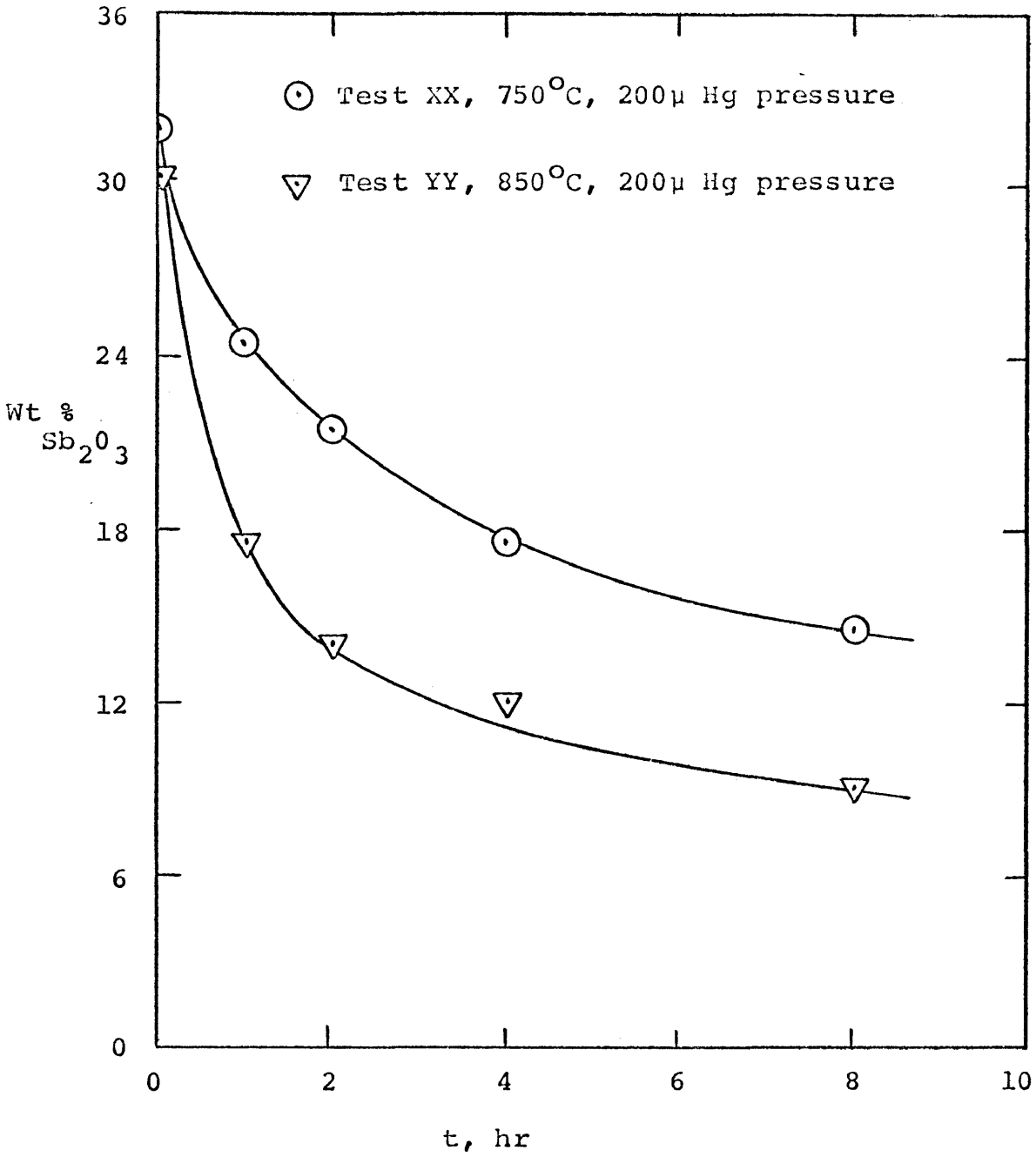

Figure 33. Removal of Sb from a 10.5 wt % SiO_2-30 wt % Sb_2O_3-PbO Slag by Vacuum Distillation at 750° and 850°C

in Figure 32 for comparison with tests PP and QQ. It is readily apparent that the decreased pressure results in a much more efficient removal of Sb_2O_3. Because of this very low pressure, however, the increased volatilization of PbO results in a significantly reduced purity of the condensate. In both tests AB and AC the concentration of PbO in the condensate was approximately 5 wt %.

In order to complete the investigation of the effects of silica additions on the rate of removal of Sb_2O_3 from lead-softening slags under reduced pressure at elevated temperatures, a final pair of tests was conducted in which the molar ratio of PbO to SiO_2 was held at a value of 1. This ratio corresponds to the point E on the phase diagram for the PbO-SiO_2 system shown in Figure 29. The greatly increased viscosity of this melt resulted in a much less efficient removal of Sb_2O_3 as shown by the results for tests TT and UU presented in Figure 34. The purity of the condensates produced in these 2 tests was the highest, however, for the condensates produced in this series of tests. Test TT yielded 73 gms of condensate containing 99.5 wt % Sb_2O_3 while test UU yielded 107 gms of condensate containing 99.25 wt % Sb_2O_3.

Quantitative information regarding the intermolecular forces in complex Pb-silicate melts would be helpful in explaining the relative ease with which Sb_2O_3 could be

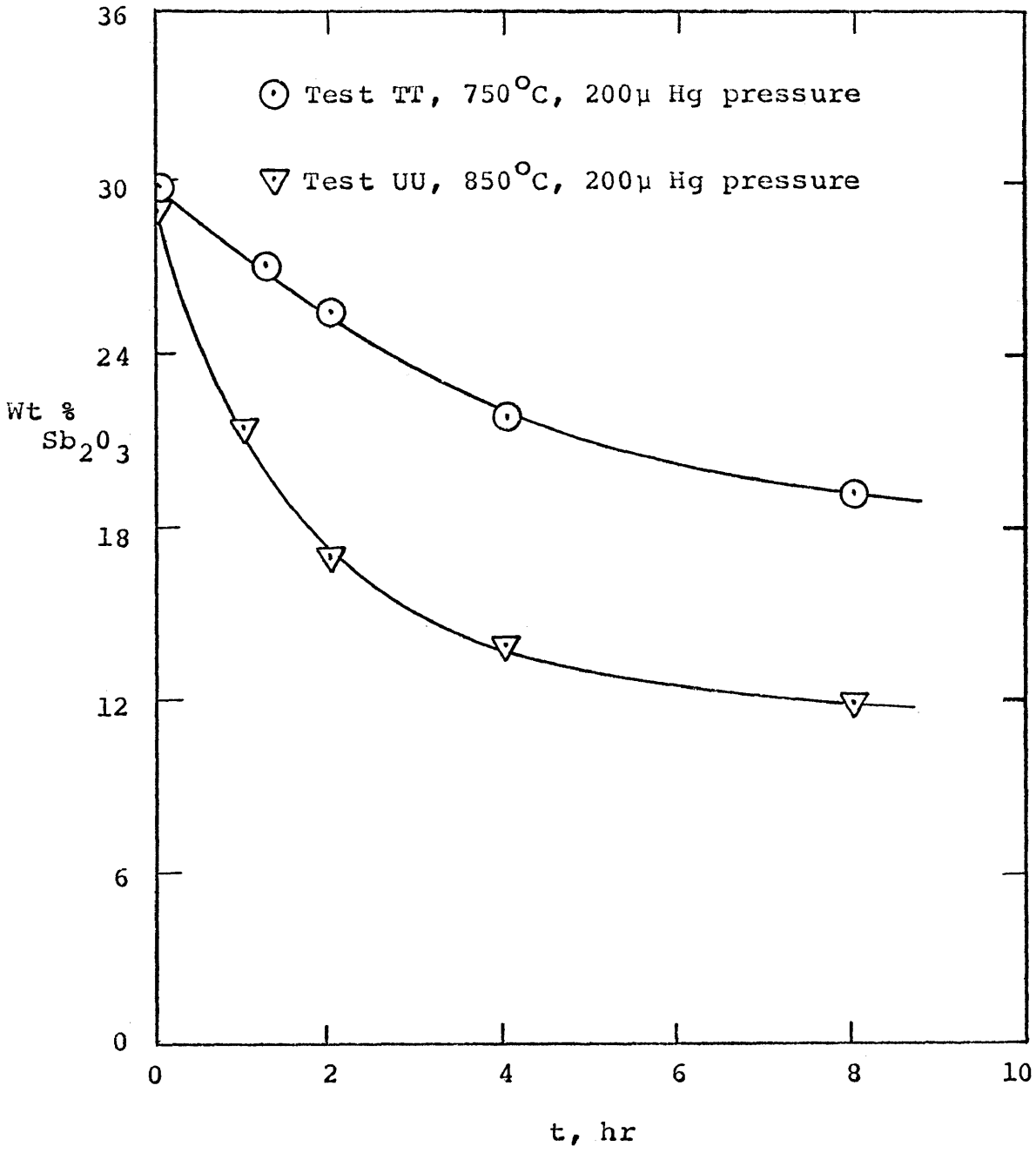

Figure 34. Removal of Sb from a 14.7 wt % SiO_2-30 wt % Sb_2O_3-PbO Slag by Vacuum Distillation at 750° and 850° C

distilled from PbO-SiO_2-Sb_2O_3 slags. However, due to a general lack of such information in the literature, no such discussion can be made here. It is possible, however, to make the qualitative statement that as the concentration of SiO_2 in these ternary slags is increased from 4.3 wt % to 10.5 wt %, the degree to which Sb_2O_3 can be distilled from them under reduced pressure is correspondingly increased. As the concentration of SiO_2 is increased above 10.5 wt %, the vacuum removal of Sb_2O_3 becomes less efficient.

In order to compare the rates at which Sb_2O_3 can be distilled from lead softening slags which contain silica additions and those which do not, some quantitative information regarding the vapor pressure of Sb_4O_6 above these slags is required. It was for this purpose that the PbO to SiO_2 ratio of 2 was selected for the vapor pressure study of PbO-SiO_2-Sb_2O_3 slags discussed in a previous section. In referring to Figure 23, it is seen that the vapor pressure of Sb_4O_6 above the Pb-silicate slags at 700°C is greater than that above the binary Sb_2O_3-PbO slags at all compositions above approximately $X_{Sb_2O_3} = 0.21$ (on PbO + Sb_2O_3 basis). This difference in vapor pressure accounts for the more rapid initial rate of removal of Sb_2O_3 observed in the case of the slags containing silica over those which do not. Using Equation (16) and the equilibrium Sb_2O_3 content for a PbO-SiO_2-Sb_2O_3 ($\frac{PbO}{SiO_2} = 2$) slag in contact

with Pb at 700°C (test BF, Table 8), a_{PbO} is calculated to be 0.571 (on $PbO+Sb_2O_3$ basis). A similar calculation has been made for the $PbO-Sb_2O_3$ system for $X_{Sb_2O_3} = 0.0683$ with the result that $a_{PbO} = 0.964$. Thus, it is apparent that the addition of SiO_2 to $PbO-Sb_2O_3$ slags results in an increase in the purity of the condensate due to the resulting decrease in the activity, and hence vapor pressure, of PbO.

The fact that the concentration of Sb_2O_3 can be reduced to much lower levels when silica is present is almost entirely due to the greatly increased fluidity of the silica-based slags. The very viscous nature of the binary $PbO-Sb_2O_3$ slags prevented the stirring action from constantly replenishing the surface of the melt with Sb_2O_3. As a result, the transport of Sb_2O_3 from the bulk solution to the surface of the melt became the rate determining step which controlled the actual rate of removal. Because of the very fluid nature of the majority of the Pb-silicate slags, stirring was very effective and the concentration of Sb_2O_3 was observed to be decreased to much lower levels than was observed for the slags containing no silica additions.

Accurate mass balances on the tests described above, from which the % recovery of Sb_2O_3 could be calculated, could not be made in this investigation. The recoveries

mentioned above are meant to be only approximate values. Due to the formation of iron oxides on the crucibles used for the tests during cleaning, a significant amount of Pb metal was formed in some of the tests. The amount of Pb formed by reduction of PbO by FeO varied with the condition of the crucible and the temperature at which the tests were carried out. No reduction of PbO was observed with new crucibles. As much as 30 gms of Pb were produced in some of the tests made at 850°C. Also, some of the Pb and PbO present in the crucible vaporized and was observed to condense in the hotter, lower portion of the condenser where the PbO reacted with the silica and thus could not be recovered for weighing.

Based on the results of the tests described in the previous section, a process using reduced pressure at elevated temperature has been developed in which the Sb_2O_3 content of a 30 wt % Sb_2O_3-PbO slag can be reduced to 10 wt % or slightly less in a period of 8 hrs at 200μ Hg pressure. The Sb_2O_3 can be recovered as a dense, non-adhering condensate containing in excess of 99 wt % Sb_2O_3.

The conditions under which this process works best are as follows:

1) temperature - 750°C
2) pressure - 200μ Hg
3) slag addition agents - 8-10 wt % SiO_2

4) residual atmosphere - inert

The degree of removal of Sb_2O_3 will be increased as either the temperature is increased or the pressure is decreased. The purity of the condensate produced will decrease in either case, however.

Selected Slag-Metal Equilibria in the Sb_2O_3-SiO_2-PbO System

The process described in the preceding section for the recovery of Sb_2O_3 from lead-softening slags has the disadvantage of leaving a somewhat high Sb_2O_3 content in the residual slag. As a result, it might be desirable to recover both the Sb and Pb values remaining. An ideal way of achieving this result would be to use the residual slag for softening additional Pb bullion. After this operation, the slag could be returned for further vacuum treatment for the recovery of the Sb_2O_3. A cyclic process such as this would have the advantage of being able to use a small recirculating slag volume which would greatly reduce the slag and dross handling problems normally encountered with the softening of Pb bullion.

The results of several slag-metal equilibrations carried out for PbO-SiO_2-Sb_2O_3 slags in contact with dilute Pb-Sb alloys are given in tabular form in Table 8. The results of these tests indicate that the Pb-silicate slags produced in the vacuum removal of Sb_2O_3 tests are not

capable of softening Pb bullion to any considerable extent. The equilibrium Sb contents are all much too high to yield a refined Pb metal of acceptable purity.

A second alternative to the disposal of these slags would be to add them directly to the lead blast furnace using Fe as a reducing agent. If a sufficient market for antimonial-Pb exists, these slags may also be converted to this product in a separate reverberatory smelting operation in which the Pb-silicate slags would be reduced by Fe and carbon.

Vapor Pressure of As_4 above Dilute As-Pb Alloys at 703°C

The removal of As from lead-softening slags as the trivalent oxide by the application of vacuum techniques was shown not to be feasible by the results of tests described in an earlier section. Since the vapor pressure of As_4 above pure As is known to be very high, the application of vacuum techniques to the removal of elemental As from Pb bullion might provide an alternative method by which lead could be softened, at least insofar as As is concerned.

The literature contains almost no information regarding attempts by earlier workers to remove As from Pb by vacuum distillation. Caldwell, Spendlove, and St. Claire (1960, pp. 1-12) have studied the vacuum distillation of Cd, Zn, Mg, Te, Sb, and As from Pb and Sn over a range of

temperatures. No mention is made, however, as to whether As was successfully removed from the alloys supposedly studied. They have determined that Sb could not be removed from a 2.3 wt % Sb-Pb alloy at 1000°C.

In view of the lack of experimental data regarding the vaporization of As from Pb-As alloys, a somewhat limited vapor pressure study was made on alloys containing from 0.5 wt % to 3.3 wt % As in Pb. The results of this study are given in tabular form in Table 5 and shown graphically in Figure 10. The vapor phase above pure As at 703°C is composed of a mixture of As_4, As_2, and As. The vapor pressures of As_2 and As are, however, negligible with respect to the pressure of As_4. The sublimation temperature of As is given by Elliott and Gleiser (1960, p. 19) as 613°C and the melting point as 817°C under a pressure of approximately 28 atm.

The results given in Table 5 have been replotted in Figure 35 together with values of $X \cdot p^{o}_{As_4}$ (for an ideal As_4 solution) for comparison. The vapor pressure of As_4 above pure As at 703°C (referred to the hypothetical, supercooled liquid) is calculated to be 16,720 mm Hg using the data of Elliott and Gleiser for the heats of sublimation and fusion of As. It is readily apparent from Figure 35 that the vapor pressure of As_4 above dilute Pb-As alloys is much too low for the efficient removal of As from such

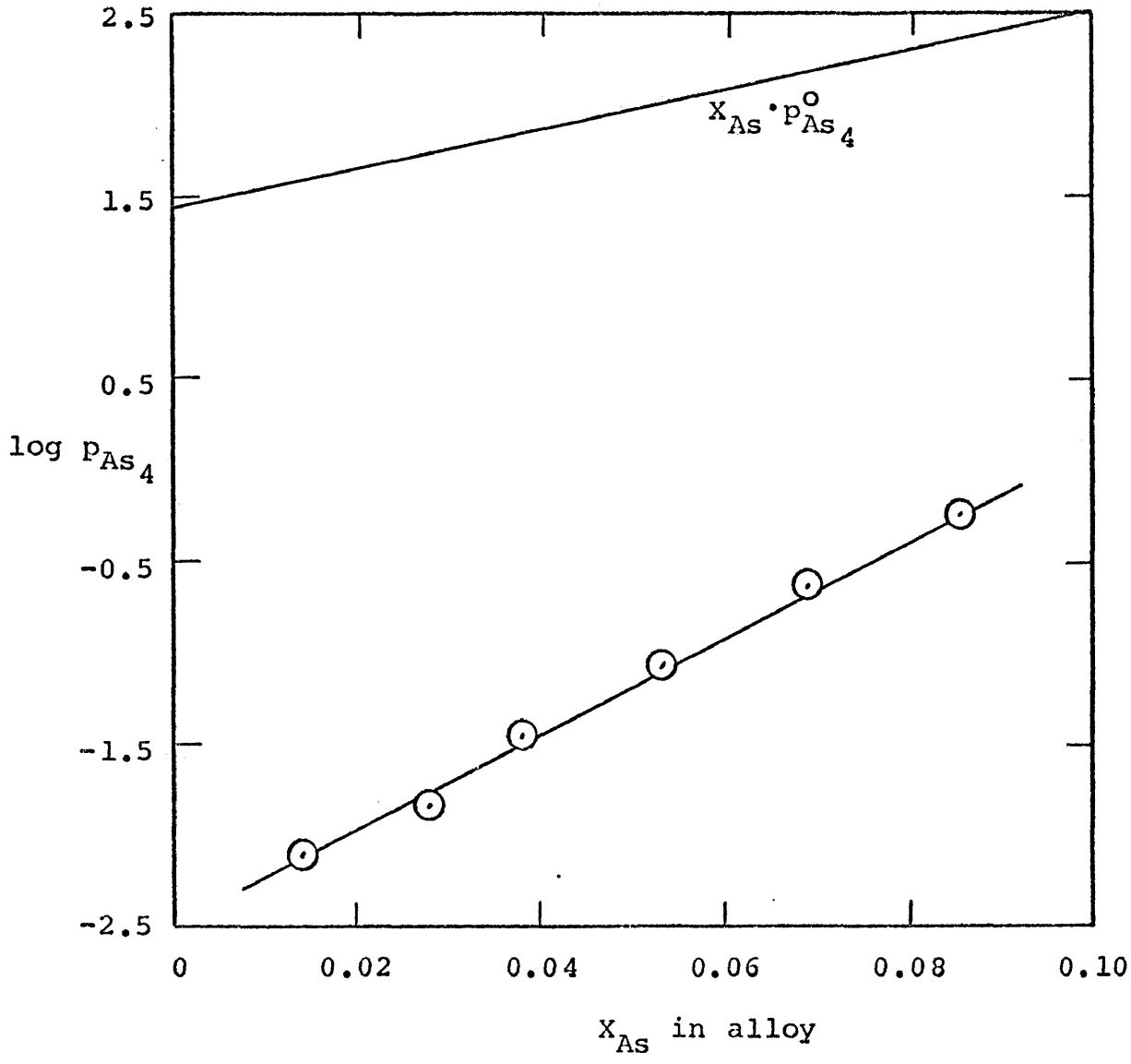

Figure 35. Vapor Pressure of As_4 above Dilute Pb-As Alloys at 703°C

alloys to concentrations much below 1 wt % As. Since the concentration of As in Pb blast-furnace bullion rarely exceeds 1 wt %, the application of vacuum techniques to the removal of As from Pb does not appear to warrant further investigation.

The data presented in Table 5 can be converted into the thermodynamic activity of As in Pb by division of p_{As_4} by $p^{o}_{As_4}$ = 16,720 mm Hg and taking the fourth root of the resulting pressure ratio. A Gibbs-Duhem integration of these activity data is presented in Table 17. A plot of the α-function for As in Pb is shown in Figure 36. It can be seen from the data of Table 17 and Figure 36 that the behaviour of As in dilute Pb-As alloys at 703°C is characterized by a near approach to ideality. Furthermore, it would appear that a regular solution model for the Pb-As system at 703°C would be a good approximation for the system for compositions above 5 mole % As due to the near-constant value of the α-function with composition. Although the slope of the α-function with composition appears to be zero for a portion of the composition range studied in this investigation, it is not safe to assume a regular solution model due to the rather narrow limits of the As concentration range. The apparent outlier represented by the alloy containing 1.43 mole % As is a result of the fact that the vapor pressure of As_4 above the alloy was barely detectable by the experimental

Table 17. Gibbs-Duhem Integration of As Activity Data Determined from Vapor Pressure Data on the Pb-As System at 703°C*

Wt % As	X_{As}	X_{Pb}	P_{As_4}, mm Hg	a_{As}	γ_{As}	$\ln\gamma_{As}$	$(X_{Pb})^2$	$\ln\frac{\gamma_{As}}{(X_{Pb})^2}$
0.52	0.0143	0.986	0.0078	0.0261	1.825	0.602	0.972	0.619
1.00	0.0279	0.972	0.0147	0.0306	1.097	0.093	0.945	0.098
1.41	0.0381	0.962	0.0351	0.0381	1.000	0.0	0.925	0.0
1.97	0.0527	0.947	0.0821	0.0471	0.894	-0.112	0.898	-0.125
2.61	0.0690	0.931	0.238	0.0614	0.890	-0.117	0.867	-0.134
3.28	0.0858	0.914	0.563	0.0762	0.888	-0.119	0.836	-0.142

* Completion of this procedure to obtain a_{Pb} is of no value due to the small number of closely-spaced data points.

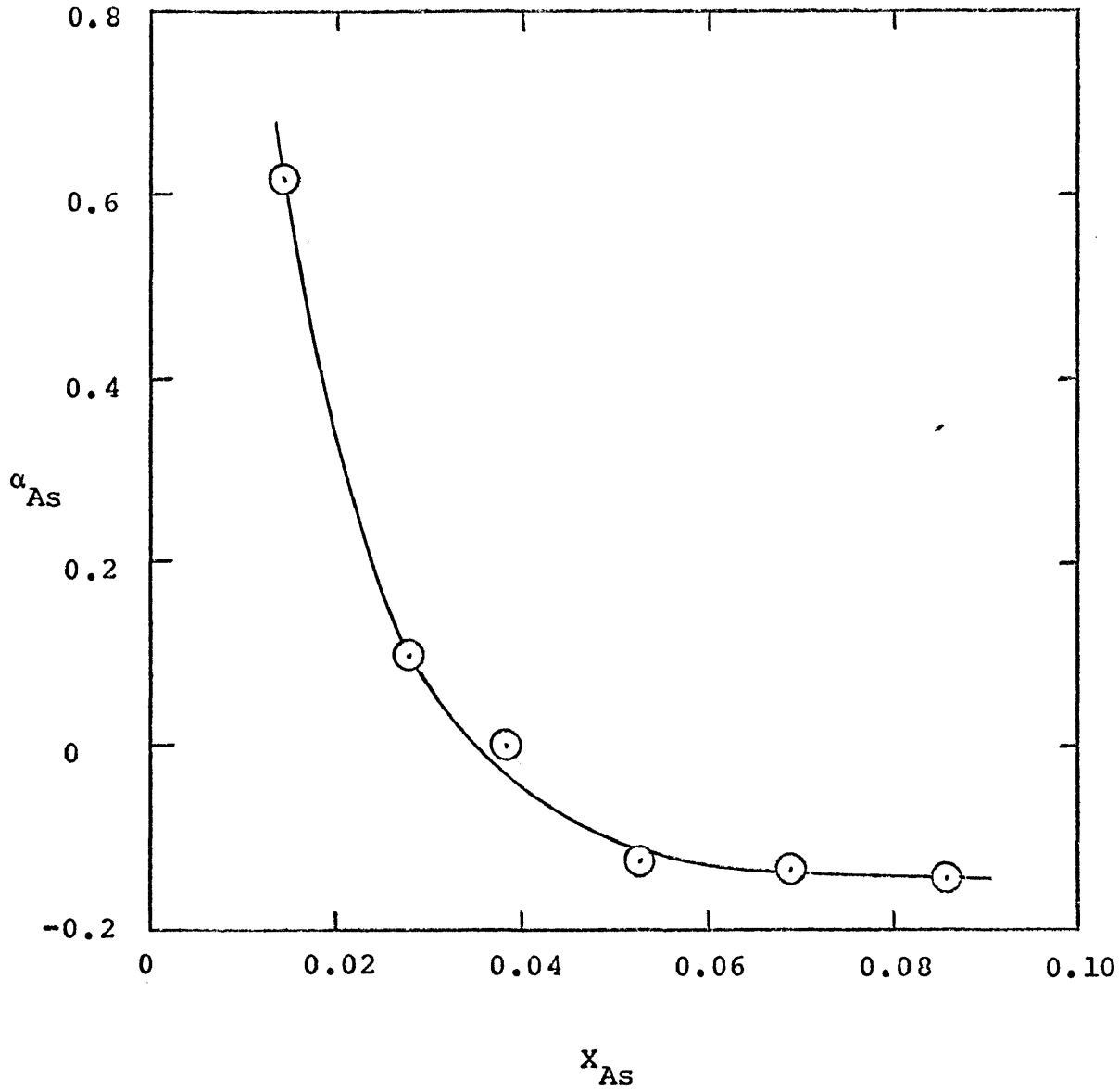

Figure 36. Variation of the As α-function with Composition for the Pb-As System at 703°C

procedure used in this investigation. Because of this, the apparent vapor pressure determined for this alloy could be in considerable error.

The activity of As in Pb determined in this investigation cannot be directly compared with the results of any previous investigators. As was mentioned previously, the literature contains very little information concerning the activity of As in Pb. J. H. Richards, Imperial Smelting Corporation Ltd. (1968, private communication) has described some thermodynamic investigations of dilute Pb-As alloys in the temperature range from 900°-1100°C. His results indicate similar pressure-composition relationships to those reported in this investigation. Moriyama and coworkers (1964, pp. 191-4) have also investigated the Pb-As system at temperatures from 450°-600°C. As a result of an emf study, they have found that the activity of Pb in this system shows a positive deviation from ideality over the entire composition range studied. The behavior of As was found to be characterized by a strong positive deviation from ideality. Since a detailed account of their work is not readily available, no English translation having been made of the original Japanese article, a thorough investigation of their results is not possible.

The activity of As in Pb determined in this investigation can be successfully predicted from the phase diagram

for the Pb-As system. The phase diagram consists of a single eutectic located at 7.6 wt % As at a temperature of 289°C. No compounds are known to exist between Pb and As, and no solid solubility has been reported for either As in Pb or Pb in As. Calculations for γ^{o}_{As}, using the Clausius-Clapeyron equation for freezing-point depression, have been made in the past by a number of investigators, among them Davey (1963, pp. 514-5). The results of such a calculation are shown in Figure 37. It is readily apparent from the figure that the regular-solution model used for the calculation represents a good approximation for a value of γ^{o}_{As} comparable to the values for the activity coefficient of As in dilute Pb-As alloys as determined in this investigation. Although the data of this investigation are somewhat limited, they indicate that γ^{o}_{As} might be slightly greater than unity. This would agree with the results of Moriyama and coworkers obtained at lower temperatures.

The results shown in Figure 38 represent an attempt to determine γ^{o}_{As} in the Pb-As system at 703°C. The very steep curvature observed at very low arsenic concentrations does not allow an accurate extrapolation to zero As concentration, however.

The results of this investigation, although far from complete, show that As in dilute Pb-As alloys at 703°C exhibits near-ideal-solution behavior. Because the vapor

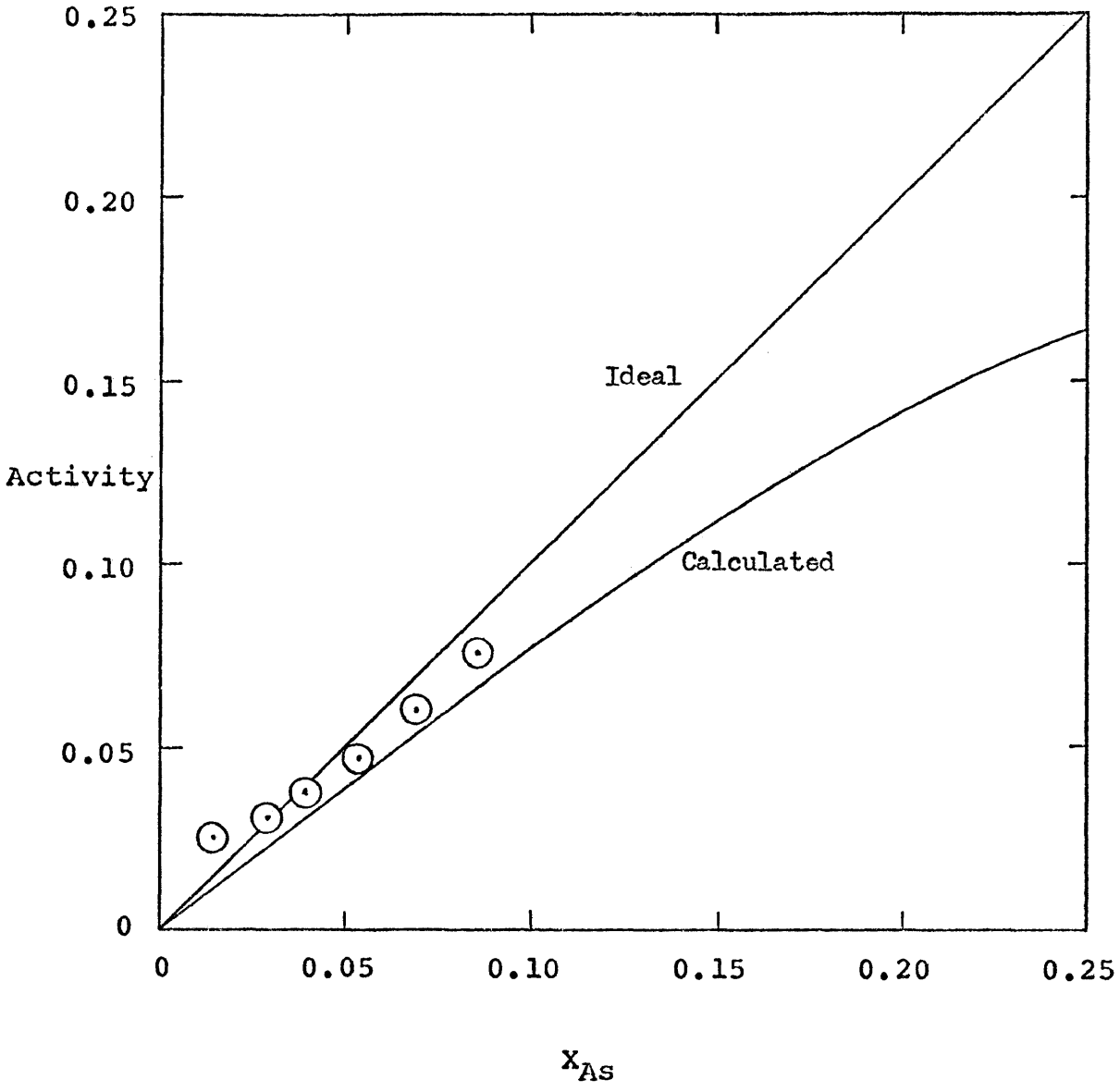

Figure 37. Activity of As in the Pb-As System at 703°C (Standard state - pure, hypothetical, supercooled liquid As)

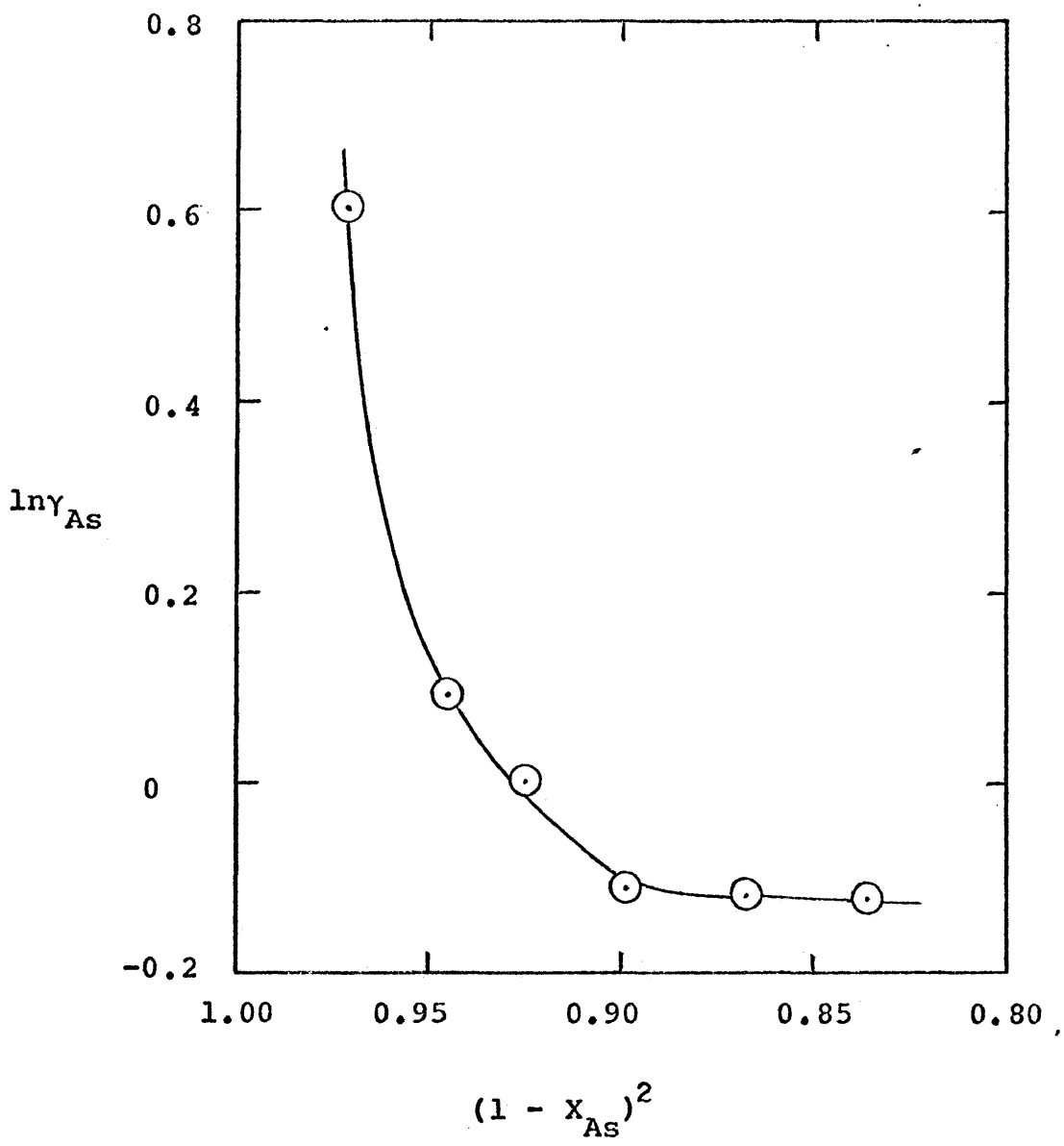

Figure 38. Variation of $\ln\gamma_{As}$ with Composition for the Pb-As System at 703°C

pressure of As_4 above Pb-As alloys is equal to $p^{o}_{As_4}(a_{As})^4$, ideality with respect to As does not insure a high pressure of As_4 above the alloys. As a result, the vacuum distillation of As from Pb blast-furnace bullion containing small amounts of dissolved As would not appear to be technically feasible at a temperature near 700°C.

CONCLUSIONS

On the basis of the experimental results obtained in this investigation, several conclusions can be made and several bases for further investigation can be proposed.

The vapor-pressure determinations which have been made in this investigation for the PbO-Sb_2O_3 system show that the behavior of Sb_2O_3 is characterized by a strong negative deviation from ideality at all compositions below 50 mole % Sb_2O_3 at 700°C. The behavior of PbO is characterized by a positive deviation from ideality at all compositions above approximately 63 mole % PbO and by a negative deviation from ideality in the range from 63 mole % to 50 mole % PbO at 700°C. In the PbO-SiO_2-Sb_2O_3 ($\frac{PbO}{SiO_2} = 2$) system, Sb_2O_3 exhibits a negative deviation from ideality at all compositions below 25 mole % Sb_2O_3. The slag systems do not form an ideal or a regular solution in either case.

Since the activities of both PbO and SiO_2 have been determined in the PbO-SiO_2 system by other investigators, the activity study in the PbO-Sb_2O_3 system reported in this investigation should be extended through the remainder of the system before suitable data can be obtained to yield

the individual component activities in the ternary $PbO-SiO_2-Sb_2O_3$ system.

In the temperature range from 650° to 750°C, the standard free energy of formation of liquid Sb_2O_3 is given by the expression: $\Delta G_f^o = -159{,}190 + 56.20\ T$. The equilibrium constant for the reaction:

$$2\ \underline{Sb}_{(1\ wt\ \%\ in\ Pb)} + 3\ PbO_{(l)} = Sb_2O_{3(l)} + 3\ Pb_{(l)}$$

is given by the expression: $\log K_{eq} = \frac{4980}{T} - 4.165$, for the temperature range from 650° to 750°C. The standard free energy of formation of $PbO \cdot Sb_2O_3$ from the elements at 604°C is calculated to be -146,580 cal.

The vacuum-removal experiments conducted in this investigation show that As and Sn cannot be efficiently removed as oxides from artificial lead-softening slags by vacuum distillation at the concentrations and temperatures normally encountered in the conventional fire-refining of lead.

A set of optimum conditions was determined to treat an artificial lead-softening slag containing 30 wt % Sb_2O_3. These optimum conditions were 200μ Hg pressure, or lower, and an addition of SiO_2 of from 8-11 wt % SiO_2. The process was successful in removing approximately 80 wt % of the original Sb_2O_3 content of the slag in 8 hr and producing a condensate containing in excess of 98 wt % Sb_2O_3 at temperatures of 750° and 850°C.

Several tests conducted in this investigation showed that successful recovery of Sb as the volatile trioxide from artificial lead-softening slags might be achieved at temperatures below the melting point of the slags. A full-scale investigation of this method would be necessary to determine if it would present major advantages over the process outlined above.

The vapor-pressure determinations made in this investigation for the Pb-As system show that As exhibits near-ideal-solution behavior, in agreement with the phase diagram, at 700°C. In view of the experimental results obtained, the vacuum distillation of As from very dilute Pb-As alloys at 700°C does not appear to be technically feasible in spite of the very high vapor pressure of pure As at this temperature.

SUMMARY

The vapor pressure of Sb_4O_6 was determined above PbO-Sb_2O_3 and PbO-SiO_2-Sb_2O_3 ($\frac{PbO}{SiO_2}$ = 2) slags at 700°C. The thermodynamic activity of Sb_2O_3 in both slag systems was calculated using the measured vapor-pressure data. In the PbO-Sb_2O_3 slag system, Sb_2O_3 was found to show a negative deviation from ideality at all slag compositions below 50 mole % Sb_2O_3. The behavior of PbO was found to be mixed. Activity coefficients for PbO, calculated by means of a Gibbs-Duhem integration of the Sb_2O_3 activity data, were found to exceed unity at all slag compositions above approximately 63 mole % PbO. At slag compositions between 63 mole % and 50 mole % PbO, activity coefficients were found to be less than unity. In the PbO-SiO_2-Sb_2O_3 ($\frac{PbO}{SiO_2}$ = 2) slag system, Sb_2O_3 was found to show a negative deviation from ideality at all slag compositions below 25 mole % Sb_2O_3. A calculation for the activities of PbO and SiO_2 in the silicate slag system was not possible due to a lack of sufficient data.

The vapor pressure of Sb_4O_6 above pure, solid, cubic Sb_2O_3 was determined for the temperature range from 422° to

599°C. The logarithm of the measured vapor pressure above cubic Sb_2O_3 was observed to vary directly with reciprocal absolute temperature.

Tests were made on the rate of removal of As, Sb, and Sn as oxides from 500 gm of 3 wt % As_2O_3-PbO, 3 wt % As_2O_3-30 wt % Sb_2O_3-PbO, 30 wt % Sb_2O_3-PbO, and 3 wt % As_2O_3-30 wt % Sb_2O_3-10 wt % SnO_2-PbO artificial lead-softening slags under reduced pressure conditions at temperatures between 500° and 850°C. The results of these tests indicated that successful removal of As and Sn as oxides, at the concentrations studied in this investigation, was not technically feasible at a reduced pressure of 200μ Hg. The results obtained for Sb, however, suggested the possibility of removing Sb as the volatile trioxide under a reduced pressure of 200μ Hg at temperatures above 700°C.

As a means of increasing the recovery of Sb from PbO-base slags, tests were made on the rate of removal of Sb from slags containing a variable SiO_2 content. The addition of SiO_2 to lead-softening slags improves the recovery of Sb as the volatile trioxide by increasing the activity of Sb_2O_3 in the slag at compositions greater than 13 mole % Sb_2O_3. In addition, it was observed that the increased fluidity of the slags containing an optimum SiO_2 concentration accounted for an increased rate of removal of Sb at low Sb_2O_3 concentrations where the activity of Sb_2O_3 was lower than that

determined for the slags containing no SiO_2 additions. The purity of the condensates produced during the tests made on slags containing SiO_2 additions was also found to be higher than that observed for similar slags containing no SiO_2 due to a reduction in the activity of PbO, and hence its vapor pressure.

A set of optimum conditions was determined to treat an artificial lead-softening slag containing 30 wt % Sb_2O_3. These optimum conditions were 200μ Hg pressure and an addition of SiO_2 of from 8-11 wt % SiO_2. The process was successful in removing approximately 80 wt % of the original Sb_2O_3 content of the slag in 8 hr and producing a condensate containing in excess of 98 wt % Sb_2O_3 at temperatures of 750° and 850°C.

Finally, the vapor pressure of As_4 was determined above dilute Pb-As alloys at 703°C as a preliminary study to a full-scale investigation of the vaporization of As from Pb-As alloys. The study proved the impossibility of recovering As from Pb-As alloys containing less than about 3 mole % As by vacuum distillation under moderately reduced pressures at 703°C. The experimental results, when converted to As activities, show that the behavior of As in Pb-As alloys containing less than 10 mole % As is characterized by near-ideal-solution behavior at 703°C.

BIBLIOGRAPHY

Alcock, C. B., and Hooper, G. W., 1959, Measurement of vapor pressures at high temperatures by the transportation method: The physical chemistry of process metallurgy-part I, New York, Interscience Publishers, p. 325-340.

American Society for Testing Materials Standards, 1967, Chemical analysis of lead- and tin-base solder metal: Chemical analysis of metals; sampling and analysis of metal bearing ores, Part 32, p. 303-310.

_____ 1965, X-ray powder data file, Cards no. 5-0534, 3-0575, 2-1385, 5-0632, 4-0566, 5-0562, 1-0260, 4-0686, 5-0651, 5-0570, 5-0467, 5-0490, 13-275, and 13-279.

Barthel, J., 1957, Oxidation of Sb in dry lead refining: Bergakadmie, v. 9, p. 630.

Bird, R. B., Stewart, W. E., and Lightfoot, E. N., 1960, Transport Phenomena: New York, John Wiley and Sons, Inc., p. 508-511, 563-575.

Caldwell, H. S., Spendlove, M. J., and St. Claire, H. W., 1960, Removing volatile metals from lead and tin by vacuum distillation: U.S. Bur. Mines Rept. Inv. 5703, 12 p.

Coughlin, J. P., 1957, Contributions to the data on theoretical metallurgy: XII Heats and free energies of formation of inorganic oxides: U.S. Bur. Mines Bull. 542, p. 8.

Davey, T. R. A., 1963, Phase systems concerned with the copper dressing of lead-Part 3: Inst. of Mining and Met. Trans., v. 72, p. 514-515.

_____ 1968, Private communication.

Elliott, J. F., and Gleiser, M., 1960, Thermochemistry of steelmaking-v. 1: Addison-Wesley Pub. Co., p. 19-22.

Folger, F., and Rodebush, W. H., 1923, The heats of vaporization of mercury and cadmium: Am. Chem. Soc. Jour., v. 45, p. 2080-2090.

Gillespie, L. J., 1939, A simple theory for separation of gases by thermal diffusion: Jour. Chem. Phys., v. 7, p. 530-535.

Glassner, A., The thermochemical properties of the oxides, fluorides, and chlorides to 2500°K: ANL Report 5750.

Hall, A. E., 1936, Softening of lead bullion: New York, Am. Inst. Mining Metall. Engineers Trans., v. 121, p. 194-205.

Hayward, C. R., 1957, An outline of metallurgical practice: New York, D. Van Nostrand Co., Inc., p. 143-219.

Henning, H., and Kohlmeyer, E. J., 1957, Untersuchungen uber das gegenseitige verhalten von blei-antimon-oxyden im schmelzflussigen zustande: Erzmetall, v. X, no. i, p. 8-15.

Hincke, W. B., 1930, The vapor pressure of antimony trioxide: Am. Chem. Soc. Jour., v. 52, p. 3869-3877.

Hoffman, H. O., 1918, Metallurgy of lead: New York, McGraw-Hill Book Co., p. 514-528.

Hultgren, R., Orr, R. L., Anderson, P. O., and Kelley, K. K., 1963, Selected values of thermodynamic properties of metals and alloys: New York, John Wiley and Sons, Inc., p. 62-67.

Kubaschewski, O., and Evans, E. LL., 1958, Metallurgical thermochemistry: New York, Pergamon Press, p. 328.

Levin, E. M., Robbins, C. R., and McMurdie, H. F., 1964, Phase disgrams for ceramists: Columbus, Am. Cer. Soc., p. 116.

Liddell, O. M., 1945, Handbook of nonferrous metallurgy-recovery of the metals, New York, McGraw-Hill Book Co., p. 144-215.

Maier, C. G., 1934, Thermodynamic data on some metallurgically important compounds of lead and the antimony-group metals and their application: U.S. Bur. Mines Rept. Inv. 3262, 53 p.

Maier, C. G., and Hincke, W. B., 1932, The system PbO-Sb_2O_3 and its relation to lead softening: New York, Am. Inst. Mining Metall. Engineers Tech. Pub. 449, 12 p.

Mariyama, J. et al, 1964, Fundamental studies on fire refining of crude lead: The activities of components in fused lead-arsenic alloys: Suiyakwai Shi, v. 15, p. 191-194 (Met Abstracts, 1965, v. 32, col. 575).

Myzenkov, F. A., and Klushin, D. N., 1965, Determination of the vapor pressure of pure antimony trioxide and antimony at high temperature: Zh. Prikl. Khim., v. 38, p. 1709-1718.

Norman, J. H., and Staley, H. G., 1964, Vaporization studies on the mixed trioxides of antimony and arsenic: Jour. Chem. Phys., v. 41, p. 1503-1504.

Pelzel, E., 1958, Reaktiensgleichgewicht zwischen flussigem blei und metalloxyden, III: Erzmetall, v. XII, no. 11, p. 558-561.

Richards, J. H., 1968, Private communication.

Rodigina, E. N., Gomel'skii, K. Z., and Luginina, V. F., 1961, Entropy and heat capacity of yellow lead oxide at high temperatures: Zh. Fiz. Khim., v. 35, p. 1799-1802.

Seltz, H., and DeWitt, B. J., 1939, A thermodynamic study of the lead-antimony system: Am. Chem. Soc. Jour., v. 61, p. 2594-2597.

_____ 1939, A thermodynamic study of the zinc-antimony system: Am. Chem. Soc. Jour., v. 61, p. 3170-3173.

Sridhar, R., and Jeffes, J. H. E., 1967, Thermodynamics of PbO and PbO-SiO_2 melts: Inst. of Mining and Met. Trans., v. 76, p. 44-50.

Wicks, C. E., and Block, F. E., 1963, Thermodynamic properties of 65 elements--their oxides, halides, carbides, and nitrides: U.S. Bur. Mines Bull. 605, p. 13-16, 63-64.

Zunkel, A. D., and Larson, A. H., 1967, Slag-metal equilibria in the Pb-PbO-Sb_2O_3 system: New York, Am. Inst. Mining Metall. Engineers Trans., v. 239, p. 473-477.

APPENDICES

Appendix I. Analysis of Reagents

Reagent	Pb	Sb	As	Cd	PbO	Sb_2O_3	As_2O_3	SnO_2
Content, %								
Pb	99.997	-	-	-	-	0.03	0.001	-
Cu	0.0001	-	-	-	-	-	-	-
As	0.0000	-	99.99	-	0.0005	0.15	-	-
Sb	0.0003	99.5	-	-	-	-	0.002	-
Sn	0.0001	-	-	-	-	-	-	-
Cd	0.0006	-	-	99.999	0.0003	-	-	-
Zn	0.00005	-	-	-	0.0006	-	-	-
Fe	0.0001	-	-	-	-	0.001	0.0005	-
Ni + Co	0.00005	-	-	-	-	-	-	-
Bi	0.0000	-	-	-	0.0001	-	-	-
S	0.0002	-	-	-	-	-	-	-
Ag	0.00015	-	-	-	0.0010	-	-	-
PbO	-	-	-	-	99.76	-	-	-
SiO_2	-	-	-	-	0.10	-	-	-
CaO	-	-	-	-	0.08	-	-	-
Fe_2O_3	-	-	-	-	0.014	-	-	-
Insol in CH_3COOH	-	-	-	-	0.042	-	-	-
Sb_2O_3	-	-	-	-	-	99.6	-	-

Appendix I. Continued

Reagent	Pb	Sb	As	Cd	PbO	Sb_2O_3	As_2O_3	SnO_2
Content, %								
Cl^-	-	-	-	-	-	0.004	0.005	0.004
$SO_4^=$	-	-	-	-	-	0.005	-	0.003
As_2O_3	-	-	-	-	-	-	99.95	-
Insol in NH_4OH	-	-	-	-	-	-	0.010	-
Sol in H_2O	-	-	-	-	-	-	-	0.10
Free alkali	-	-	-	-	-	-	-	0.04

Appendix II. Methods of Chemical Analysis

A. Chemical Analysis for As and Sb in Lead Oxide Slags by the Distillation-Bromate Method (ASTM Analysis E46-66);

1. A 0.25 gm sample was transferred to a 500 ml Erlenmeyer flask.
2. To the flask and to a second flask carried through the procedure as a blank, 15 gm $KHSO_4$ and 20 ml H_2SO_4 were added.
3. The flask was gently heated to decompose the sample, and when decomposition was complete, it was strongly heated over an open flame to expel or wash down the sulfur on the walls of the flask.
4. The flask was then cooled and 10 ml H_2O were added to hydrate the H_2SO_4. The sample was finally cooled to room temperature.
5. 50 ml HCl and 10 gm NaCl were added to the flask.
6. The flask was connected to the distillation apparatus (see figure below) and 200 ml H_2O were added to the receiving beaker. The distillation flask was heated on a hot plate until the temperature of the vapor inside the flask reached 105°C. The distillation flask was then disconnected and removed from the hot plate.

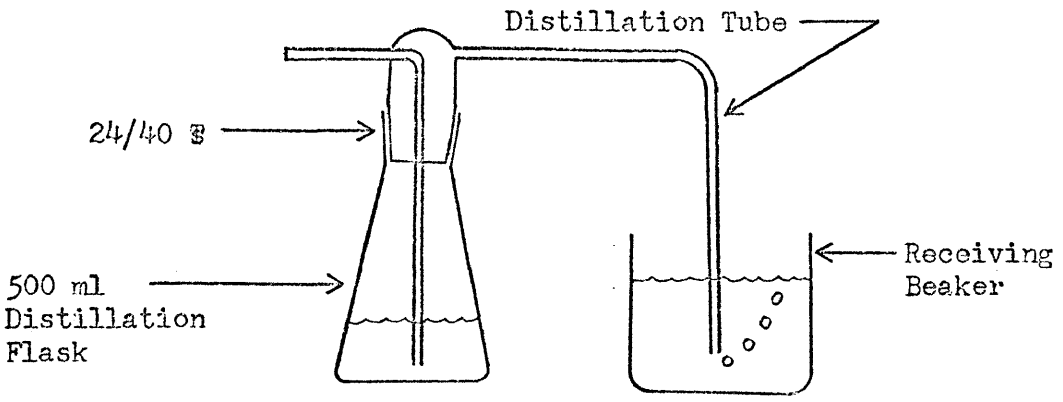

7. The distillate was heated to boiling and boiled gently for 10 min to expel sulfur compounds.
8. The distillate was then titrated at 80-90°C with 0.1N $KBrO_3$ solution and methyl orange indicator added near the end of the titration.
9. This titration determined As_2O_3 in PbO-slags by the following formula:

$$\text{wt \% } As_2O_3 = \frac{(A-B)(0.1)(0.0375)(100)}{C} \times 1.32$$

where: A = ml $KBrO_3$ to titrate sample
B = ml $KBrO_3$ to titrate blank
C = wt of sample in gm

10. To the solution remaining in the distillation flask, 25 gm NaCl were added and the solution diluted to 350 ml with boiling water.
11. The solution was titrated hot with 0.1N $KBrO_3$ and methyl orange indicator.

12. This titration determined Sb_2O_3 in PbO-slags by the following formula:

$$\text{wt \% } Sb_2O_3 = \frac{(A-B)(0.1)(0.0609)(100)}{C} \times 1.20$$

where: A = ml $KBrO_3$ to titrate sample

B = ml $KBrO_3$ to titrate blank

C = wt of sample in gm

B. Chemical Analysis for As and Sb in Pb by the Distillation-Bromate Method:

The same method as outlined above was used to determine As and Sb in Pb with the exceptions that 1.0 gm samples and 0.01N $KBrO_3$ were used. The calculations for wt % As and wt % Sb were modified as follows:

$$\text{wt \% As} = \frac{(A-B)(0.01)(0.0375)(100)}{C} \times 1.32$$

and,

$$\text{wt \% Sb} = \frac{(A-B)(0.01)(0.0609)(100)}{C} \times 1.20$$

C. Chemical Analysis for Sn by the Iodimetric Titration Method (ASTM Analysis E57-60):

1. A 1.0 gm sample was transferred to a 500 ml Erlenmeyer flask.
2. To the flask and to a second flask carried through the procedure as a blank, 5 gm $KHSO_4$ and 20 ml H_2SO_4 were added.
3. The flask was gently heated to decompose the sample, and when decomposition was complete, it

was strongly heated over an open flame to expel or wash down the sulfur on the walls of the flask.

4. The flask was then cooled and 180 ml H_2O were added.
5. 60 ml HCl and 10 gm pure Fe wire were added to the flask.
6. The flask was connected to the distillation apparatus (described above) and a saturated $NaHCO_3$ solution was added to the receiving beaker. The contents of the flask were heated to boiling and boiled for 30 min (some undissolved Fe should remain after boiling).
7. When reduction was complete, the contents of the flask were cooled to $10^{\circ} \pm 2^{\circ}C$ under a CO_2 atmosphere.
8. Maintaining the CO_2 atmosphere, 5 ml starch solution were added to the flask and the solution was titrated in the presence of Fe with standardized KIO_3 solution.
9. This titration determined SnO_2 in PbO-slags by the following formula:

$$\text{wt \% } SnO_2 = \frac{(A)(B)(100)}{C} \times 1.27$$

where: A = ml KIO_3 to titrate sample

B = Sn equivalent of KIO_3 solution (0.0594 gm/ml)

C = wt of sample in gm

10. The standard KIO_3 solution was prepared as follows: 3.5670 gm KIO_3 were dissolved in 200.0 ml H_2O containing 1.0 gm NaOH; 10.0 gm KI were then added to the solution. The resulting solution was added to a 1000 ml flask and diluted with water to 1000.0 ml. This solution was then standardized against a known SnO_2-PbO slag.
11. The starch solution was prepared as follows: 0.80 gm soluble starch was dissolved in 400 ml hot H_2O and allowed to cool to room temperature. The starch solution was prepared fresh daily.

D. Chemical Analysis for Pb and Sb in Oxide Condensates by Atomic Absorption Techniques:

1. A 0.5 gm sample was weighed into a 150 ml beaker.
2. 10 ml of a mixture of conc. HCl and conc. HNO_3 (10:1) was added to the samples and allowed to stand overnight with intermittent swirling at room temperature.
3. 20 ml of a 10% tartaric acid solution was added to the samples, with stirring, and the samples quantitatively transferred to 100 ml volumetric flasks and diluted to volume with distilled water.
4. Suitable aliquotes were then taken for analysis.

5. Standard solutions were prepared from B & A test lead metal (99.99+% Pb) and Sb metal (AS&R 99.999+% Sb). Solution was affected in the same manner as described above. The standard samples were diluted to the concentrations desired for calibration of the atomic absorption spectrophotometer.

6. Conditions for obtaining the calibration curve for Sb were as follows:

   Instrument -- Perkin-Elmer Model 303 Atomic Absorption Spectrophotometer

   Wavelength -- 2311.5 Å

   Slit -- 3-2

   Source and Current -- Australian-made hollow cathode lamp at 20 ma.

   Fuel -- acetylene at 8 psi

   Oxidant -- air at 30 psi

   Burner -- 3-slot Boling Burner head

7. The data for the calibration curve for the Sb analyses is as follows:

log % absorption	μ gm Sb/ml
0.9465	10.0
1.1838	20.0
1.4589	40.0
1.5163	50.0
1.5887	60.0
1.6290	70.0
1.6676	80.0
1.6990	90.0
1.7285	100.0

Appendix III. Sample Calculation for p_{Cd} above pure Cd from Weight-loss Data

The molecular weight of Cd is 112.40 gm/mol.

$$p_{Cd}\ (\text{atm}) = \frac{n_{Cd}}{n_{argon}} P_t\ (\text{atm}) \qquad (\text{if } n_{Cd} << n_{argon})$$

$$n_{Cd} = \frac{\Delta w,\ \text{gm}}{112,40}$$

Assuming that argon behaves as an ideal gas,

$$n_{argon} = \frac{P_t V}{R T_r}$$

$$\text{Therefore, } p_{Cd}\ (\text{mm Hg}) = \frac{(\Delta w,\ \text{gm})(P_t,\ \text{atm})(760) R T_r}{(P_t,\ \text{atm})(V,\ \text{liters})(112.40)}$$

$$p_{Cd}\ (\text{mm Hg}) = \frac{(\Delta w,\ \text{mg})(0.08205)(760) T_r}{(V,\ \text{liters})(112.40)(1000\ \text{mg/gm})}$$

$$p_{Cd}\ (\text{mm Hg}) = \frac{(\Delta w,\ \text{mg})}{(V,\ \text{liters})} \times T_r \times 5.550 \times 10^{-4}$$

where: T_r = temperature at which volume of argon was measured, ^{o}K.

Appendix IV. Experimental data for vapor-pressure determinations on Cd, Sb_2O_3, $PbO-Sb_2O_3$ and $PbO-SiO_2-Sb_2O_3$ slags, and Pb-As alloys.

1. Cadmium

Test	Temp, °C	Room Temp, °C	Flow Rate, cc/min	Flow Rate, cc/min at STP	Reaction Time, min	Weight loss, grams	mg/liter
C-19	393	25	98	73	120	0.05745	4.885
C-20	393	24	133	199	125	0.07075	4.256
C-21	393	25	115	86	108	0.05924	4.770
C-22	393	26	85	63.5	150	0.07057	5.535
C-23	393	24	68	51	93	0.03592	5.680
C-24	393	27	53	39.5	120	0.03900	6.132*
C-25	393	27	45	33.5	138	0.03845	6.192*
C-26	393	23	34	25.5	129	0.02677	6.104*
C-27	393	23	21.5	16	115	0.01486	6.009*
C-28	393	28	12	9	185	0.01540	6.937
C-29	393	26	5	4	159	0.00669	8.415
C-30	393	26	25	18.5	201	0.03116	6.199
C-32	254	25	67.5	50.5	275	0.00091	0.0489
C-33	254	26	98	73	247	0.00078	0.0323*

* Denotes tests used to calculate mean vapor pressure

Appendix IV. Cont'd.

1. Cadmium Cont'd

Test	Temp, °C	Room Temp, °C	Flow Rate, cc/min	Flow Rate, cc/min at STP	Reaction Time, min	Weight loss grams	Weight loss mg/liter
C-34	254	23	128	95.5	253	0.00105	0.0324*
C-35	254	22	152	113.5	540	0.00269	0.0328*
C-36	254	25	169	126	255	0.00140	0.0325*
C-37	254	24	187	140	283	0.00169	0.0320*
C-38	254	23	217	162	250	0.00129	0.0238
C-39	254	27	89	66.5	210	0.00061	0.0321*
C-40	297	29	82	61.5	255	0.00460	0.220*
C-41	297	27	143	107	320	0.00982	0.215*
C-42	346	25	52	39	149	0.01217	1.571
C-43	346	27	98	73	163	0.01917	1.197*
C-44	346	23	71	53	184	0.01756	1.344*
C-45	346	26	82	61.5	155	0.01692	1.331*
C-46	346	22	58	43.5	155	0.01253	1.394*

Appendix IV. Cont'd.

2. Sb_2O_3

Test	Temp, °C	Room Temp, °C	Flow Rate, cc/min	Flow Rate cc/min at STP	Reaction Time, min	Weight loss grams	Weight loss mg/liter
S-1	422	26	29	21.5	195	0.00046	0.0813
S-2	422	27	62	46.5	159	0.00060	0.0609
S-3	422	25	112	83.5	146	0.00083	0.0510*
S-4	422	25	85	63.5	805	0.00344	0.0503*
S-5	422	27	134	100	155	0.00106	0.0510*
S-6	422	27	158	118	126	0.00091	0.0456
S-7	454	27	52	39	115	0.00163	0.272
S-8	454	28	71	53	123	0.00209	0.239*
S-9	454	29	107	80	83	0.00214	0.241*
S-10	454	29	94	70.5	208	0.00466	0.238*
S-11	454	27	134	100	120	0.00386	0.240*
S-12	454	28	148	110.5	140	0.00429	0.207
S-13	454	30	117	87.5	77	0.00214	0.238*
S-14	454	30	33	24.5	90	0.00134	0.451

Appendix IV. Cont'd.

2. Sb_2O_3 Cont'd.

Test	Temp, °C	Room Temp, °C	Flow Rate, cc/min	Flow Rate, cc/min at STP	Reaction Time, min	Weight loss grams	Weight loss mg/liter
S-15	485	29	30	22.5	68	0.00271	1.328
S-16	485	30	55	41	75	0.00422	1.023
S-17	485	30	77	57.5	60	0.00392	0.849*
S-18	485	30	97	72.5	172	0.01419	0.851*
S-19	485	30	128	95.5	157	0.01729	0.860*
S-20	485	29	142	106	60	0.00662	0.777*
S-21	485	29	170	127	65	0.00835	0.756
S-22	514	31	30	22.5	80	0.01106	4.608
S-23	514	31	48	36	62	0.01087	3.653
S-24	514	31	74	55.5	74	0.01597	2.916*
S-25	514	31	91	68	45	0.01166	2.847*
S-26	514	31	112	83.5	46	0.01468	2.849*
S-27	514	30	136	101.5	127	0.04985	2.886*

Appendix IV. Cont'd.

2. Sb_2O_3 Cont'd.

Test	Temp, °C	Room Temp, °C	Flow Rate, cc/min	Flow Rate, cc/min at STP	Reaction Time, min	Weight loss, grams	Weight loss, mg/liter
S-28	547	28	30	22.5	90	0.04427	16.396
S-29	547	29	48	36	80	0.05356	13.948
S-30	547	30	68	51	63	0.04987	11.641
S-31	547	30	88	65.5	51	0.04566	10.174*
S-32	547	29	110	82	62	0.07118	10.437*
S-33	547	28	137	102	166	0.22880	10.061*
S-34	547	28	165	123	104	0.14558	8.484
S-35	568	28	52	39	79	0.13017	31.687
S-36	568	29	31	23	74	0.08643	37.677
S-37	568	29	74	55.5	58	0.10901	25.398
S-38	568	29	92	68.5	35	0.06852	21.280*
S-39	568	29	115	86	35	0.08735	21.702*
S-40	568	29	133	99.5	31	0.08550	20.737*
S-41	568	29	123	92	35	0.09292	21.584*
S-42	568	29	165	123	48	0.13509	17.057

Appendix IV. Cont'd.

2. Sb_2O_3 Cont'd.

Test	Temp, °C	Room Temp, °C	Flow Rate, cc/min	Flow Rate, cc/min at STP	Reaction Time, min	Weight loss grams	Weight loss mg/liter
S-43	568	31	30	22.5	75	0.01166	5.182
S-44	568	31	51	38	65	0.01336	4.030
S-45	568	31	73	54.5	61	0.01408	3.162
S-46	568	31	92	68.5	60	0.01448	2.623
S-47	568	31	114	85	63	0.01639	2.282
S-48	568	30	137	102.5	50	0.01404	2.050
S-49	599	29	53	39.5	73	0.29685	76.725
S-50	599	31	73	54.5	31	0.12126	53.584*
S-51	599	32	94	70.5	26	0.12825	52.475*
S-52	599	32	112	83.5	20	0.12367	55.210*
S-53	599	30	129	96.5	30	0.19002	49.101
S-54	599	30	155	116	38	0.23879	40.542

Appendix IV. Cont'd.

3. $PbO-Sb_2O_3$ slags

Test	$X_{Sb_2O_3}$	Temp, °C	Room Temp, °C	Flow Rate, cc/min	Flow Rate cc/min at STP	Reaction Time, min	Weight loss grams	Weight loss mg/liter
S-101	0.280	700	27	57	42.5	30	0.00664	3.883*
S-102	0.280	700	29	82	61.5	40	0.01285	3.918*
S-103	0.280	700	30	95	71	38	0.01419	3.931*
S-104	0.280	700	31	110	82	33	0.01409	3.882*
S-105	0.280	700	29	30	22.5	56	0.00758	4.512
S-106	0.212	700	29	35	26	62	0.00456	2.101
S-107	0.212	700	30	47	35	59	0.00487	1.756*
S-108	0.212	700	30	65	48.5	46	0.00516	1.726*
S-109	0.212	700	27	98	73.5	64	0.01077	1.717*
S-110	0.176	700	26	32	24	60	0.00362	1.885
S-111	0.176	700	26	51	38	60	0.00369	1.206*
S-112	0.176	700	27	74	55.5	63	0.00545	1.169*
S-113	0.176	700	29	97	72.5	54	0.00614	1.172*

Appendix IV. Cont'd.

3. $PbO-Sb_2O_3$ slags Cont'd.

Test	$X_{Sb_2O_3}$	Temp, °C	Room Temp, °C	Flow Rate, cc/min	Flow Rate, cc/min at STP	Reaction Time, min	Weight loss grams	Weight loss mg/liter
S-114	0.137	700	30	35	26	70	0.00250	1.020
S-115	0.137	700	25	51	38	61	0.00281	0.903*
S-116	0.137	700	27	78	58.5	55	0.00393	0.916*
S-117	0.137	700	30	94	70	56	0.00469	0.891*
S-118	0.108	700	30	38	28.5	37	0.00153	1.088
S-119	0.108	700	30	51	38	45	0.00212	0.924*
S-120	0.108	700	30	72	54	53	0.00343	0.899*
S-121	0.108	700	31	95	71	54	0.00457	0.891*
S-122	0.0442	700	32	34	25.5	50	0.00258	1.518
S-123	0.0442	700	32	50	37.5	56	0.00273	0.975*
S-124	0.0442	700	28	70	52.5	34	0.00223	0.937*
S-125	0.0442	700	29	93	69.5	35	0.00296	0.909*

Appendix IV. Cont'd.

3. $PbO-Sb_2O_3$ slags Cont'd.

Test	$X_{Sb_2O_3}$	Temp, °C	Room Temp, °C	Flow Rate cc/min	Flow Rate cc/min at STP	Reaction Time, min	Weight loss, grams	Weight loss, mg/liter
S-126	0.495	700	27	32	25.5	22	0.03885	55.185
S-127	0.495	700	26	50	37.5	20	0.04168	41.680
S-128	0.495	700	26	60	45	20	0.04681	39.008*
S-129	0.495	700	26	79	59	20	0.06110	38.671*
S-130	0.495	700	26	87	65	20	0.06634	38.128*
S-131	0.0442	750	27	62	46.5	44	0.00427	1.565*
S-132	0.0442	750	28	89	66.5	33	0.00475	1.617*
S-133	0.108	750	28	90	67.5	36	0.00514	1.586*
S-134	0.108	750	29	60	45	49	0.00462	1.571*
S-135	0.108	650	29	57	42.5	46	0.00133	0.507*
S-136	0.108	650	29	89	66.5	43	0.00188	0.491*
S-137	0.176	650	29	89	66.5	35	0.00151	0.485*
S-138	0.176	650	29	62	46.5	35	0.00109	0.502*

Appendix IV. Cont'd.

4. $PbO-SiO_2-Sb_2O_3$ slags

Test	$X_{Sb_2O_3}$	Temp, °C	Room Temp, °C	Flow Rate, cc/min	Flow Rate, cc/min at STP	Reaction Time, min	Weight loss grams	Weight loss mg/liter
S-60	0.0296	700	30	55	41	37	0.00006	0.0295
S-61	0.0296	700	30	74	55.5	203	0.00025	0.0166*
S-62	0.0296	700	31	95	71	120	0.00019	0.0167*
S-63	0.0296	700	29	111	83	105	0.00019	0.0163*
S-64	0.0296	700	30	127	95	112	0.00023	0.0162*
S-65	0.0296	700	30	152	113.5	131	0.00034	0.0171*
S-66	0.0634	700	28	53	39.5	127	0.00059	0.0877*
S-67	0.0634	700	28	68	50.5	135	0.00075	0.0817*
S-68	0.0634	700	28	92	68.5	157	0.00124	0.0859*
S-69	0.0634	700	27	111	83	120	0.00116	0.0871*
S-70	0.0634	700	26	127	95	158	0.00140	0.0698
S-71	0.0634	700	27	30	22.5	125	0.00050	0.133

Appendix IV. Cont'd.

4. $PbO-SiO_2-Sb_2O_3$ slags Cont'd.

Test	$X_{Sb_2O_3}$	Temp, °C	Room Temp, °C	Flow Rate, cc/min	Flow Rate cc/min at STP	Reaction Time, min	Weight loss grams	Weight loss mg/liter
S-72	0.0945	700	28	31	23	150	0.00138	0.297
S-73	0.0945	700	29	48	36	136	0.00155	0.237*
S-74	0.0945	700	28	77	57.5	88	0.00164	0.242*
S-75	0.0945	700	29	87	65	83	0.00169	0.234*
S-76	0.0945	700	31	112	83.5	75	0.00196	0.233*
S-77	0.0945	700	31	128	95.5	65	0.00176	0.212
S-78	0.130	700	26	33	24.5	73	0.00250	1.038
S-79	0.130	700	26	52	39	65	0.00279	0.825*
S-80	0.130	700	27	74	55.5	66	0.00416	0.852*
S-81	0.130	700	27	92	68.5	60	0.00447	0.810*
S-82	0.130	700	27	112	83.5	62	0.00564	0.812*
S-83	0.130	700	27	136	101.5	48	0.00446	0.683

Appendix IV. Cont'd.

4. $PbO-SiO_2-Sb_2O_3$ slags Cont'd.

Test	$X_{Sb_2O_3}$	Temp, °C	Room Temp, °C	Flow Rate, cc/min	Flow Rate, cc/min at STP	Reaction Time, min	Weight loss grams	Weight loss mg/liter
S-84	0.167	700	27	32	24	60	0.00647	3.370
S-85	0.167	700	28	53	39.5	60	0.00791	2.488*
S-86	0.167	700	27	79	59	60	0.01197	2.525*
S-87	0.167	700	28	108	80.5	43	0.01153	2.483*
S-88	0.206	700	26	35	26	48	0.01400	8.333
S-89	0.206	700	29	53	39.5	48	0.01623	6.380*
S-90	0.206	700	29	73	54.5	46	0.02019	6.013*
S-91	0.206	700	29	92	68.5	44	0.02644	6.532*
S-92	0.206	700	28	115	86	52	0.03236	5.414
S-93	0.246	700	29	34	25.5	77	0.03877	14.809
S-94	0.246	700	29	56	42	35	0.02691	13.730*
S-95	0.246	700	28	67	50	35	0.03204	13.663*
S-96	0.246	700	28	84	63	35	0.04005	13.622*
S-97	0.246	700	28	109	81.5	46	0.06224	12.413

Appendix IV. Cont'd.

5. Pb-As alloys

Test	X_{As}	Temp, °C	Room Temp, °C	Flow Rate, cc/min	Flow Rate cc/min at STP	Reaction Time, min	Weight loss, grams	Weight loss, mg/liter
A-3	0.0690	703	27	99	74	30	0.01153	3.882*
A-4	0.0690	703	28	120.5	90	25.5	0.01136	3.667*
A-5	0.0690	703	29	141	105	23	0.01243	3.833*
A-6	0.0690	703	29	84	63	31	0.00959	3.683*
A-7	0.0690	703	29	67	50	32	0.00911	4.249
A-8	0.0690	703	29	43	32	31	0.00609	4.569
A-9	0.0690	703	24	178	133	31	0.01322	2.396
A-11	0.0279	703	29	25	18.5	48	0.00041	0.342
A-12	0.0279	703	29	45.5	34	50	0.00055	0.242*
A-14	0.0279	703	29	33.5	25	58	0.00045	0.232*
A-15	0.0279	703	28	77	57.5	46	0.00087	0.246*
A-16	0.0279	703	28	105	78.5	59	0.00136	0.220*
A-17	0.0279	703	29	135	101	55	0.00130	0.175

Appendix IV. Cont'd.

5. Pb-As alloys Cont'd.

Test	X_{As}	Temp, °C	Room Temp, °C	Flow Rate, cc/min	Flow Rate, cc/min at STP	Reaction Time, min	Weight loss grams	Weight loss mg/liter
A-18	0.0143	703	30	39	29	90	0.00069	0.197
A-19	0.0143	703	31	76	57	88	0.00086	0.129*
A-21	0.0143	703	30	129	96.5	65	0.00102	0.122*
A-22	0.0143	703	31	108	80.5	72	0.00093	0.120*
A-23	0.0143	703	32	154	115	60	0.00081	0.088
A-24	0.0143	703	32	16	12	89	0.00037	0.260
A-26	0.0858	703	30	104	77.5	19	0.01762	8.917*
A-27	0.0858	703	30	128	95.5	20	0.02041	7.973
A-28	0.0858	703	29	155	116	21	0.02228	6.845
A-29	0.0858	703	29	75	56	22	0.01587	9.618
A-31	0.0858	703	28	37	27.5	27	0.01323	13.243
A-32	0.0858	703	28	20	15	30	0.00940	15.667
A-33	0.0858	703	30	84	63	25	0.01870	8.905*
A-34	0.0858	703	30	95	71	25	0.02133	8.981*
A-35	0.0858	703	30	64	48	24	0.01617	10.527

1171

Appendix IV. Cont'd.

5. Pb-As alloys Cont'd.

Test	X_{As}	Temp, °C	Room Temp. °C	Flow Rate, cc/min	Flow Rate cc/min at STP	Reaction Time, min	Weight loss grams	Weight loss mg/liter
A-36	0.0381	703	29	25	18.5	77	0.00186	0.966
A-37	0.0381	703	29	54	40.5	82	0.00336	0.759
A-38	0.0381	703	30	77	57.5	93	0.00425	0.593*
A-39	0.0381	703	31	97	72.5	80	0.00415	0.535*
A-40	0.0381	703	31	131	98	75	0.00510	0.519
A-41	0.0381	703	29	149	111.5	98	0.00635	0.435
A-42	0.0381	703	29	86.5	64.5	75	0.00350	0.540*
A-43	0.0381	703	29	112	83.5	60	0.00378	0.563*
A-44	0.0527	703	30	112	83.5	75	0.01112	1.324*
A-45	0.0527	703	30	92	68.5	63	0.00949	1.637
A-46	0.0527	703	30	76	57	63	0.00839	1.752
A-47	0.0527	703	30	53	39.5	50	0.00542	2.045
A-49	0.0527	703	29	137	102.5	60	0.01049	1.276*

Appendix IV. Cont'd.

5. Pb-As alloys Cont'd.

Test	X_{As}	Temp, °C	Room Temp, °C	Flow Rate, cc/min	Flow Rate, cc/min at STP	Reaction Time, min	Weight loss, grams	Weight loss, mg/liter
A-50	0.0527	703	31	151	113	62	0.01225	1.309*
A-51	0.0527	703	31	98	73	60	0.00872	1.483
A-52	0.0527	703	30	169	126	60	0.01202	1.185
A-53	0.0527	703	31	27	20	60	0.00410	2.531

Appendix V. X-ray Powder Diffraction Data for PbO, Pb, Sb, Sb_2O_3, Sb_2O_4, Sb_2O_5, As, As_2O_3, As_2O_5, Sn, SnO_2, $2PbO \cdot SiO_2$, α-$4PbO \cdot SiO_2$, and γ-$4PbO \cdot SiO_2$ as Compiled from the ASTM Powder Data Index

Element or Compound	d_{hkl}, A°	2θ, °	Relative Intensity
yellow PbO	5.893	15.02	6
	3.067	29.10	100
	2.946	30.32	31
	2.744	32.60	28
	2.493	36.00	< 1
	2.377	37.80	20
red PbO	5.018	17.66	5
	3.115	28.64	100
	2.809	31.82	62
	2.510	35.74	18
Pb	2.85	31.36	100
	2.47	36.34	50
	1.74	52.54	50
	1.49	62.24	50
Sb	3.753	23.68	25
	3.538	25.14	4
	3.109	28.68	100
	2.248	40.08	70
$Sb_2O_{3(o)}$	4.57	19.40	17
	3.494	25.48	25
	3.174	28.08	20
	3.142	28.38	100
	3.118	28.60	75
	2.738	32.68	9
	2.712	33.00	9
	2.650	33.78	13
	2.456	36.42	9
$Sb_2O_{3(c)}$	6.44	13.74	12
	3.218	27.40	100
	2.788	32.08	40
	2.559	35.04	11
	2.276	39.56	2

Appendix V. Cont'd.

Element or Compound	d_{hkl}, A°	2θ, °	Relative Intensity
Sb_2O_4	5.90	15.00	3
	4.46	19.88	9
	3.60	24.70	3
	3.445	25.84	35
	3.073	29.04	100
	3.033	29.42	5
	2.942	30.36	45
	2.718	32.92	9
	2.651	33.78	25
	2.470	36.34	7
	2.404	37.38	17
	2.235	40.32	11
Sb_2O_5	5.952	14.86	25
	3.108	28.70	20
	2.976	30.00	100
	2.577	34.78	30
	2.365	38.02	4
	2.102	43.00	2
As	3.52	25.28	26
	3.112	28.66	6
	2.771	32.28	100
	2.050	44.14	24
As_2O_3	6.394	13.84	63
	3.920	22.66	< 1
	3.195	27.90	100
	2.768	32.32	28
	2.541	35.28	38
	2.262	39.82	12
	2.132	42.36	17
As_2O_5	7.1	12.46	30
	5.6	15.80	30
	4.88	18.16	100
	4.01	22.16	10
	3.58	24.84	60
	3.40	26.18	60
	3.21	27.76	20
	3.05	29.26	50
	2.70	33.14	20
	2.62	34.20	40
	2.34	38.42	10
	2.26	39.86	20

Appendix V. Cont'd.

Element or Compound	d_{hkl}, A°	2θ, °	Relative Intensity
α-Sn	3.751	23.70	100
	2.294	39.24	83
	1.956	46.38	53
β-Sn	2.915	30.64	100
	2.793	32.02	90
	2.062	43.87	34
SnO_2	3.351	26.58	100
	2.644	33.88	81
	2.369	37.95	24
	2.309	38.98	5
	2.120	42.61	2
$2PbO \cdot SiO_2$	6.03	14.68	40
	4.29	20.68	6
	3.71	23.96	25
	3.56	25.00	18
	3.22	27.68	100
	3.13	28.50	85
	3.00	29.76	60
	2.95	30.27	20
	2.89	30.92	20
	2.80	31.94	35
	2.58	34.74	20
	2.55	35.16	25
	2.43	36.96	14
	2.41	37.28	10
	2.37	37.93	18
	2.23	40.41	14
α-$4PbO \cdot SiO_2$	3.64	24.40	40
	3.36	26.50	40
	3.10	28.78	100
	3.03	29.46	80
	2.91	30.70	40
	2.83	31.58	60
	2.70	33.16	60
	2.49	36.04	40
	2.31	38.96	40
	2.25	40.04	40

Appendix V. Cont'd.

Element or Compound	d_{hkl}, A°	2θ °	Relative Intensity
γ-4PbO·SiO_2	3.22	27.68	6
	3.12	28.58	100
	3.02	29.55	35
	2.95	30.27	18
	2.92	30.59	16
	2.72	32.90	20
	2.66	33.66	6
	2.54	35.30	4
	2.49	36.04	6
	1.961	46.26	4

Appendix VI. Reference X-ray Powder Diffraction Data for $PbO \cdot Sb_2O_3$ and $PbO \cdot SiO_2$

Compound	d_{hkl}, Å	2θ, °	Relative Intensity
$PbO \cdot Sb_2O_3$	3.601	24.70	w
	3.361	26.50	w
	3.246	27.45	vs
	3.025	29.50	m
	2.673	33.50	w
	2.635	34.00	w
$PbO \cdot SiO_2$	3.527	25.23	m
	3.500	25.43	m
	3.304	26.96	m
	3.193	27.92	m
	3.062	29.14	vw
	3.012	29.63	w
	2.953	30.24	w
	2.885	30.97	w
	2.558	31.30	vw
	2.779	32.18	w
	2.699	33.16	w
	2.650	33.80	vw
	2.329	38.62	s
	2.281	39.48	vs
	2.189	41.20	vw
	2.046	44.22	w
	2.018	44.88	w

Appendix VII. Calculation of ΔG° for the Reaction $PbO_{(s)} = PbO_{(l)}$ below the Melting Point of PbO.

The melting point of PbO = 1170°K and ΔH_f° = 6,110 cal/mole (Rodigina, Gomel'skii, and Luginina, 1961, p. 1801).

$$\Delta G_f^{\circ} = \Delta H_f^{\circ} - T\Delta S_f^{\circ}$$

$$\Delta S_f^{\circ} = \frac{\Delta H_f^{\circ}}{T_f}$$

Assuming $\Delta C_p = 0$, then $\Delta G_f^{\circ} = \Delta H_f^{\circ} - T\left(\frac{\Delta H_f^{\circ}}{T_f}\right) = 6110 - T\left(\frac{6110}{1170}\right)$

Therefore, $\Delta G_f^{\circ} = 6110 - 5.23\ T$

At 973°K, $\Delta G_{f_{973}}^{\circ} = 6110 - 5.23\ (973) = 6110 - 5080 = 1030$ cal

Appendix VIII. Calculation of ΔG^{o} for the Reaction

$$Sb_{(l)} = \underline{Sb}_{1 \text{ wt \% in Pb}}$$

Since Sb in Pb obeys Henry's law up to about 3.9 wt % at 700°C, the following equation applies for a change in standard state from pure liquid Sb to Sb dissolved in Pb at 1 wt %:

$$\Delta G^{o}_{T} = RT \ln a_{Sb_{1 \text{ wt \%}}} = RT \ln \gamma^{o} X_{Sb_{1 \text{ wt \%}}}$$

At 973°K, $\gamma^{o}_{Sb} = 0.798$. This value was obtained by extrapolating the data of Hultgren, Orr, Anderson, and Kelley (1960, p. 896) and Seltz and DeWitt (1939, p. 2595).

$$X_{Sb} \text{ at 1 wt \% Sb in Pb} = \frac{\frac{1}{121.76}}{\frac{1}{121.76} + \frac{99}{207.21}} = 0.0136$$

At 973°K, $\Delta G^{o}_{973} = (4.58)(973) \log (0.798)(0.0136)$

$$= 4456(-1.867)$$

$$\Delta G^{o}_{973} = -8320 \text{ cal}$$

Appendix IX. Determination of ΔH_m^o for the Reaction

$$PbO_{(s)} = PbO_{(l)}$$

The literature contains two entirely distinct values for the heat of fusion of PbO. Wicks and Block (1963, p. 63) report a value of 2,800 cal/mole whereas Rodigina, Gomel'skii, and Luginina (1961, p. 1801) report a value of 6,110 cal/mole. The lower value of 2,800 cal/mole represents an average of values obtained from freezing-point depression calculations made on a number of $PbO\text{-}Me_xO_y$ systems without any direct component activity data.

By use of the data of Sridhar and Jeffes (1967, p. 50), a value for ΔH_m^o can be calculated which is the same as that reported by Rodigina, Gomel'skii, and Luginina.

The activity of PbO in the $PbO\text{-}SiO_2$ system has been determined by Sridhar and Jeffes and has been shown to be temperature-independent above approximately 80 mole % PbO in the temperature range from 850° to 1050°C. Therefore, the activity of PbO measured at 1000°C should be equal to the activity of PbO calculated from the depression of the freezing point using the phase diagram shown in Figure 29.

The activity of PbO in the $PbO\text{-}SiO_2$ system, using the data of Sridhar and Jeffes and Figure 29, is shown in Figure 39 as a function of reciprocal temperature. A calculation for ΔH_m^o from the slope of the log a_{PbO} versus $\frac{1}{T}$ curve has been made with the result that ΔH_m^o = 6,110 cal/mole

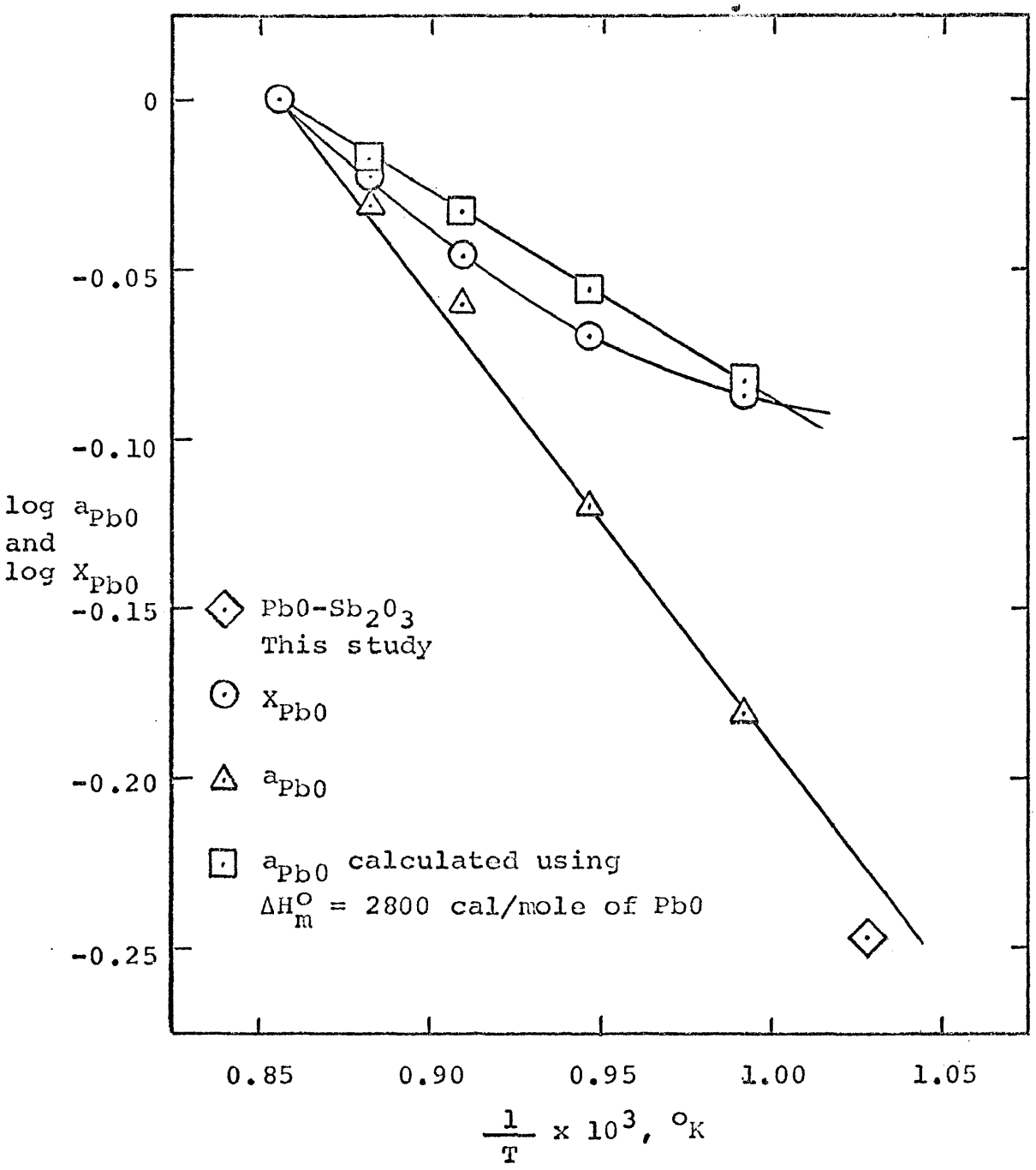

Figure 39. Log a_{PbO} and log X_{PbO} Versus Reciprocal Temperature for the $PbO-SiO_2$ System

Appendix IX. Cont'd.

of PbO. This value is the same as that reported by Rodigina, Gomel'skii, and Luginina. The freezing-point depression as a function of mole fraction of PbO is seen to be nearly tangent to this curve at mole fractions approaching unity.

A third curve shown in Figure 39 was plotted from the freezing-point depression of PbO by SiO_2 using a value of 2,800 cal/mole of PbO for ΔH^o_m. The discrepancy in the slope of this curve at mole fractions of PbO approaching unity indicates that the value of 2,800 cal/mole of PbO for ΔH^o_m is much too low.

The results of this investigation can be compared with those of Sridhar and Jeffes by use of the data presented in Table 14. The activity of PbO, relative to pure, solid PbO, in a liquid containing 14.4 mole % Sb_2O_3 in equilibrium with α solid solution at 700°C was calculated to be 0.964. By use of T_b = 1789°K and ΔH^o_{vap} = 49,350 cal/mole of PbO from Rodigina, Gomel'skii, and Luginina, the vapor pressure above pure, liquid PbO can be calculated with the result that,

$$\log p_{PbO} \text{ (mm Hg)} = 8.909 - \frac{10,790}{T}$$

Also, using their values for T_m = 1170°K and ΔH^o_m = 6,110 cal/mole of PbO, the vapor pressure above pure, solid PbO

Appendix IX. Cont'd.

can be calculated with the result that,

$$\log p_{PbO} \text{ (mm Hg)} = 10.050 - \frac{12,120}{T}$$

The calculated activity of PbO given above can now be referred to the pure, supercooled, liquid standard state by multiplying it by the ratio of the vapor pressure above pure, solid PbO at 700°C to the vapor pressure above pure, supercooled, liquid PbO at 700°C obtained from the above equations:

$$a_{PbO_{(l)}} = 0.964 \left(\frac{0.00392}{0.00668}\right) = 0.566$$

This value is included in Figure 39 and is found to agree with the value of 6,110 cal/mole of PbO reported by Rodigina, Gomel'skii, and Luginina for the heat of fusion of PbO.

VITA

The author was born on February 14, 1943, in Niagara Falls, New York. He received his primary and secondary education in Ashtabula, Ohio, and Lewiston, New York.

He entered the University of Missouri School of Mines and Metallurgy, Rolla, Missouri, in September 1961. He received his Bachelor of Science degree in Metallurgical Engineering from the University of Missouri at Rolla in June 1965.

He has been enrolled in the Graduate School of the Colorado School of Mines from June 1965 to the present. He received his Master of Science degree in Metallurgical Engineering from the Colorado School of Mines in June 1966.

While enrolled in the Graduate School of the Colorado School of Mines, the author was a research assistant on a project supported by the National Science Foundation from June 1965 to September 1965 and held a National Defense Education Act Fellowship from September 1965 to the present.